Aus dem Zentrum für Orthopädie und Unfallchirurgie (ZOU)

der Universitätsmedizin der Johannes Gutenberg-Universität Mainz

Referenzwerte für die dreidimensionale Haltungs-und Bewegungsanalyse gesunder Probanden basierend auf videorasterstereographisch erhobenen Wirbelsäulendaten während des Stehens und des Gehens auf einem Laufband

Inauguraldissertation

zur Erlangung des Doktorgrades der

physiologischen Wissenschaften

der Universitätsmedizin

der Johannes Gutenberg-Universität Mainz

Vorgelegt von

Janine Huthwelker

aus Kassel

Mainz, 2024

Wissenschaftlicher Vorstand:	Univ.-Prof. Dr. Hansjörg Schild
1. Gutachter:	---
2. Gutachter:	---
3. Gutachter:	---
Tag der Promotion:	23. September 2024

Inhaltsverzeichnis

Verzeichnisübersicht

Abkürzungsverzeichnis

SGZ	Standardisierter Gangzyklus
VRS	Videorasterstereographie
C7	Siebter Halswirbelkörper
L4	Vierter Lendenwirbelkörper

Abbildungsverzeichnis

Tabellenverzeichnis

1 Zusammenfassung

Die Beurteilung der Haltung ist ein wichtiger Bestandteil der Untersuchung von Patienten mit muskuloskeletalen Beschwerden. In der Praxis erfolgt dies oft durch visuelle Beobachtungen, welche zwar einfach und schnell durchführbar sind, deren Reliabilität jedoch limitiert ist (Fedorak et al., 2003). In Kombination mit akkurateren Messverfahren ließe sich die Qualität dieser Haltungsanalysen jedoch potentiell verbessern (Fedorak et al., 2003). Hierfür stehen verschiedenste Möglichkeiten zur Verfügung, von denen eine die Videorasterstereographie (VRS) darstellt.

Bei der VRS handelt es sich um ein ursprünglich für die strahlenfreie Verlaufskontrolle von Skoliosen entwickeltes (Drerup, 2014, Betsch et al., 2015), reliables, valides und nicht-invasives Messverfahren zur dreidimensionalen wirbelsäulenspezifischen Haltungsanalyse (Krott et al., 2020). Dabei wird mit Hilfe eines Lichtprojektors ein horizontales Linienraster auf die Rückenoberfläche des Patienten projiziert, welches sich durch die individuelle Oberflächentopographie krümmt und von einer Kamera aufgezeichnet wird (Betsch et al., 2015) (Abbildung 1a). Mit Hilfe einer Computersoftware wird im Anschluss eine Art dreidimensionaler „virtueller Gipsabdruck“ der Rückenoberfläche erstellt (Betsch et al., 2015, Drerup et al., 2001). Anhand charakteristischer Krümmungsmuster auf dieser Oberfläche (bspw. die Lumbalgrübchen, der Vertebra Prominens und die Symmetrielinie) und mittels eines mathematischen Algorithmus, basierend auf mehreren hundert Röntgenaufnahmen, wird ein dreidimensionales Wirbelsäulenmodell rekonstruiert (Betsch et al., 2015, Drerup et al., 2001, Drerup und Hierholzer, 1992a, Drerup und Hierholzer, 1992b). So lassen sich verschiedenste Wirbelsäulenparameter, wie bspw. der Skoliosewinkel, die thorakale Kyphose, die lumbale Lordose u.v.a. ableiten und analysieren.

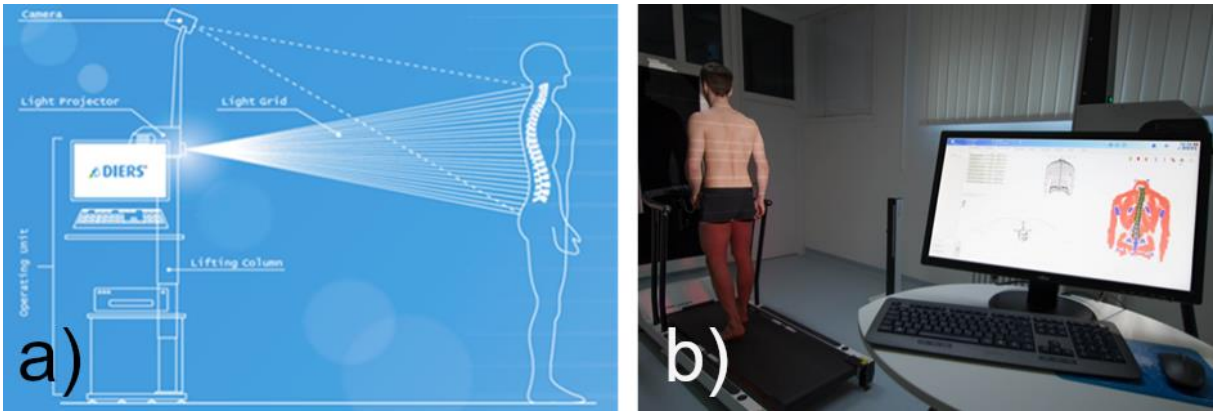

Abbildung 1 *Schematische Illustration des VRS-Messsystems (a) und VRS-Messung eines Probanden während des Gehens (b).*
Abbildung entnommen aus Huthwelker et al. (2023).

Das Verfahren hat sich in den letzten Jahrzehnten zunehmend klinisch etabliert (Applebaum et al., 2020, Betsch et al., 2015) und kann auch unter dynamischen Bedingungen im Rahmen von laufbandgestützten Ganganalysen, zur Untersuchung der Wirbelsäulenbewegung herangezogen werden (Betsch et al., 2013, Betsch et al., 2015) (Abbildung 1b). Hier wurde bereits die Genauigkeit der Markererkennung (Betsch et al., 2013), als auch die Reproduzierbarkeit der Messergebnisse im Gang (Gipsman et al., 2014) mit positivem Ergebnis untersucht.

Um klinisch und wissenschaftlich generierte Messergebnisse in einem funktionellen Kontext interpretieren und geeignete Behandlungsempfehlungen daraus ableiten zu können, fehlt es in der Literatur aber noch an ausreichend geeigneten Referenzdaten. Solche sind für statische VRS-Messungen aktuell für Kinder (Furian et al., 2013)), für sehr homogene Gruppen junger Erwachsener (Schröder et al., 2011, Schröder et al., 2014, Michalik et al., 2020) oder für junge Erwachsene und Erwachsene mittleren Alters (Degenhardt et al., 2017, Degenhardt et al., 2020) verfügbar. Mögliche Unterschiede zwischen den Geschlechtern oder physiologische, altersbedingte Veränderungen der Wirbelsäule werden dabei bisher jedoch nicht ausreichend berücksichtigt.

Auch die Interpretation dynamischer, im Rahmen von Ganganalysen erhobener, VRS-Messergebnisse ist noch immer komplex. Dies liegt zum einen daran, dass das funktionelle physiologische Bewegungsverhalten der Wirbelsäule im Gang, auf Grund eines fehlenden Gold-Standards zu dessen Erfassung, generell noch nicht abschließend beschrieben ist. Hier hat die VRS, durch ihre alternative, zugrundeliegende Messmethodik, im Vergleich zu anderen markerbasierten Systemen, durchaus Potential den Erkenntnisgewinn weiter voranzutreiben. Da die Entwicklung der dynamischen VRS im Verhältnis jedoch noch relativ neu ist (Betsch et al., 2013), stehen bisher nur wenige Referenzdaten für vereinzelte Wirbelsäulenparameter im Gang zur Verfügung (Michalik et al., 2020).

An diese Lücken knüpft das vorliegende Dissertationsprojekt an, mit dem Ziel entsprechend systematische Referenzdaten sowohl für statische, als auch für dynamische VRS-Messergebnisse, in zeitlicher Relation zum Gangzyklus, zur Verfügung zu stellen. Dafür wurden nach erfolgreicher Freigabe durch die Ethikkommission der Landesärztekammer Rheinland-Pfalz (Bearbeitungsnummer: 837.194.16 (10513)) und der Registrierung im Deutschen Register Klinischer Studien (INT: DRKS00010834), 201 gesunde Probanden im Alter von 18-70 Jahren rekrutiert. Als Einschlusskriterien wurde eine adäquate Gangsicherheit (ermittelt durch den Timed-up-and-Go Test (Bischoff et al., 2003)), eine alters- und geschlechtsentsprechende Gehgeschwindigkeit (ermittelt durch den 2-Minuten Gehtest (Bohannon et al., 2015)), eine physiologische Wirbelsäulenfunktion (ermittelt durch die Back Performance Scale (Myklebust et al., 2007)), sowie eine für das physiologische Gehen

erforderliche, aktive Gelenkbeweglichkeit der großen Gelenke (Perry und Burnfield, 2010) vorausgesetzt. Gleichzeitig wurden Probanden von der Studienteilnahme ausgeschlossen, die bereits eine Operation oder Fraktur im Messbereich (vom siebten Halswirbelkörper (C7) bis zum Becken) erlitten hatten, oder die in den letzten 12 Monaten vor der Datenerhebung auf Grund von Schmerzen oder Funktionsstörungen im Messbereich (C7 bis zum Becken), bzw. in den letzten 6 Monaten vor der Datenerhebung auf Grund von Schmerzen oder Funktionsstörungen am restlichen muskuloskeletalen System, einen Arzt oder Therapeuten aufsuchen mussten.

Die Datenerhebung erfolgte mit dem DIERS “4D motion® Lab” (bestehend aus dem formetric III 4D; dem leg axis, dem leg axis lateral und dem pedogait System (einer laufbandintegrierten kapazitiven Fußdruckmessplatte)), sowie der zugehörigen DICAM 3 Software (Software Version 3.7.1.7). Alle 201 Probanden wurden einmal im Stand und anschließend in randomisierter Reihenfolge bei 2 km/h, 3 km/h, 4 km/h und 5 km/h während des Gehens auf einem Laufband vermessen und einer von drei Alterskohorten („jung“: 18-30 Jahre; „mittel“: 31-50 Jahre; „alt“: 51-70 Jahre), mit jeweils 67 Probanden und einem Geschlechterverhältnis von 2:1 (44 weiblich; 23 männlich) zugeteilt (Tabelle 1).

Tabelle 1 *Probandencharakteristika.*
Tabelle adaptiert und übersetzt aus Huthwelker et al. (2022).

		Alle Probanden	**Geschlecht**		**Alterskohorte “jung”**		
			Alle Frauen	Alle Männer	Alle „jungen“ Probanden	„junge“ Frauen	„junge“ Männer
N		201	132	69	67	44	23
Alter (Jahre)	**Mittelwert**	**41,3**	**41,3**	**41,3**	**25,9**	**26,0**	**25,6**
	Standard Abweichung	13,4	13,0	14,3	2,9	2,7	3,3
BMI (kg/m²)	**Mittelwert**	**23,5**	**22,9**	**24,6**	**22,7**	**22,0**	**23,9**
	Standard Abweichung	2,8	2,8	2,4	2,9	2,9	2,6
		Alterskohorte “mittel”			**Alterskohorte “alt”**		
		Alle „mittleren“ Probanden	„mittlere“ Frauen	„mittlere“ Männer	Alle „alten“ Probanden	„alte“ Frauen	„alte“ Männer
N		67	44	23	67	44	23
Alter (Jahre)	**Mittelwert**	**41,4**	**42,2**	**39,8**	**56,6**	**55,7**	**58,3**
	Standard Abweichung	6,4	6,5	6,2	4,3	3,9	4,5
BMI (kg/m²)	**Mittelwert**	**23,7**	**23,0**	**25,0**	**24,1**	**23,6**	**25,0**
	Standard Abweichung	2,8	2,8	2,3	2,5	2,5	2,2

Da in der damaligen Standardversion des Messsystems keine Möglichkeit bestand, die dynamischen Wirbelsäulendaten in zeitlicher Relation zum Gangzyklus als Rohdaten zu exportieren, konnte die Arbeitsgruppe des MotionLab gemeinsam mit dem Hersteller, im

Rahmen eines vorgelagerten Entwicklungsprozesses, erfolgreich eine entsprechende Softwareschnittstelle erarbeiten und so die wissenschaftliche Nutzbarkeit des Systems weiter verbessern. In der nachfolgenden Datenauswertung war es dadurch möglich, neben den klinisch etablierten und bei VRS-Messungen üblicherweise verwendeten „globalen Wirbelsäulenparametern“ (z.B. „thorakale Kyphose“, „lumbale Lordose“, „Seitabweichung“, „Oberflächenrotation“ etc.), auch „spezifische Wirbelsäulenparameter“ auszuwerten und in Form von Referenzdaten sowohl für klinische, als auch für Forschungszwecke zu präsentieren. Die spezifischen Parameter beschreiben in diesem Zusammenhang die isolierten Positions- bzw. Bewegungsdaten jedes einzelnen Wirbelkörpers (von C7 bis zum vierten Lendenwirbelkörper (L4)) in allen drei Bewegungsrichtungen, sowohl im Stand, als auch während des Gehens auf einem Laufband in zeitlicher Relation zum Gangzyklus. Hierfür war im Vorfeld die Aufbereitung der exportierten Rohdaten erforderlich.

Für die Standmessungen, welche im Messprogramm „4D average“ (12 automatische Serienmessungen innerhalb von 6 Sekunden) erhoben wurden, beinhaltete diese Aufbereitung zunächst eine Zusammenfassung der 12 vorhandenen Einzelmessungen, zu einem gemittelten Wert pro Proband und pro exportiertem Parameter. Mit Hilfe deskriptiver Statistik wurden diese gemittelten Werte anschließend über alle Teilnehmer der entsprechenden Subgruppen als „Mittelwert der Mittelwerte“ mit ihren zugehörigen Standardabweichungen dargestellt. Unter Anwendung explorativer statistischer Verfahren konnte außerdem auf mögliche Unterschiede zwischen den analysierten Subgruppen (zweifaktorielle Varianzanalyse), sowie auf signifikante Abweichungen der Haltung von der Nulllinie (Wilcoxon Test) getestet werden.

Für die Beschreibung der dynamischen Messergebnisse wurden pro Proband die Wirbelsäulendaten von drei aufeinanderfolgenden Gangzyklen (beginnend mit dem rechten Referenzbein) aus der Software exportiert. Um verschiedene Messparameter zwischen den Probanden miteinander vergleichbar zu machen, war mit Hilfe einer interpolierenden Splinefunktion die Überführung der Rohdaten in einen geglätteten standardisierten Gangzyklus (SGZ) erforderlich. Die hierfür eigens entwickelten Software-Skripte wurden öffentlich zugänglich gemacht (Konradi, 2022d, Konradi, 2022b, Konradi, 2022a, Konradi, 2022c, Schmidtmann und Konradi, 2022, Westphal und Konradi, 2022). Mit Hilfe deskriptiver statistischer Verfahren wurden die mittleren Kurvenverläufe der gesamten Probandengruppe (n=201), für alle spezifischen Wirbelsäulenparameter (C7-L4) und das Becken, umrahmt von ihren jeweiligen 2,5 und 97,5 Perzentilkurven dargestellt. Die individuellen links- und rechtsseitigen Rotationsmaxima der einzelnen Probanden wurden mit Hilfe von Vorhersageellipsen und in Relation zu ihrem zeitlichen Auftreten im SGZ präsentiert. Außerdem wurde das auf VRS-Messungen basierende, Bewegungsverhalten der Wirbelsäule

in Relation zum bisherigen funktionellen Verständnis der rotatorischen Wirbelsäulenbewegung im Gang analysiert.

Nach der statistischen Aufbereitung, erfolgte die Veröffentlichung der ersten Teil-Ergebnisse dieses umfangreichen Referenzdatensatzes in zwei internationalen Publikationen (Huthwelker et al., 2022, Huthwelker et al., 2023), welche nachfolgend zusammengefasst werden:

Der erste Artikel "**Reference Values for 3D Spinal Posture Based on Videorasterstereographic Analyses of Healthy Adults**" wurde am 15. Dezember 2022 im MDPI Journal "Bioengineering" veröffentlicht (Impact Faktor 2022: 4,6; Habilitationswert 2022: B). In dieser Arbeit wurden Referenzdaten sowohl für globale als auch für spezifische Wirbelsäulenparameter im Stand in allen drei Bewegungsebenen und in Abhängigkeit des Geschlechts und des Alters der Probanden beschrieben. Die Ergebnisse der globalen Parameter waren dabei annähernd vergleichbar mit denen früherer VRS-Studien (Schröder et al., 2011, Schröder et al., 2014, Michalik et al., 2020, Degenhardt et al., 2020, Degenhardt et al., 2017) und zeigten zusätzlich funktionelle Übereinstimmungen mit Ergebnissen anderer klinischer Untersuchungsverfahren (Arshad et al., 2019, Zappalá et al., 2021). So wiesen bspw. Frauen in der vorliegenden Studie, ähnlich wie in der Literatur bereits beschrieben (Arshad et al., 2019), eine stärkere Lordoseausprägung auf als Männer und bei älteren Probanden zeigte sich im Vergleich zu jüngeren eine stärkere thorakale Kyphose, ähnlich den Ergebnissen von Zappalá et al. (2021), basierend auf radiologischen Cobb-Winkel Berechnungen.

Auch die Auswertung der spezifischen Wirbelsäulenparameter, also die Beschreibung der dreidimensionalen Positionsdaten jedes einzelnen Wirbelkörpers, deuteten auf funktionelle Übereinstimmungen mit radiologischen Messverfahren hin (Janssen et al., 2009, Kouwenhoven et al., 2006). In der Sagittalebene wurde bspw. deutlich, dass Frauen, ähnlich den Ergebnissen von Janssen et al. (2009), in der durchgeführten VRS-Studie, stärker in Extension (bzw. weniger stark in Flexion) positionierte Wirbelkörper aufwiesen als Männer. Gleichzeitig zeigten sich, besonders in der Transversalebene, sehr systematische Asymmetrien und somit Abweichungen von der erwarteten Rotationsnullstellung der Wirbelsäule im aufrechten Stand (Abbildung 2). Auch diese Ergebnisse wurden bereits, basierend auf CT und MRT Untersuchungen, beschrieben (Kouwenhoven et al., 2006) und konnten zumindest teilweise durch die Organanatomie begründet werden (Kouwenhoven et al., 2007).

In Verbindung mit dem hohen Maß an Individualität der erhobenen Haltungsdaten, welches durch die großen Standardabweichungen der Daten für die einzelnen Parameter deutlich

wurde, bleibt die Frage zu diskutieren, ob therapeutische Interventionen immer auf eine möglichst symmetrische, aufrechte Haltung abzielen (Wolf et al., 2021) und inwieweit die persönlichen Haltungsvoraussetzungen eines Individuums noch stärker bei der Ergebnisinterpretation berücksichtigt werden sollten.

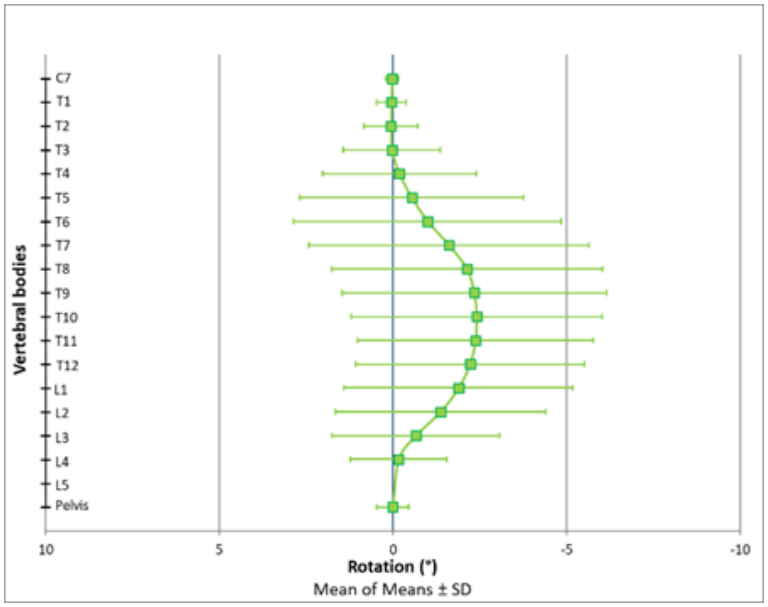

Abbildung 2 *Rotationsstellung der analysierten spezifischen Wirbelsäulenparameter (Wirbelkörper C7-L4 und des Beckens) im Stand.*
Positive Werte bedeuten eine Rotation des Wirbelkörpers nach links (gegen den Uhrzeigersinn), negative Werte bedeuten eine Rotation des Wirbelkörpers nach rechts (im Uhrzeigersinn). Aufgrund der besseren Interpretierbarkeit wurden die Werte auf der X-Achse angepasst.
Abbildung entnommen aus Huthwelker et al. (2022).

Zusammenfassend konnte der erste Artikel die bestehenden Referenzdatensets im Bereich der globalen Wirbelsäulenparameter, um eine systematische Auswertung nach Geschlecht und Alter ergänzen und zusätzlich um die präsentierten spezifischen Wirbelsäulenparameter erweitern, welche eine systematische Asymmetrie der Wirbelsäule insbesondere in der Transversalebene offenbarten. Neben der Vergleichbarkeit mit den Ergebnissen vorangegangener VRS Studien, zeigte sich dabei eine hohe funktionelle Übereinstimmung der Messergebnisse mit denen etablierter klinischer Untersuchungsverfahren. Dies deutet darauf hin, dass sich die VRS, durch ihre nicht-invasive Messmethodik, besonders für die Beantwortung funktioneller klinischer Fragestellungen und die Evaluierung intraindividueller Therapieeffekte eignet.

Der zweite Artikel “**Reference values and functional descriptions of transverse plane spinal dynamics during gait based on surface topography**” wurde am 06. Januar 2023 im Elsevier Journal “Human Movement Science” publiziert (Impact Faktor 2022: 2,1;

Habilitationswert 2022: C). In dieser Arbeit wurde das rotatorische Bewegungsverhalten der einzelnen gemessenen Wirbelkörper (von C7-L4) und des Beckens in der Transversalebene, bei einer Gehgeschwindigkeit von 5 km/h beschrieben. Die Ergebnisse offenbarten ebenfalls hochindividuelle spinale Bewegungsmuster, was sich deutlich anhand der breiten Abstände der ermittelten Perzentilkurven, sowie der großen Flächen der beschriebenen Vorhersageellipsen ableiten ließ. Demgegenüber steht, ähnlich wie im Stand, ein überraschend systematisches, rotatorisches Bewegungsverhalten der Wirbelsäule, wenn die gemittelten Ergebnisse aller 201 Probanden betrachtet werden (Abbildung 3).

Das sich hieraus ergebende Bewegungsmuster, weicht dabei deutlich vom bisherigen funktionellen Verständnis der Wirbelsäulenbewegung im Gang ab und stellt dieses in Frage. Bisher wurde die Brustwirbelsäule als dynamisch stabilisiert im Gang beschrieben, mit einem frontotransversalen Thoraxdurchmesser der rechtwinklig zur Fortbewegungsebene steht (Suppé und Bongarz, 2013). Auf Höhe der mittleren Brustwirbelsäule wurde ein annähernd statischer „Umkehrpunkt“ vermutet, um den herum sich die funktionelle Verschraubung der Wirbelsäule zwischen dem Becken und dem Schultergürtel während der aufrechten Fortbewegung vollzieht (Gregersen und Lucas, 1967). Im Gegensatz dazu, zeigten die Wirbelkörper der mittleren Brustwirbelsäule bei videorasterstereographischen Messungen jedoch den größten rotatorischen Bewegungsausschlag der, ebenso wie im Stand, eine leicht rechtsseitige verschobene Asymmetrie aufwies (Abbildung 3).

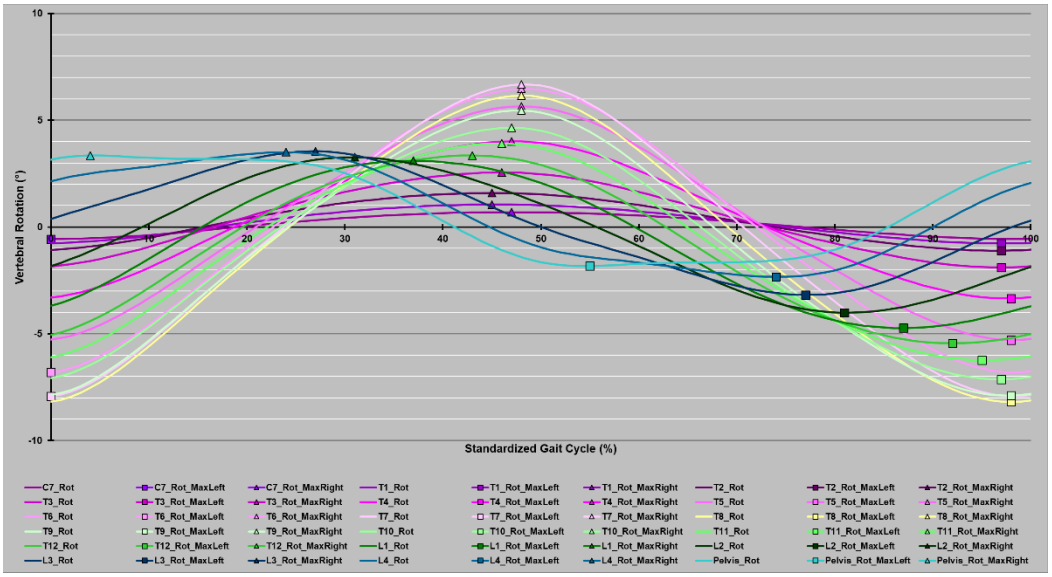

Abbildung 3 *Rotationskurven der analysierten spezifischen Wirbelsäulenparameter (Wirbelkörper C7-L4 und des Beckens) innerhalb des SGZ bei einer Gehgeschwindigkeit von 5 km/h.*
Positive Werte bedeuten eine Rotation des Wirbelkörpers nach links (gegen den Uhrzeigersinn), negative Werte bedeuten eine Rotation des Wirbelkörpers nach rechts (im Uhrzeigersinn). Die jeweiligen Rotationsmaxima nach links Δ und rechts □ sind markiert.
Abbildung entnommen aus Huthwelker et al. (2023).

Darüber hinaus wurde deutlich, dass die gemessene Rotationsbewegung vom Becken eingeleitet wurde. Alle darüber liegenden Wirbelkörper folgten dieser Bewegung nacheinander von kaudal nach kranial, wodurch sich ein dynamischer „Umkehrpunkt“ in der rotatorischen Wirbelsäulenbewegung offenbarte, der in zwei Schwingungen systematisch von kaudal nach kranial verlief und so der vom Becken eingeleiteten Bewegung folgte (Abbildung 4).

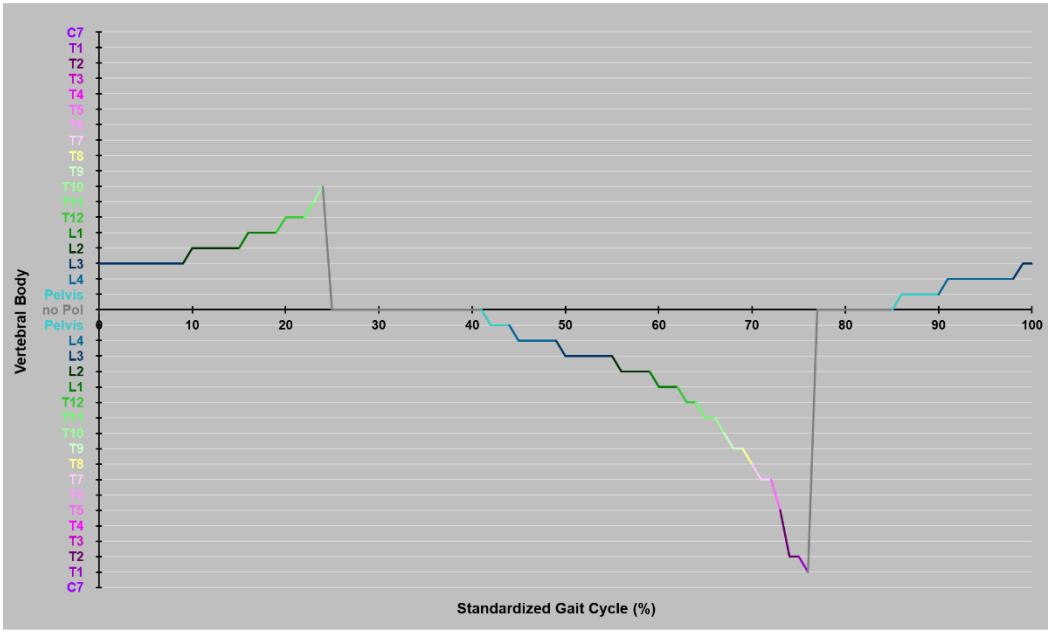

Abbildung 4 *Verlauf des rotatorischen „Umkehrpunktes“ (Point of Intersection) innerhalb des SGZ. Abbildung entnommen aus Huthwelker et al. (2023).*

Die beiden publizierten Arbeiten stellen den Auftakt einer geplanten Publikationsserie dar, in der umfassende VRS-Referenzdaten sowohl für den Stand, als auch für die vier erhobenen Gehgeschwindigkeiten (bei 2 km/h, 3 km/h, 4 km/h und 5 km/h) präsentiert werden sollen. Die vorliegenden Teilergebnisse können dabei bereits jetzt, sowohl für klinische, als auch für wissenschaftliche Anwender desselben Messsystems, von großer praktischer Bedeutung sein, da sie eine erste Orientierung und Einordnung erhobener individueller Messergebnisse in Relation zu einer entsprechend gesunden Alters- und Geschlechtskohorte ermöglichen.

Aufgrund großer Abweichungen vom bisherigen funktionellen Verständnis, ist es jedoch erforderlich zu überprüfen, ob die bisher präsentierten Ergebnisse durch weitere Arbeitsgruppen und Labore, insbesondere auch mit anderen Messverfahren, bei einem sonst ähnlichen Studiendesign reproduzierbar sind.

2 Publikationen

2.1 Reference values for 3D spinal posture based on videorasterstereographic analyses of healthy adults

bioengineering

MDPI

Article

Reference Values for 3D Spinal Posture Based on Videorasterstereographic Analyses of Healthy Adults

Janine Huthwelker [1,*], Jürgen Konradi [1], Claudia Wolf [1], Ruben Westphal [2], Irene Schmidtmann [2], Philipp Drees [3] and Ulrich Betz [1]

[1] Institute of Physical Therapy, Prevention and Rehabilitation, University Medical Center of the Johannes Gutenberg University Mainz, Langenbeckstraße 1, D-55131 Mainz, Germany
[2] Institute of Medical Biostatistics, Epidemiology and Informatics, University Medical Center of the Johannes Gutenberg University Mainz, Obere Zahlbacher Straße 69, D-55131 Mainz, Germany
[3] Department of Orthopedics and Trauma Surgery, University Medical Center of the Johannes Gutenberg University Mainz, Langenbeckstraße 1, D-55131 Mainz, Germany
* Correspondence: janine.huthwelker@unimedizin-mainz.de

Abstract: Visual examinations are commonly used to analyze spinal posture. Even though they are simple and fast, their interrater reliability is poor. Suitable alternatives should be objective, non-invasive, valid and reliable. Videorasterstereography (VRS) is a corresponding method that is increasingly becoming established. However, there is a lack of reference data based on adequate numbers of participants and structured subgroup analyses according to sex and age. We used VRS to capture the spinal posture of 201 healthy participants (aged 18–70 years) divided into three age cohorts. Three-dimensional reference data are presented for the global spine parameters and for every vertebral body individually (C7-L4) (here called the specific spine parameters). The vertebral column was found to be systematically asymmetric in the transverse and the coronal planes. Graphical presentations of the vertebral body posture revealed systematic differences between the subgroups; however, large standard deviations meant that these differences were not significant. In contrast, several global parameters (e.g., thoracic kyphosis and lumbar lordosis) indicated differences between the analyzed subgroups. The findings confirm the importance of presenting reference data not only according to sex but also according to age in order to map physiological posture changes over the life span. The question also arises as to whether therapeutic approximations to an almost symmetrical spine are biomechanically desirable.

Keywords: surface topography; rasterstereographic back shape analysis; normative data; healthy adults; posture analysis; spine

Citation: Huthwelker, J.; Konradi, J.; Wolf, C.; Westphal, R.; Schmidtmann, I.; Drees, P.; Betz, U. Reference Values for 3D Spinal Posture Based on Videorasterstereographic Analyses of Healthy Adults. *Bioengineering* **2022**, *9*, 809. https://doi.org/10.3390/bioengineering9120809

Academic Editors: Christina Zong-Hao Ma, Zhengrong Li, Chen He and Aurélien Courvoisier

Received: 14 November 2022
Accepted: 12 December 2022
Published: 15 December 2022

1. Introduction

The spine connects the pelvis and the head with 24 vertebral bodies that can move against each other in three directions of movement. It stabilizes the torso and enables verticalization. The posture and movements of the spine are individually varied and highly characteristic of each person [1]. Visual inspection and posture analyses are important aspects of the basic examination of patients affected by spinal disorders [2]. Many musculoskeletal examiners have reported that visual estimations are one of their most commonly used assessment tools when analyzing spinal posture in clinical practice [3]. Although these visual assessments are simple and quick to perform, their results are relatively subjective, and their interrater reliability is statistically poor [3,4]. This becomes problematic when the results contribute to the clinical decision making process or are used in follow-up examinations to assess the progress and outcomes of the initiated therapies [5]. In order to address this problem, the collection of data regarding spinal posture should be objective and standardized using valid, reliable and reproducible measurement approaches. It is crucial for the assessments to be non-invasive for the patient and quick and easy to conduct

in daily clinical routines. Videorasterstereography (VRS) seems to be a corresponding method that is increasingly becoming established in clinical practice [6–8].

The VRS system is based on a horizontal light line pattern projected onto the patient's unclothed back and creates a virtual plaster cast of the individual back surface within only a few seconds [7]. In addition to information about the surface topographic curvature picture, the system is able to precisely estimate the position of every vertebral body (from C7 to L4) and the pelvis in a virtually constructed three-dimensional model of the human vertebral column [7,9–12]. VRS has evolved since its initial development in the 1980s and has been described in various publications [6,7,13]. The system has been proven to be valid and highly reliable compared to the clinical gold standard (X-ray imaging) [8,14–17].

In order to implement VRS for spinal posture analysis as a routine assessment in clinical practice, it is essential to have systematic reference data available for comparison with the potential pathological findings. Unfortunately, the current datasets are only conditionally able to fulfill these requirements, as they have several limitations.

Thus far, there are reference data for the global spine parameters of children [18], young adults [19–21] and young and middle-aged adults [22,23]. Either relatively heterogeneous study cohorts with very small numbers of participants have been analyzed without any further subgroup specifications [22,23], or subgroup-analyses have focused only on the potential differences between female and male participants in young, relatively homogenous study cohorts [19–21]. Possible changes in physiologic spinal posture according to sex and/or age over the adult life span have not yet been investigated. This knowledge, however, is essential for the consultation of reference data in clinical practice, in which not only young but also older patients are examined using VRS measurement devices.

In order to close this gap in our knowledge, the first aim of the current study was to provide practitioners and researchers with an additional set of VRS reference data that, firstly, included a preferably high number of healthy participants. Secondly, structured subgroup analyses were used depict possible physiologic changes in the spinal posture parameters according to sex and age over an adult life span of 18 to 70 years.

The second aim of this study was to provide the respective reference data for specific spine parameters: the isolated position of each vertebral body from C7 to L4 in all three dimensions of movement. These data are currently missing from the literature. As of up to a few years ago, only global spine parameters such as the thoracic kyphosis and lumbar lordosis angles were exportable from the DICAM 3 software. Meanwhile, the three-dimensional position of each vertebral body can be analyzed using an additional export interface.

In contrast to the work previously published by our own research group, describing a subgroup analysis of 100 asymptomatic females based on the dataset included here [24], this project involved a more differentiated analysis providing reference data for three different age cohorts (18–30 years, 31–50 years and 51–70 years) and for both sexes, respectively.

2. Materials and Methods

The data analyzed in this work were part of a prospective, explorative, cross-sectional and monocentric study assessing the three-dimensional spinal posture and movement behavior of healthy participants in the upright standing position and at four different walking speeds (2 km/h, 3 km/h, 4 km/h and 5 km/h). Ethical approval was obtained from the responsible ethics committee of the Rhineland-Palatinate Medical Association, and the study is registered with the World Health Organization (WHO) (INT: DRKS00010834). Based on a statistical sample size calculation, 201 healthy participants (sex ratio of 2/3 females to 1/3 males, aged 18–70 years) who gave their informed consent prior to participation were included in three different age cohorts (young (18–30 years), middle (31–50 years) and old (51–70 years)).

2.1. Participants

In order to participate, the volunteers had to be free of pain, and due to data capture requirements, their body mass index (BMI) had to be $\leq$30.0 kg/m^2. All the participants had to demonstrate adequate gait stability (timed up-and-go test [25]), an age- and sex-accorded walking speed (two-minute walk test [26]) and spinal function (back performance scale [27]), as well as an appropriate joint mobility in order, theoretically, to be able to perform a physiological gait pattern [28]. Interested volunteers were excluded from participation in cases where they reported a history of surgery or fracture between the spinal segments of C7 and the pelvis. Further exclusion criteria were medical or therapeutic treatments due to spinal or pelvic girdle complaints (C7-pelvis) within the last 12 months or medical or therapeutic treatments due to musculoskeletal problems (musculoskeletal system except for C7-pelvis) within the last six months prior to the investigation.

2.2. Experimental Setup and Data Capture

In the study, "4D average" posture analyses were performed on all the participants using the DIERS Formetric III 4D measuring device (software versions DICAM v3.7.1.7 (DIERS International GmbH, Schlangenbad, Germany) for the data collection and DICAM v3.5.0Beta11 (DIERS International GmbH, Schlangenbad, Germany) for the data export), a VRS system based on the principle of triangulation [13]. A slide projector, used as the optical equivalent to an inverse camera, projects horizontal and parallel light lines onto the unclothed back of the participant, who is standing upright on a treadmill (height: ~18 cm) at a predefined distance from the measuring device (~2 m), with the eyes looking towards a standardized point ~2 m away and 20 cm below the individual's body height (measured from the ground). Twelve series recordings of the transformed line pattern (due to back surface curvatures) were captured for a period of 6 s with an associated camera system. The three-dimensional scatter plot derived (consisting of up to 150,000 individual data points, depending on the body size) was used to create a virtual plaster cast of the surface of the participant's back. The three-dimensional position of the underlying spine and the pelvis was estimated based on this information in combination with a clinically validated correlational model [11–13].

Even though it is technically not required for static VRS posture analyses, all the participants were marked with seven reflective markers prior to the data capture (on the spinal process of C7, the spinous processes between the medial parts of the spinae scapulae (~T3) and the thoracolumbar transitions (~T12), the left and right posterior superior iliac spine (PSIS) and on both acromia). This was necessary because the superior study protocol meant that the data for the dynamic gait analyses were also captured on the same measurement appointment. In order to best control for potential palpation or measurement bias, however, the same investigator (physical therapist) always performed the complete procedure themselves, including the entrance examinations (checking for inclusion and exclusion criteria), palpation, marker attachments and the VRS measurements, following a strict and standardized protocol. A static control scan was also performed to check for the correct placement of the markers. Where there were clinically inconclusive measurement results or any uncertainty on the part of the investigator, the placement of the markers was checked, palpated again, and corrected, if necessary, until the final marker position was defined. The measurements were repeated if the first graphical data output revealed clinically incomprehensible, inconsistent measuring artefacts or apparent software misinterpretations. For reasons of quality assurance, the investigator and an additional technician, who were both highly familiar with the software and the measuring device, further inspected all the pictures and the graphical data output visually after completion of the data collection phase for further abnormal spinal representations or other measuring artefacts and corrected them if necessary. In total, 46 specific and 14 global spine parameters were exported using the export interface of the DICAM v3.5.0Beta11 software. The Statistical Analysis System (SAS version 9.4) was used to combine all the exported

files into one editable sheet of raw data. Figure 1 provides a schematic flow chart of the experimental process.

Figure 1. Schematic flow chart of the experimental process.

2.3. Data Analysis

The "4D average" measurement approach used meant that 12 individual values per participant were exported for every spine parameter. Several clinically inconclusive extreme values and, for one participant, isolated missing data points were identified in a preliminary visual data review. The Statistical Package of the Social Sciences (IBM SPSS Statistics for Windows, Version 23.0. Armonk, NY, USA: IBM Corp.) was used to systematically identify these values for every analyzed parameter, and all the extreme outliers revealed by the stem-and-leaf plot were removed from the raw dataset. The missing values were treated as extreme outliers, and the respective cells were removed from the raw dataset as well. The remaining values for every parameter were aggregated to finally create one mean value for every participant and for every parameter of interest.

Descriptive statistics were used to describe the reference values for all the specific (C7–L4 and the pelvis) and global spine parameters according to the mean of means (MoM) and the standard deviation (SD) in all three dimensions for the entire group, for all the female and all the male participants, and for the female and male participants within the three different age cohorts, respectively. An explorative two-way analysis of variance (two-way ANOVA) was used to check for possible differences between the groups according to sex, age cohort or a combination of both (level of significance $p < 0.05$). Possible deviations from the symmetrical zero positions of the different spine parameters were checked by one-sample Wilcoxon signed rank tests (level of significance $p < 0.05$). Graphical figures were created using Microsoft Excel (Microsoft Corporation, Version 2016. Redmond, WA, USA).

The authors do not include a detailed definition or description of the analyzed global and specific spine parameters. Instead, the reader is referred to the respective previous publications [19,24].

3. Results

3.1. Participants

A total of 201 healthy participants (132 females and 69 males) were included in the data analyses and were subdivided into three different age cohorts (67 participants per group). Their detailed characteristics, according to age and BMI, are presented in Table 1.

3.2. Data Analysis

The spinal posture data were analyzed using descriptive and explorative statistics. Reference values for the specific and global spine parameters are presented in Table 2 for the transversal plane, in Table 3 for the coronal plane and in Table 4 for the sagittal plane. Figure 2 (transversal), Figure 3 (coronal) and Figure 4 (sagittal) are the respective graphical representations of the specific spine parameters for those three investigated planes. The results of the explorative statistical analyses are presented in Table 5.

Table 1. Participant characteristics.

		All Participants	Sex		Age Cohort "Young"			Age Cohort "Middle"			Age Cohort "Old"		
			All Females	All Males	All Young Participants	Young Females	Young Males	All Middle Participants	Middle Females	Middle Males	All Old Participants	Old Females	Old Males
N		201	132	69	67	44	23	67	44	23	67	44	23
Age (years)	Mean	41.3	41.3	41.3	25.9	26.0	25.6	41.4	42.2	39.8	56.6	55.7	58.3
	SD	13.4	13.0	14.3	2.9	2.7	3.3	6.4	6.5	6.2	4.3	3.9	4.5
BMI (kg/m²)	Mean	23.5	22.9	24.6	22.7	22.0	23.9	23.7	23.0	25.0	24.1	23.6	25.0
	SD	2.8	2.8	2.4	2.9	2.9	2.6	2.8	2.8	2.3	2.5	2.5	2.2

Table 2. Results of the descriptive statistical analyses (MoM ± SD) of the spinal parameters in the transversal plane.

			Specific Parameters																			Global Parameters			
			Sh (°)	C7 (°)	T1 (°)	T2 (°)	T3 (°)	T4 (°)	T5 (°)	T6 (°)	T7 (°)	T8 (°)	T9 (°)	T10 (°)	T11 (°)	T12 (°)	L1 (°)	L2 (°)	L3 (°)	L4 (°)	Pel (°)	Surface Rotation RMS (°)	Surface Rotation MAX (°)	(Right Side) Surface Rotation +Max (°)	(Left Side) Surface Rotation −Max (°)
	All Participants	N	198	199	201	200	200	197	197	198	198	198	200	201	201	201	201	200	200	200	200	200	201	198	201
		MoM	−0.3	0.0	0.0	0.1	0.0	−0.2	−0.5	−1.0	−1.6	−2.1	−2.3	−2.4	−2.4	−2.2	−1.9	−1.4	−0.7	−0.2	0.0	2.3	−1.9	1.5	−3.3
		SD	2.0	0.2	0.4	0.8	1.4	2.2	3.2	3.9	4.0	3.9	3.8	3.6	3.4	3.3	3.3	3.0	2.4	1.4	0.5	0.9	4..0	1.4	2.3
Sex	All Females	N	130	131	132	131	131	129	129	130	130	130	131	132	132	132	132	131	131	131	132	131	132	130	132
		MoM	−0.3	0.0	0.1	0.1	0.1	−0.1	−0.4	−0.8	−1.4	−1.9	−2.2	−2.2	−2.1	−2.0	−1.7	−1.2	−0.6	−0.1	0.0	2.2	−1.8	1.5	−3.2
		SD	2.0	0.2	0.4	0.7	1.3	2.0	3.0	3.6	3.8	3.7	3.7	3.6	3.5	3.5	3.6	3.3	2.6	1.4	0.5	0.9	4.0	1.4	2.3
	All Males	N	68	68	69	69	69	68	68	68	68	68	69	69	69	69	69	69	69	69	68	69	69	68	69
		MoM	−0.3	0.0	0.0	0.0	−0.1	−0.4	−0.8	−1.4	−2.1	−2.6	−2.7	−2.8	−2.8	−2.6	−2.3	−1.6	−0.9	−0.2	0.1	2.3	−2.1	1.7	−3.6
		SD	2.0	0.2	0.5	0.9	1.6	2.5	3.6	4.3	4.4	4.2	4.1	3.6	3.2	2.8	2.7	2.5	2.1	1.3	0.4	0.9	4.0	1.4	2.3
Age Cohort "Young"	All Young Participants	N	67	67	67	67	67	67	67	67	67	66	66	67	67	67	67	66	66	66	67	67	67	66	67
		MoM	−0.1	0.0	0.0	−0.1	−0.2	−0.5	−1.0	−1.5	−2.1	−2.7	−2.9	−2.7	−2.7	−2.5	−2.1	−1.5	−0.6	0.0	0.1	2.3	−2.3	1.4	−3.5
		SD	2.1	0.2	0.4	0.7	1.3	2.1	3.1	3.7	3.9	3.6	3.4	3.4	3.1	3.1	3.2	2.9	2.3	1.3	0.5	0.9	3.6	1.2	2.2
	Young Females	N	44	44	44	44	44	44	44	44	44	43	43	44	44	44	44	43	43	43	44	44	44	43	44
		MoM	0.1	0.0	0.0	0.0	−0.2	−0.4	−0.9	−1.5	−2.0	−2.6	−2.8	−2.5	−2.4	−2.3	−1.9	−1.4	−0.5	0.0	0.0	2.4	−2.4	1.3	−3.5
		SD	2.0	0.2	0.4	0.7	1.3	2.1	3.1	3.7	3.9	3.4	3.3	3.4	3.2	3.3	3.6	3.2	2.5	1.4	0.5	0.9	3.8	1.3	2.3
	Young Males	N	23	23	23	23	23	23	23	23	23	23	23	23	23	23	23	23	23	23	23	23	23	23	23
		MoM	−0.4	0.0	0.0	−0.1	−0.3	−0.6	−1.1	−1.7	−2.3	−2.8	−3.0	−3.0	−3.2	−3.0	−2.6	−1.9	−0.9	−0.2	0.3	2.2	−2.3	1.7	−3.6
		SD	2.2	0.2	0.4	0.7	1.3	2.1	3.2	3.8	4.1	4.0	3.7	3.3	3.0	2.6	2.4	2.2	1.8	1.1	0.4	0.8	3.4	1.2	2.2
	All Middle Participants	N	66	67	67	67	67	67	67	67	67	67	67	67	67	67	67	67	67	67	67	67	67	67	67
		MoM	−0.5	0.0	0.1	0.1	0.1	0.0	−0.2	−0.6	−1.2	−1.7	−2.1	−2.3	−2.3	−2.3	−2.0	−1.5	−0.8	−0.3	−0.1	2.1	−2.3	1.4	−3.4
		SD	2.1	0.2	0.4	0.7	1.3	2.2	3.2	3.7	3.9	3.8	3.7	3.6	3.5	3.4	3.5	3.3	2.7	1.6	0.4	1.0	3.6	1.4	2.2
Age Cohort "Middle"	Middle Females	N	43	44	44	44	44	44	44	44	44	44	44	44	44	44	44	44	44	44	44	44	44	44	44
		MoM	−0.4	0.0	0.1	0.1	0.2	0.2	0.0	−0.4	−0.9	−1.4	−1.9	−2.1	−2.3	−2.2	−2.0	−1.5	−0.9	−0.4	−0.1	2.0	−2.2	1.3	−3.3
		SD	2.1	0.2	0.3	0.6	1.2	1.9	2.8	3.2	3.4	3.4	3.4	3.4	3.5	3.5	3.7	3.5	2.8	1.6	0.4	0.8	3.4	1.4	2.0
	Middle Males	N	23	23	23	23	23	23	23	23	23	23	23	23	23	23	23	23	23	23	23	23	23	23	23
		MoM	−0.6	0.0	0.0	0.0	−0.1	−0.3	−0.6	−1.1	−1.7	−2.3	−2.6	−2.6	−2.5	−2.3	−1.9	−1.3	−0.5	−0.1	−0.1	2.3	−2.4	1.5	−3.6
		SD	2.1	0.2	0.4	0.9	1.6	2.6	3.8	4.6	4.7	4.5	4.3	3.9	3.5	3.2	3.0	2.9	2.6	1.7	0.4	1.1	3.8	1.4	2.6
	All Old Participants	N	65	65	67	66	66	63	63	64	64	65	67	67	67	67	67	67	67	67	66	66	67	65	67
		MoM	−0.3	0.0	0.1	0.1	0.2	−0.1	−0.4	−0.8	−1.5	−2.0	−2.1	−2.2	−2.1	−1.9	−1.6	−1.1	−0.6	−0.2	0.1	2.3	−1.1	1.8	−3.1
		SD	2.0	0.2	0.5	0.9	1.6	2.3	3.4	4.1	4.3	4.3	4.3	3.9	3.6	3.4	3.2	2.9	2.2	1.3	0.4	0.9	4.6	1.7	2.4
Age Cohort "Old"	Old Females	N	43	43	44	43	43	41	41	42	42	43	44	44	44	44	44	44	44	44	44	44	44	43	44
		MoM	−0.6	0.0	0.1	0.2	0.3	0.1	−0.3	−0.5	−1.3	−1.7	−1.8	−1.9	−1.7	−1.5	−1.2	−0.8	−0.3	0.0	0.1	2.3	−0.9	1.8	−2.9
		SD	2.0	0.2	0.4	0.8	1.4	2.0	3.1	3.9	4.1	4.3	4.3	4.0	3.8	3.6	3.5	3.1	2.4	1.4	0.4	0.9	4.6	1.7	2.4
	Old Males	N	22	22	23	23	23	22	22	22	22	22	23	23	23	23	23	23	23	23	22	23	23	22	23
		MoM	0.3	0.1	0.0	0.1	0.1	−0.3	−0.8	−1.4	−2.1	−2.6	−2.5	−2.8	−2.8	−2.6	−2.2	−1.7	−1.2	−0.5	0.0	2.5	−1.4	1.8	−3.5
		SD	1.8	0.2	0.6	1.1	1.9	2.9	4.0	4.6	4.6	4.3	4.4	3.8	3.1	2.8	2.6	2.4	1.8	1.0	0.4	0.9	4.8	1.7	2.3

Abbreviations: MoM = mean of means; SD = standard deviation; Sh = shoulder; Pel = pelvis; N = number.

Table 3. Results of the descriptive statistical analyses (MoM ± SD) of the spinal parameters in the coronal plane.

			Specific Parameters																			Global Parameters					
			Sh (°)	C7 (°)	T1 (°)	T2 (°)	T3 (°)	T4 (°)	T5 (°)	T6 (°)	T7 (°)	T8 (°)	T9 (°)	T10 (°)	T11 (°)	T12 (°)	L1 (°)	L2 (°)	L3 (°)	L4 (°)	Pel (°)	Trunk Imbalance VP-DM (°)	Trunk Imbalance VP-DM (mm)	Apical Deviation RMS (mm)	Apical Deviation MAX (mm)	(Right Side) Apical Deviation VP-DM +Max (mm)	(Left Side) Apical Deviation VP-DM Max (mm)
	All Participants	N	200	197	195	194	199	198	198	198	201	201	200	200	200	199	198	198	198	200	194	194	195	196	201	198	198
		MoM	−1.1	−1.1	−1.5	−1.7	−1.3	−0.5	0.3	1.0	1.2	1.1	0.8	0.5	0.3	0.3	0.0	−0.2	0.1	0.7	−0.1	−0.2	−1.7	3.6	−1.8	3.2	−4.9
		SD	1.3	2.1	2.3	2.6	3.1	3.0	2.6	2.1	2.0	2.2	2.1	1.9	1.9	1.9	1.6	1.7	2.4	3.1	0.8	0.8	7.3	1.7	7.1	3.0	3.3
	All Females	N	131	129	128	127	132	131	131	131	132	132	131	131	131	130	129	129	129	131	127	126	128	130	132	131	130
		MoM	−1.3	−1.2	−1.6	−1.8	−1.4	−0.7	0.1	0.8	1.1	1.1	0.8	0.5	0.3	0.3	0.1	−0.1	0.3	1.0	−0.1	−0.2	−1.6	3.5	−2.3	2.9	−4.9
		SD	1.4	2.2	2.3	2.5	3.1	3.0	2.5	1.9	1.9	2.1	2.0	1.9	2.0	2.0	1.7	1.8	2.5	3.2	0.8	0.9	7.7	1.7	6.7	2.8	3.3
Sex	All Males	N	69	68	67	67	67	67	67	67	69	69	69	69	69	69	69	69	69	69	67	68	67	66	69	67	68
		MoM	−0.9	−1.0	−1.3	−1.3	−1.1	−0.3	0.6	1.2	1.4	1.2	0.8	0.5	0.4	0.2	−0.1	−0.4	−0.3	0.2	−0.3	−0.2	−2.0	3.8	−0.8	3.8	−4.7
		SD	1.3	2.1	2.3	2.8	3.1	3.2	2.8	2.3	2.3	2.4	2.3	2.0	1.8	1.8	1.5	1.5	2.2	2.8	0.8	0.8	6.6	1.6	7.7	3.4	3.2
	All Young Participants	N	67	66	66	66	67	66	66	66	67	67	67	67	67	67	67	67	66	66	64	66	66	65	67	66	66
		MoM	−1.0	−0.9	−1.2	−1.3	−0.6	0.2	0.9	1.2	1.0	0.7	0.5	0.4	0.4	0.4	0.0	−0.3	0.4	1.2	−0.1	−0.3	−2.5	3.5	−0.9	3.3	−4.4
		SD	1.2	1.7	2.0	2.4	2.8	2.7	2.4	1.9	1.8	1.9	1.9	2.0	2.0	1.9	1.6	1.8	2.6	3.0	0.9	0.8	6.5	1.6	7.0	2.9	3.1
Age Cohort "Young"	YoungFemales	N	44	43	43	43	44	43	43	43	44	44	44	44	44	44	44	44	43	43	42	43	43	42	44	43	43
		MoM	−1.1	−1.1	−1.4	−1.4	−0.6	0.4	0.9	1.1	0.9	0.7	0.5	0.4	0.5	0.4	0.1	−0.1	0.6	1.5	−0.1	−0.3	−2.6	3.4	−1.1	3.1	−4.4
		SD	1.3	1.7	2.0	2.5	3.0	2.7	2.2	1.7	1.7	1.8	1.7	1.9	2.1	2.0	1.5	1.9	2.7	3.2	0.9	0.8	6.7	1.6	7.2	2.7	3.1
	Young Males	N	23	23	23	23	23	23	23	23	23	23	23	23	23	23	23	23	23	23	22	23	23	23	23	23	23
		MoM	−0.7	−0.6	−0.9	−1.1	−0.7	0.0	0.7	1.3	1.3	0.9	0.4	0.2	0.3	0.3	−0.2	−0.5	−0.2	0.6	−0.1	−0.2	−2.3	3.6	−0.4	3.8	−4.4
		SD	1.1	1.8	2.0	2.3	2.4	2.8	2.7	2.2	2.0	2.3	2.3	2.1	1.9	2.0	1.7	1.6	2.2	2.6	0.8	0.7	6.3	1.6	6.7	3.1	3.1
	All Middle Participants	N	67	65	63	63	67	67	67	67	67	67	66	66	66	65	66	65	66	67	64	66	66	66	67	66	66
		MoM	−1.2	−1.1	−1.6	−1.9	−1.5	−0.8	0.0	0.7	1.1	1.1	1.0	0.8	0.4	0.4	0.1	−0.2	0.1	0.8	−0.2	−0.2	−1.9	3.8	−2.9	2.9	−5.3
		SD	1.3	2.3	2.4	2.7	3.3	3.2	2.7	2.0	1.9	2.1	2.0	1.9	2.1	2.0	1.7	1.4	2.2	3.2	0.8	0.8	7.0	1.8	7.0	3.2	3.3
Age Cohort "Middle"	Middle Females	N	44	42	41	41	44	44	44	44	44	44	43	43	43	42	43	42	43	44	41	43	43	44	44	44	43
		MoM	−1.3	−1.0	−1.7	−2.2	−1.7	−1.1	−0.3	0.5	1.0	1.1	1.1	0.9	0.4	0.4	0.2	−0.1	0.2	0.8	−0.1	−0.2	−1.8	3.6	−3.3	2.8	−5.3
		SD	1.4	2.4	2.4	2.7	3.3	2.9	2.4	1.9	2.0	2.1	1.9	1.9	2.3	2.2	1.9	1.4	2.3	3.3	0.7	0.9	7.4	1.9	6.4	2.9	3.3
	Middle Males	N	23	23	22	22	23	23	23	23	23	23	23	23	23	23	23	23	23	23	23	23	23	22	23	22	23
		MoM	−1.0	−1.3	−1.3	−1.3	−1.1	−0.4	0.4	1.1	1.3	1.2	0.9	0.6	0.5	0.3	0.0	−0.3	0.0	0.7	−0.4	−0.2	−2.2	4.1	−2.2	3.2	−5.4
		SD	1.1	2.3	2.3	2.7	3.5	3.7	3.3	2.2	1.8	2.0	2.2	2.0	1.8	1.8	1.5	1.4	2.0	2.8	0.9	0.7	6.2	1.7	8.0	3.7	3.4
	All Old Participants	N	66	66	66	65	65	65	65	65	67	67	67	67	67	67	65	66	66	67	66	62	63	65	67	66	66
		MoM	1.2	1.3	1.7	1.8	1.7	1.0	0.0	1.0	1.6	1.5	1.0	0.4	0.1	0.0	0.0	0.2	0.2	0.2	0.1	0.1	0.8	3.6	1.5	3.3	4.8
		SD	1.4	2.2	2.4	2.7	3.0	3.1	2.8	2.3	2.3	2.4	2.2	1.9	1.7	1.7	1.6	1.8	2.5	3.0	0.8	0.9	8.3	1.6	7.3	3.1	3.3
	Old Females	N	43	44	44	43	44	44	44	44	44	44	44	44	44	44	42	43	43	44	44	40	42	44	44	44	44
		MoM	−1.3	−1.3	−1.6	−1.9	−1.9	−1.2	−0.2	0.8	1.5	1.4	0.9	0.3	0.0	0.0	0.1	−0.1	0.1	0.6	0.0	−0.2	−0.4	3.5	−2.4	2.8	−5.1
		SD	1.3	2.3	2.4	2.4	2.9	3.1	2.9	2.1	1.9	2.2	2.2	1.9	1.6	1.8	1.7	2.0	2.5	3.0	0.8	1.0	8.8	1.7	6.5	2.7	3.5
Age Cohort "Old"	Old Males	N	23	22	22	22	21	21	21	21	23	23	23	23	23	23	23	23	23	23	22	22	21	21	23	22	22
		MoM	−1.0	−1.2	−1.8	−1.6	−1.3	−0.4	0.6	1.4	1.7	1.6	1.2	0.7	0.3	0.0	−0.3	−0.5	−0.7	−0.6	−0.2	−0.1	−1.4	3.7	0.3	4.4	−4.3
		SD	1.6	2.0	2.5	3.4	3.3	3.0	2.5	2.6	3.0	2.8	2.3	2.0	1.9	1.6	1.3	1.5	2.3	2.8	0.7	0.9	7.4	1.6	8.5	3.6	3.0

Abbreviations: MoM = mean of means; SD = standard deviation; Sh = shoulder; Pel = pelvis; N = number.

Table 4. Results of the descriptive statistical analyses (MoM ± SD) of the spinal parameters in the sagittal plane.

				Specific Parameters																		Global Parameters			
				Sh (°)	C7 (°)	T1 (°)	T2 (°)	T3 (°)	T4 (°)	T5 (°)	T6 (°)	T7 (°)	T8 (°)	T9 (°)	T10 (°)	T11 (°)	T12 (°)	L1 (°)	L2 (°)	L3 (°)	L4 (°)	Pel (°)	Trunk Inclination (VP-DM) (°)	Trunk Inclination (VP-DM) (mm)	Thoracic Kyphosis (ICT-ITL) (°)	Lumbar Lordosis (ITL-ILS) (°)
Sex	All Participants	N	-	201	201	200	200	199	200	199	200	201	201	201	200	200	200	199	201	201	201	198	198	200	201
		MoM	-	25.5	25.5	23.6	18.6	13.7	10.0	7.2	4.4	0.2	−5.4	−11.0	−15.3	−17.6	−17.4	−13.7	−2.7	10.7	18.4	3.1	26.0	49.9	40.9
		SD	-	7.5	6.3	6.4	6.5	5.3	4.6	3.9	3.7	3.8	3.9	4.2	4.5	4.9	5.1	5.7	7.4	7.7	8.9	2.1	17.5	8.3	9.2
	All Females	N	-	132	132	131	132	132	132	131	132	132	132	132	131	131	131	130	132	132	132	130	130	131	132
		MoM	-	26.2	25.6	22.5	16.9	12.1	8.8	6.3	3.6	−0.6	−6.3	−11.9	−16.3	−18.5	−17.7	−13.0	−0.6	13.9	19.1	3.1	25.6	50.1	44.0
		SD	-	7.6	6.4	6.4	6.3	5.1	4.4	3.8	3.7	3.6	3.7	4.2	4.5	5.1	5.5	5.8	7.5	6.6	8.9	2.1	17.6	8.2	8.5
	All Males	N	-	69	69	69	68	67	68	68	68	68	69	69	69	69	69	69	69	69	69	68	68	69	69
		MoM	-	24.1	25.4	25.7	21.9	16.7	12.4	9.0	6.0	1.9	−3.7	−9.1	−13.5	−16.0	−16.9	−15.1	−6.7	4.5	17.0	3.0	26.7	49.6	34.9
		SD	-	7.1	6.0	5.7	5.4	4.3	4.0	3.4	3.3	3.7	3.6	3.7	4.0	4.1	4.3	5.2	5.5	5.5	8.7	2.0	17.4	8.6	7.3
Age Cohort "Young"	All Young Participants	N	-	67	67	66	67	67	67	67	67	67	67	67	67	67	67	67	67	67	67	66	66	66	67
		MoM	-	23.4	23.7	22.2	17.1	12.5	9.2	6.8	4.4	0.5	−5.0	−10.5	−14.7	−16.9	−16.8	−13.4	−2.7	10.9	21.6	2.9	24.8	46.5	40.1
		SD	-	6.9	6.0	5.9	6.2	5.3	4.7	4.0	3.8	3.9	3.8	4.2	4.7	5.0	5.2	5.8	7.0	7.7	8.3	2.2	18.4	7.1	8.9
	Young Females	N	-	44	44	43	44	44	44	44	44	44	44	44	44	44	44	44	44	44	44	43	43	43	44
		MoM	-	23.9	23.4	20.7	15.0	10.7	7.9	5.7	3.3	−0.4	−5.8	−11.1	−15.3	−17.6	−17.0	−12.9	−1.3	13.2	22.1	2.8	22.6	46.9	43.0
		SD	-	7.4	6.5	5.5	5.5	4.9	4.6	4.0	3.9	4.1	4.0	4.6	5.1	5.5	5.4	5.9	7.3	7.7	8.9	2.1	17.5	6.9	8.7
	Young Males	N	-	23	23	23	23	23	23	23	23	23	23	23	23	23	23	23	23	23	23	23	23	23	23
		MoM	-	22.6	24.3	25.0	21.2	16.1	11.8	9.0	6.4	2.2	−3.5	−9.1	−13.4	−15.6	−16.5	−14.6	−5.4	6.5	20.7	3.3	28.9	45.8	34.5
		SD	-	5.8	5.1	5.7	5.4	4.3	3.8	3.2	2.7	2.9	2.8	3.1	3.5	3.7	4.7	5.8	5.6	5.6	6.9	2.2	19.7	7.7	6.5
Age Cohort "Middle"	All Middle Participants	N	-	67	67	67	67	66	66	66	66	67	67	67	67	67	67	66	67	67	67	67	67	67	67
		MoM	-	27.7	26.7	23.1	17.9	13.3	10.1	7.7	4.9	0.6	−5.1	−10.6	−15.3	−18.1	−17.9	−14.5	−3.8	9.9	17.8	3.2	27.0	49.7	41.0
		SD	-	6.8	5.9	6.5	6.4	4.7	3.7	3.2	3.3	3.6	3.9	4.2	4.5	4.9	4.7	5.2	7.5	7.4	8.8	2.0	17.0	7.7	9.0
	Middle Females	N	-	44	44	44	44	44	44	44	44	44	44	44	44	44	44	43	44	44	44	44	44	44	44
		MoM	-	28.5	26.7	21.7	16.0	11.9	9.0	6.9	4.1	−0.4	−6.3	−11.9	−16.8	−19.5	−18.2	−13.5	−1.0	13.5	18.4	3.2	26.3	49.3	43.7
		SD	-	6.0	5.5	6.5	6.0	4.4	3.4	3.0	3.3	3.3	3.6	4.0	4.2	4.9	5.4	5.6	7.1	5.6	8.6	2.1	17.3	7.6	9.0
	Middle Males	N	-	23	23	23	23	22	22	22	22	23	23	23	23	23	23	23	23	23	23	23	23	23	23
		MoM	-	26.1	26.8	25.7	21.4	16.1	12.3	9.4	6.3	2.6	−2.8	−8.2	−12.4	−15.4	−17.2	−16.3	−9.2	3.0	16.7	3.2	28.3	50.5	35.7
		SD	-	8.1	6.6	5.7	5.8	3.9	3.5	3.0	2.9	3.4	3.5	3.4	3.7	3.8	2.9	3.6	4.9	5.2	9.1	1.9	16.7	7.9	6.2
Age Cohort "Old"	All Old Participants	N	-	67	67	67	66	66	67	66	67	67	67	67	66	66	66	66	67	67	67	65	65	67	67
		MoM	-	25.4	26.1	25.5	20.8	15.2	10.7	7.2	3.9	−0.4	−6.2	−11.8	−16.0	−17.9	−17.6	−13.2	−1.7	11.3	15.7	3.1	26.1	53.4	41.6
		SD	-	8.2	6.5	6.3	6.3	5.5	5.1	4.2	4.0	3.9	3.8	4.2	4.4	4.8	5.4	6.1	7.7	7.9	8.6	2.1	17.4	8.7	9.7
	Old Females	N	-	44	44	44	44	44	44	43	44	44	44	44	43	43	43	43	44	44	44	43	43	44	44
		MoM	-	26.3	26.7	25.0	19.6	13.8	9.5	6.5	3.3	−1.1	−6.9	−12.7	−16.8	−18.3	−17.8	−12.6	0.4	13.0	16.8	3.4	27.8	54.0	45.3
		SD	-	8.7	6.7	6.5	6.7	5.5	4.9	4.1	3.8	3.4	3.4	4.0	4.1	4.8	5.6	6.0	8.0	6.4	8.4	2.2	18.2	8.7	7.7
	Old Males	N	-	23	23	23	22	22	23	23	23	23	23	23	23	23	23	23	23	23	23	22	22	23	23
		MoM	-	23.5	25.0	26.4	23.2	18.1	13.0	8.7	5.2	0.8	−4.7	−10.1	−14.6	−17.0	−17.1	−14.3	−3.7	4.1	13.7	2.6	22.8	52.4	34.4
		SD	-	6.9	6.1	6.0	4.9	4.5	4.7	4.1	4.1	4.5	4.2	4.2	4.8	4.7	5.1	6.0	5.3	5.2	8.9	1.8	15.5	9.0	9.1

Abbreviations: MoM = mean of means; SD = standard deviation; Sh = shoulder; Pel = pelvis; N = number.

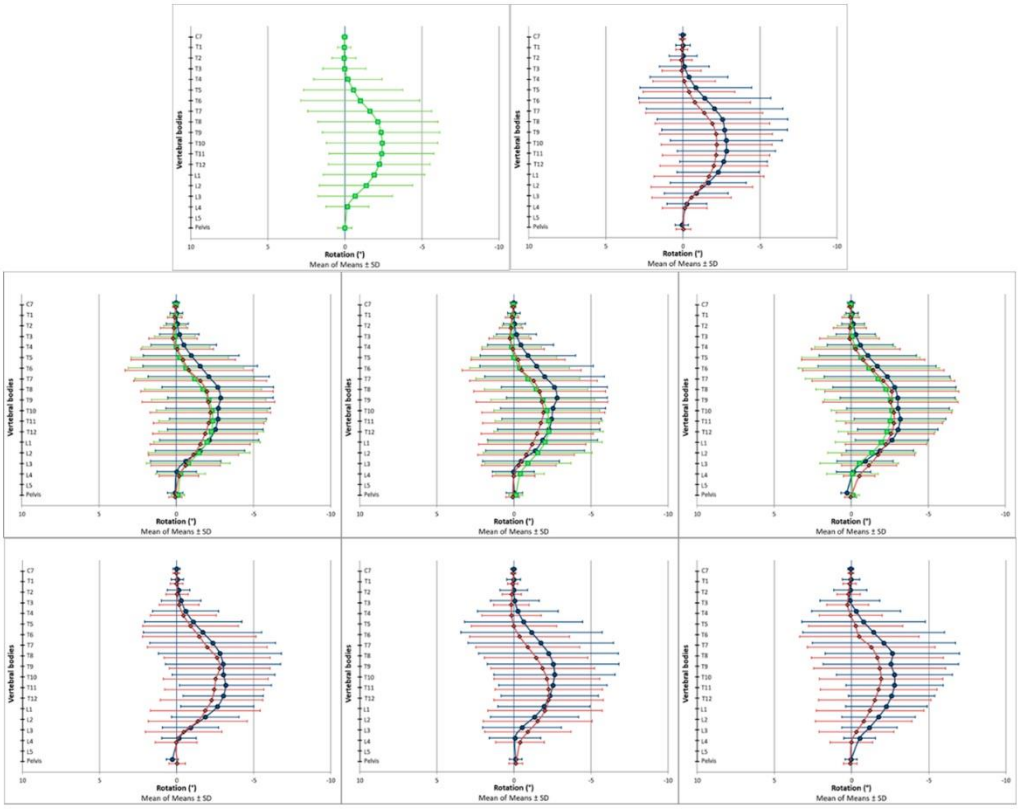

Figure 2. Vertebral body positions in the transversal plane. Positive values represent a rotation of the vertebral bodies to the left (counterclockwise), and negative values represent a rotation of the vertebral bodies to the right (clockwise). The scale of the *x*-axis is turned to enhance the intuitive visual interpretability of the results: (**Upper row**) (left picture: all participants (■, green); right picture: all female (◆, red) and all male (●, blue) participants). (**Middle row**) (left picture: all participants of the respective age cohorts: young (●, blue), middle (■, green) and old (◆, red); middle picture: all female participants of the respective age cohorts: young (●, blue), middle (■, green) and old (◆, red); right picture: all male participants of the respective age cohorts: young (●, blue), middle (■, green) and old (◆, red)). (**Lower row**) (left picture: all young female (◆, red) and all young male (●, blue) participants; middle picture: all middle-aged female (◆, red) and all middle-aged male (●, blue) participants; right picture: all old female (◆, red) and all old male (●, blue) participants).

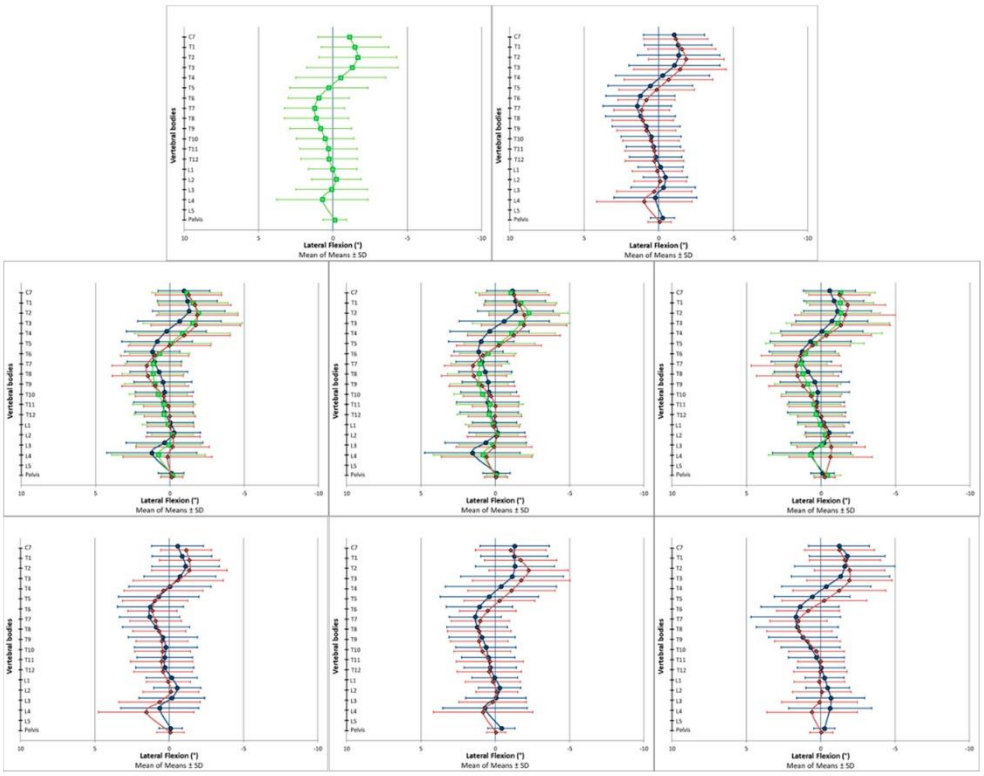

Figure 3. Vertebral body positions in the coronal plane. Positive values represent a tilt of the vertebral bodies to the left, and negative values represent a tilt of the vertebral bodies to the right. The scale of the *x*-axis is turned to enhance the intuitive visual interpretability of the results: (**Upper row**) (left picture: all participants (■, green); right picture: all female (◆, red) and all male (●, blue) participants). (**Middle row**) (left picture: all participants of the respective age cohorts: young (●, blue), middle (■, green) and old (◆, red); middle picture: all female participants of the respective age cohorts: young (●, blue), middle (■, green) and old (◆, red); right picture: all male participants of the respective age cohorts: young (●, blue), middle (■, green) and old (◆, red)). (**Lower row**) (left picture: all young female (◆, red) and all young male (●, blue) participants; middle picture: all middle-aged female (◆, red) and all middle-aged male (●, blue) participants; right picture: all old female (◆, red) and all old male (●, blue) participants).

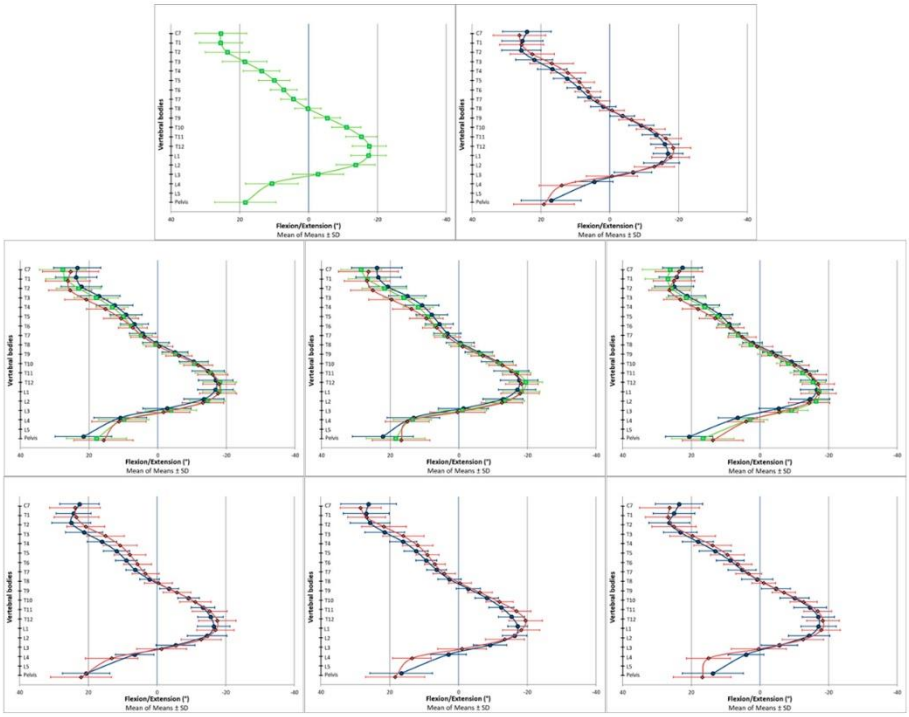

Figure 4. Vertebral body positions in the sagittal plane. Positive values represent a tilt of the vertebral bodies towards spinal flexion, and negative values represent a tilt of the vertebral bodies towards spinal extension. The scale of the *x*-axis is turned to enhance the intuitive visual interpretability of the results: (**Upper row**) (left picture: all participants (■, green); right picture: all female (◆, red) and all male (●, blue) participants). (**Middle row**) (left picture: all participants of the respective age cohorts: young (●, blue), middle (■, green) and old (◆, red); middle picture: all female participants of the respective age cohorts: young (●, blue), middle (■, green) and old (◆, red); right picture: all male participants of the respective age cohorts: young (●, blue), middle (■, green) and old (◆, red)). (**Lower row**) (left picture: all young female (◆, red) and all young male (●, blue) participants; middle picture: all middle-aged female (◆, red) and all middle-aged male (●, blue) participants; right picture: all old female (◆, red) and all old male (●, blue) participants.

3.2.1. Descriptive Data Analysis

In the transverse plane, the spine was not in a neutral rotary position. Instead, a systematic vertebral rotation to the right side was identified from T5 to L3 among all the investigated subgroups (Figure 2 and Table 2). In the coronal plane, a systematic deviation from the neutral centerline was also apparent. The vertebrae above T5 were laterally flexed to the right side, and around the fifth thoracic vertebrae, the side of lateral flexion changed in direction to the left (Figure 3 and Table 3). In the sagittal plane, T8 was found to be in an almost neutral position, indicating that it was the thoracic kyphosis apex (Figure 4 and Table 4). The vertebrae above (C7–T7) were tilted towards spinal flexion, while the vertebrae below were positioned in spinal extension (T9–~L3). The height of the lumbar lordosis apex, meaning the reverse change in direction from spinal extension to spinal flexion, differed between the analyzed subgroups but was systematically located between L2 and L4.

Table 5. Results of the explorative statistical analyses (one-sample Wilcoxon signed rank test and two-way analyses of variance) of the spinal parameters in all three planes of movement.

		Specific Parameters																		Global Parameters					
		Transversal Plane																							
		Sh (°)	C7 (°)	T1 (°)	T2 (°)	T3 (°)	T4 (°)	T5 (°)	T6 (°)	T7 (°)	T8 (°)	T9 (°)	T10 (°)	T11 (°)	T12 (°)	L1 (°)	L2 (°)	L3 (°)	L4 (°)	Pel (°)	Surface Rotation RMS (°)		Surface Rotation MAX (°)	(Right Side) Surface Rotation +Max (°)		(Left Side) Surface Rotation −Max (°)
AP vs. HM = 0 (One-Sample Wilcoxon Signed Rank Test)	Observed Median	−0.12	0.06	0.15	0.06	−0.04	−0.27	−0.73	−1.03	−1.60	−2.21	−2.56	−2.60	−2.74	−2.33	−1.98	−1.23	−0.69	−0.18	0.03	2.11		−2.73	1.17		−3.22
	Standardized Test Statistic	−1.71	2.35	1.43	0.87	0.06	−1.22	−2.33	−3.52	−5.22	−6.80	−7.48	−7.93	−8.16	−7.96	−7.10	−5.73	−3.86	−1.95	0.81	12.26		−6.28	11.44		−12.14
	p-Value	0.09	**0.02** *	0.15	0.39	0.96	0.22	**0.02** *	**0.00** *	**0.00** *	**0.00** *	**0.00** *	**0.00** *	**0.00** *	**0.00** *	**0.00** *	**0.00** *	**0.00** *	0.05	0.42	**0.00** *		**0.00** *	**0.00** *		**0.00** *
Between-Subject Effects (Two-Way ANOVA)	Sex (Sig)	0.84	0.82	0.29	0.38	0.41	0.37	0.37	0.27	0.27	0.27	0.34	0.26	0.19	0.19	0.23	0.36	0.40	0.53	0.17	0.45		0.71	0.35		0.37
	Age Cohort (Sig)	0.50	0.63	0.40	0.30	0.27	0.48	0.30	0.48	0.52	0.47	0.52	0.76	0.66	0.60	0.67	0.82	0.99	0.71	**0.01** *	0.45		0.17	0.25		0.69
	Sex * Age Cohort (Sig)	0.15	0.92	0.97	0.99	0.98	0.94	0.92	0.87	0.93	0.85	0.92	0.95	0.83	0.69	0.62	0.57	0.37	0.23	0.06	0.49		0.94	0.71		0.84
	Young vs. Old (Sig)	0.87	0.77	0.43	0.34	0.26	0.63	0.74	0.63	0.82	0.68	0.56	0.71	0.57	0.49	0.57	0.81	1.00	0.92	1.00	1.00		0.16	0.33		0.56
	Young vs. Middle (Sig)	0.52	0.94	0.92	0.72	0.54	0.48	0.44	0.44	0.47	0.41	0.58	0.80	0.83	0.89	0.97	1.00	0.97	0.67	**0.05** *	0.55		1.00	0.99		0.97
	Middle vs. Old (Sig)	0.93	0.97	1.00	1.00	0.95	1.00	0.97	0.99	0.94	0.97	1.00	0.99	0.91	0.77	0.73	0.88	0.97	0.96	0.07	0.47		0.18	0.22		0.71
		Coronal Plane																							
		Sh (°)	C7 (°)	T1 (°)	T2 (°)	T3 (°)	T4 (°)	T5 (°)	T6 (°)	T7 (°)	T8 (°)	T9 (°)	T10 (°)	T11 (°)	T12 (°)	L1 (°)	L2 (°)	L3 (°)	L4 (°)	Pel (°)	Trunk Imbalance (VP-DM) (°)	Trunk Imbalance (VP-DM) (mm)	Apical Deviation RMS (mm)	Apical Deviation MAX (mm)	(Right Side) Apical Deviation (VP-DM) +max (mm)	(Left Side) Apical Deviation (VP-DM) −max (mm)
AP vs. HM = 0 (One-Sample Wilcoxon Signed Rank Test)	Observed Median	−1.08	−1.11	−1.55	−1.68	−1.38	−0.73	0.11	0.93	1.23	1.30	1.02	0.68	0.43	0.21	0.05	−0.29	0.04	0.51	−0.07	−0.24	−2.35	3.19	−3.30	2.70	−4.52
	Standardized Test Statistic	−9.52	−6.77	−7.89	−7.80	−5.52	−2.30	1.22	5.92	7.62	6.61	5.15	3.74	2.41	1.97	0.22	−1.82	0.38	2.91	−1.70	−3.54	−3.39	12.14	−3.54	11.34	−12.11
	p-Value	**0.00** *	**0.00** *	**0.00** *	**0.00** *	**0.00** *	**0.02** *	0.22	**0.00** *	**0.00** *	**0.00** *	**0.00** *	**0.00** *	**0.02** *	**0.05** *	0.83	0.07	0.70	**0.00** *	0.09	**0.00** *	**0.00** *	**0.00** *	**0.00** *	**0.00** *	**0.00** *
Between-Subject Effects (two-way ANOVA)	Sex (Sig)	0.08	0.72	0.47	0.20	0.43	0.40	0.29	0.18	0.32	0.61	0.95	0.94	0.81	0.78	0.35	0.19	0.09	0.10	0.11	0.73	0.76	0.23	0.16	**0.04** *	0.61
	Age Cohort (Sig)	0.47	0.56	0.35	0.42	0.19	0.15	0.23	0.31	0.38	0.18	0.24	0.49	0.67	0.49	0.81	0.91	0.47	0.13	0.62	0.58	0.53	0.48	0.26	0.58	0.25
	Sex * Age Cohort (Sig)	1.00	0.55	0.70	0.76	0.75	0.44	0.49	0.81	0.95	0.99	0.80	0.60	0.77	0.99	0.92	0.92	0.76	0.60	0.49	0.93	0.88	0.88	0.72	0.55	0.79
	Young vs. Old (Sig)	0.63	0.78	0.50	0.53	0.12	0.07	0.19	0.96	0.44	0.12	0.38	1.00	0.67	0.62	1.00	1.00	0.40	0.14	1.00	0.86	0.54	0.93	0.88	1.00	0.70
	Young vs. Middle (Sig)	0.57	0.94	0.73	0.41	0.26	0.12	0.14	0.45	1.00	0.56	0.34	0.52	1.00	1.00	0.93	0.98	0.82	0.79	0.88	1.00	1.00	0.60	0.23	0.74	0.20
	Middle vs. Old (Sig)	1.00	0.98	0.98	1.00	0.97	0.99	1.00	0.75	0.66	0.61	1.00	0.63	0.73	0.59	0.94	1.00	0.78	0.57	0.93	1.00	1.00	0.90	0.48	0.77	0.64

Table 5. *Cont.*

		Specific Parameters																		Global Parameters				
			Sagittal Plane																					
		Sh (°)	C7 (°)	T1 (°)	T2 (°)	T3 (°)	T4 (°)	T5 (°)	T6 (°)	T7 (°)	T8 (°)	T9 (°)	T10 (°)	T11 (°)	T12 (°)	L1 (°)	L2 (°)	L3 (°)	L4 (°)	Pel (°)	Trunk Inclination (VP-DM) (°)	Trunk Inclination (VP-DM) (mm)	Thoracic Kyphosis (ICT-ITL) (°)	Lumbar Lordosis (ITL-ILS) (°)
AP vs. HM = 0 (One-Sample Wilcoxon Signed Rank Test)	Observed Median	-	25.01	25.24	23.95	19.04	13.65	10.36	7.91	4.83	0.23	−5.69	−10.98	−15.07	−17.42	−17.61	−14.08	−3.58	10.52	18.40	2.98	26.15	50.54	40.98
	Standardized Test Statistic	-	12.29	12.29	12.26	12.26	12.23	12.25	12.15	10.91	0.89	−11.74	−12.29	−12.26	−12.26	−12.26	−12.23	−4.97	11.74	12.27	11.84	11.84	12.26	12.29
	p-Value	-	**0.00** *	**0.00** *	**0.00** *	**0.00** *	**0.00** *	**0.00** *	**0.00** *	**0.00** *	0.38	**0.00** *	**0.00** *	**0.00** *	**0.00** *	**0.00** *	**0.00** *	**0.00** *	**0.00** *	**0.00** *	**0.00** *	**0.00** *	**0.00** *	**0.00** *
Between-Subject Effects (two-way ANOVA)	Sex (Sig)	-	**0.05** *	0.80	**0.00** *	**0.00** *	**0.00** *	**0.00** *	**0.00** *	**0.00** *	**0.00** *	**0.00** *	**0.00** *	**0.00** *	**0.00** *	0.32	**0.01** *	**0.00** *	**0.00** *	0.10	0.74	0.68	0.66	**0.00** *
	Age Cohort (Sig)	-	**0.01** *	**0.03** *	**0.03** *	**0.01** *	**0.01** *	0.19	0.47	0.30	0.14	0.11	0.13	0.20	0.42	0.59	0.33	0.13	0.31	**0.00** *	0.85	0.80	**0.00** *	0.70
	Sex * Age Cohort (Sig)	-	0.84	0.50	0.35	0.44	0.77	0.93	0.70	0.67	0.70	0.62	0.49	0.24	0.26	0.95	0.84	0.26	0.12	0.86	0.24	0.22	0.60	0.58
	Young vs. Old (Sig)	-	0.38	0.07	**0.01** *	**0.00** *	**0.00** *	0.15	1.00	0.84	0.30	0.16	0.13	0.20	0.56	0.80	0.99	1.00	0.94	**0.00** *	0.96	0.96	**0.00** *	0.52
	Young vs. Middle (Sig)	-	**0.00** *	**0.02** *	0.80	0.84	0.75	0.70	0.47	0.82	0.98	1.00	0.96	0.78	0.38	0.58	0.66	1.00	0.60	**0.03** *	0.88	0.84	0.06	0.80
	Middle vs. Old (Sig)	-	0.21	0.84	0.06	**0.01** *	0.06	1.00	1.00	0.34	0.21	0.20	0.22	0.71	0.99	0.98	0.46	0.22	0.40	0.34	0.99	0.99	**0.02** *	0.89

Bold and * = $p < 0.05$. Abbreviations: Sh = shoulder; Pel = pelvis; AP = group of all participants; HM = hypothetical median; Sig = significance.

The graphical data output of the specific spine parameters indicated systematic differences between the female and male participants and between the participants in the different age cohorts. In the transverse plane, these subgroup-dependent visual differences were present among almost all the investigated vertebral bodies. In the coronal plane, the differences seemed to be locally limited to the upper thoracic spine. In the sagittal plane, the curves of the analyzed subgroups ran more in parallel compared to the other two planes. In this regard, the differently scaled x-axes have to be considered.

3.2.2. Explorative Data Analysis

The graphically apparent deviations of the vertebral bodies from the symmetrical zero position in the transverse and the coronal planes could be confirmed by statistical data analyses. The deviations were significant from T5 to L3 in the transverse plane and from C7 to T4, from T6 to T12 and for the pelvis in the coronal plane when that data of the entire group were considered and tested versus a hypothetical median of zero. Likewise, all the global parameters in the two respective planes deviated significantly from the respective symmetrical spine position (Table 5). The visual differences between the analyzed subgroups, however, could not be statistically confirmed for the transverse and coronal plane data. Here, only the isolated parameters revealed statistical trends pointing towards a possible existing difference (for "Pelvis Rotation" between the young and middle participants ($p = 0.05$) and for "Right Side Apical Deviation VP-DM + max (mm)" ($p = 0.04$) between the female and male participants).

In the sagittal plane, systematic deviations from a straight upright spine position existed in all the vertebral bodies except for T8 (neutral vertebrae of the thoracic kyphosis) and all the global spine parameters. In contrast with the two other planes, the statistical analyses also revealed systematic trends pointing towards possible differences between the analyzed subgroups. The global parameter of "Lumbar Lordosis (ITL-ILS) (°)" differed between the female and male participants ($p < 0.001$), while the parameter of "Thoracic Kyphosis (ICT-ITL) (°)" indicated a trend towards a difference between the participants in the different age cohorts ($p < 0.001$). The systematic trend behind these findings becomes apparent when observing the specific spine parameters. Sex-specific differences could be found for all the specific parameters except for the two major turning points (meaning the most flexed (T1) and the most extended (L1) vertebrae). Differences between the age cohorts in the global parameter of "Thoracic Kyphosis (ICT-ITL) (°)" were also apparent at the level of the specific spine parameters. The systematic differences due to the participants' belonging to different age cohorts can be seen here in the isolated upper thoracic vertebrae (C7–T4) and the pelvis (Table 5).

3.3. Literature Comparison

Table 6 compares the results for the global spine parameters of the current study with those derived from previous publications using the same VRS measurement device [18–23]. Most of the results were found to be almost comparable; however, there was a trend towards slightly lower values derived from the current study for the parameters of the transverse and the coronal plane when compared to those of previous research.

Table 6. Comparison of the results for the global spine parameters from the current study with those of previous research.

				Transversal Plane					Coronal Plane						Sagittal Plane			
				Surface Rotation RMS (°)	Surface Rotation MAX (°)	(Right Side) Surface Rotation +Max (°)	(Left Side) Surface Rotation −Max (°)	Trunk Imbalance (VP-DM) (°)	Trunk Imbalance (VP-DM) (mm)	Apical Deviation RMS (mm)	Apical Deviation MAX (mm)	(Right Side) Apical Deviation (VP-DM) +Max (mm)	(Left Side) Apical Deviation (VP-DM) −Max (mm)	Trunk Inclination (VP-DM) (°)	Trunk Inclination (VP-DM) (mm)	Thoracic Kyphosis (ICT-ITL) (°)	Lumbar Lordosis (ITL-ILS) (°)
Current Study	All Participants		MoM	2.3	−1.9	1.5	−3.3	−0.2	−1.7	3.6	−1.8	3.2	−4.9	3.1	26.0	49.9	40.9
			SD	0.9	4.0	1.4	2.3	0.8	7.3	1.7	7.1	3.0	3.3	2.1	17.5	8.3	9.2
	Sex	All Females	MoM	2.2	−1.8	1.5	−3.2	−0.2	−1.6	3.5	−2.3	2.9	−4.9	3.1	25.6	50.1	44.0
			SD	0.9	4.0	1.4	2.3	0.9	7.7	1.7	6.7	2.8	3.3	2.1	17.6	8.2	8.5
		All Males	MoM	2.3	−2.1	1.7	−3.6	−0.2	−2.0	3.8	−0.8	3.8	−4.7	3.0	26.7	49.6	34.9
			SD	0.9	4.0	1.4	2.3	0.8	6.6	1.6	7.7	3.4	3.2	2.0	17.4	8.6	7.3
	All Young Participants		MoM	2.3	−2.3	1.4	−3.5	−0.3	−2.5	3.5	−0.9	3.3	−4.4	2.9	24.8	46.5	40.1
			SD	0.9	3.6	1.2	2.2	0.8	6.5	1.6	7.0	2.9	3.1	2.2	18.4	7.1	8.9
	Age Cohort "Young"	Young Females	MoM	2.4	−2.4	1.3	−3.5	−0.3	−2.6	3.4	−1.1	3.1	−4.4	2.8	22.6	46.9	43.0
			SD	0.9	3.8	1.3	2.3	0.8	6.7	1.6	7.2	2.7	3.1	2.1	17.5	6.9	8.7
		Young Males	MoM	2.2	−2.3	1.7	−3.6	−0.2	−2.3	3.6	−0.4	3.8	−4.4	3.3	28.9	45.8	34.5
			SD	0.8	3.4	1.2	2.2	0.7	6.3	1.6	6.7	3.1	3.1	2.2	19.7	7.7	6.5
	All Middle Participants		MoM	2.1	−2.3	1.4	−3.4	−0.2	−1.9	3.8	−2.9	2.9	−5.3	3.2	27.0	49.7	41.0
			SD	1.0	3.6	1.4	2.2	0.8	7.0	1.8	7.0	3.2	3.3	2.0	17.0	7.7	9.0
	Age Cohort "Middle"	Middle Females	MoM	2.0	−2.2	1.3	−3.3	−0.2	−1.8	3.6	−3.3	2.8	−5.3	3.2	26.3	49.3	43.7
			SD	0.8	3.4	1.4	2.0	0.9	7.4	1.9	6.4	2.9	3.3	2.1	17.3	7.6	9.0
		Middle Males	MoM	2.3	−2.4	1.5	−3.6	−0.2	−2.2	4.1	−2.2	3.2	−5.4	3.2	28.3	50.5	35.7
			SD	1.1	3.8	1.4	2.6	0.7	6.2	1.7	8.0	3.7	3.4	1.9	16.7	7.9	6.2
	All Old Participants		MoM	2.3	−1.1	1.8	−3.1	−0.1	−0.8	3.6	−1.5	3.3	−4.8	3.1	26.1	53.4	41.6
			SD	0.9	4.6	1.7	2.4	0.9	8.3	1.6	7.3	3.1	3.3	2.1	17.4	8.7	9.7
	Age Cohort "Old"	Old Females	MoM	2.3	−0.9	1.8	−2.9	−0.2	−0.4	3.5	−2.4	2.8	−5.1	3.4	27.8	54.0	45.3
			SD	0.9	4.6	1.7	2.4	1.0	8.8	1.7	6.5	2.7	3.5	2.2	18.2	8.7	7.7
		Old Males	MoM	2.5	1.4	1.8	3.5	0.1	1.4	3.7	0.3	4.4	4.3	2.6	22.8	52.4	34.4
			SD	0.9	4.8	1.7	2.3	0.9	7.4	1.6	8.5	3.6	3.0	1.8	15.5	9.0	9.1
Literature Comparison	Degenhardt et al., 2017 [22]	Young-Middle Participants	Mean	3.8	1.8	5.6	−4.6	0.1	1.0	5.6	3.6 ‡	7.9	−5.0	3.1	26.0	48.1	35.6
			SD	1.4	7.2	3.4	2.9	0.8	7.2	3.0	10.3 †	5.8	4.1	2.3	18.7	9.1	8.4
	Degenhardt et al., 2020 [23]	Young-Middle Participants	Mean	3.8	2.0	5.7	−4.5	0.2	1.3	5.4	4.3	8.0	−4.6	3.2	26.2	48.5	35.4
			SD	1.0	6.0	2.8	2.4	0.7	5.6	2.5	8.7	5.1	2.9	2.2	17.7	8.3	7.6
	Michalik et al., 2020 [19]	Young Females	Mean	3.6	-	-	-	−0.1	-	5.6	-	-	-	2.1	-	44.0 †	37.4 †
			SD	1.6	-	-	-	0.9	-	2.3	-	-	-	2.4	-	8.6 †	9.8 †
		Young Males	Mean	3.5	-	-	-	−0.1	-	5.1	-	-	-	1.9	-	44.6 †	29.0 †
			SD	1.6	-	-	-	1.0	-	2.1	-	-	-	1.9	-	7.8 †	7.7 †
	Schröder et al., 2011 [20]	Young Females	Mean	3.6	-	-	-	-	6.9	5.5	-	-	-	-	12.3	47.1	42.7
			SD	1.8	-	-	-	-	4.6	2.3	-	-	-	-	17.9	8.6	8.2
		Young Males	Mean	3.1	-	-	-	-	7.7	5.8	-	-	-	-	10.3	49.2	35.8
			SD	1.5	-	-	-	-	7.2	2.5	-	-	-	-	16.4	9.3	6.6
	Schröder et al., 2014 [21]	Young Females	Mean	3.4	-	-	-	-	7.7	4.2	-	-	-	16.6 *	-	45.4	44.0
			SD	1.7	-	-	-	-	4.6	2.0	-	-	-	15.5 *	-	8.1	9.4
		Young Males	Mean	3.6	-	-	-	-	6.9	4.5	-	-	-	20.8 *	-	47.2	35.9
			SD	1.4	-	-	-	-	4.6	2.1	-	-	-	15.2 *	-	7.3	8.2
	Furian et al., 2013 [18]	Girls	Mean	-	-	-	-	-	5.7	-	4.9 ‡	-	-	-	2.6 *	47.1 †Δ	42.1 †Δ
			SD	-	-	-	-	-	0.7	-	0.7 ‡	-	-	-	0.7 *		
		Boys	Mean	-	-	-	-	-	7.4	-	4.7 ‡	-	-	-	3.0 *	7.5 †Δ	9.9 †Δ
			SD	-	-	-	-	-	0.8	-	0.4 ‡	-	-	-	0.2 *		

Abbreviations: MoM = mean of means; SD = standard deviation; ‡ = parameters could not be clearly assigned; * = values not comprehensible (unit of measurement questionable); † = parameters differ slightly from those used in the current study ("Thoracic Kyphosis VP-T12"; "Lumbar Lordosis T12-DM"); Δ = results are only available as one mean and SD for the entire group (n = 345) and not for the subgroups, respectively. [22]: n = 30 participants, age = 30.2 ± 9.8 years; [23]: n = 29 participants, age = 30.1 ± 10.1 years; [19]: n = 56 females, age = 23.6 ± 2.0 years and n = 65 males, age = 24.3 ± 2.2 years; [20]: n = 89 females, age = 26.4 ± 4.5 years and n = 88 males, age = 27.7 ± 4.4 years; [21]: n = 52 females, age = 26.1 ± 6.9 years and n = 51 males, age = 28.2 ± 7.4 years; [18]: n = 168 girls, age = 8.3 ± 1.3 years and n = 177 boys, age = 8.6 ± 1.2 years.

4. Discussion

Various studies have analyzed spinal posture and its possible adaptations to different spinal and other musculoskeletal pathologies using VRS [29–31]. However, reference values for the comparison of the possible pathological findings are only available for global spine parameters that mainly derived from children [18], younger adults [19–21], or young and middle-aged adults, but these are based on very small numbers of participants [22,23]. Systematically collected normative data, which differentiates between subgroups according to sex and age, which can be used to identify possible changes in spinal posture over the adult life span, were missing. One aim of this study was, therefore, to complement existing knowledge with a further reference dataset that meets those requirements. Spinal posture data were thus captured and analyzed based on 201 healthy participants according to sex and age over an adult life span of 18 to 70 years. A further aim was to expand the current knowledge by providing an additional reference dataset of specific spine parameters that contains three-dimensional posture data for every vertebral body (from C7 to L4 and the pelvis).

4.1. Global Spine Parameters

The results for the global spine parameters derived from the current study did not differ greatly from those of previous publications using the same VRS measurement device ([19–23]; Table 6). However, there seems to be a trend towards slightly lower measurement results for the parameters in the transverse and the coronal planes. Possible explanations for the deviation of the results could be, in addition to the different cohort compositions and cohort sizes, differences in the measurement protocol and data analysis. To obtain the most accurate data quality, we used a high standardization of the measurement protocol, the use of additional markers in the course of the vertebral column (~T3 and ~T12) and the systematic removal of extreme outliers from the raw dataset. Since the comparative studies do not provide corresponding information, the question regarding the reasons for the differences cannot be answered in a well-established manner.

In the current study, significant trends towards possible differences in several global spine parameters according to sex and age cohort were revealed through explorative data analyses. While these differences were not found to be systematic for the coronal plane parameter of the "(Right Side) Apical Deviation VP-DM + max (mm)", the results for the respective sagittal plane parameters were considered highly important. The "Lumbar Lordosis (ITL-ILS) (°)" angle revealed a trend towards a significant difference between the female and male participants, with females showing greater lordosis angles than their male counterparts. This is in accordance with previous publications using the same VRS measuring device [19–21]. These findings also match the results of a recent systematic review and meta-analysis describing age- and sex-based effects on the lumbar lordosis angles and the range of motion based on different clinically established measurement approaches (radiological and non-radiological). The authors also found significant differences according to sex, with females having greater lumbar lordosis angles than men, but in contrast to the current findings, they also revealed indications that age possibly affected the respective spine parameters [32]. Similar correlations between VRS- and X-ray-measured results were found for the sagittal plane parameter of "Thoracic Kyphosis". The current study found a trend towards significant differences between young and old ($p < 0.001$) and between middle and old ($p < 0.02$) participants, indicating an increase in the VRS-measured parameter with increasing age. Comparable results were published in a recent systematic review based on radiography-based Cobb angle calculations [33]. The authors described an increase in thoracic kyphosis with aging but did not find that sex affected the spine parameters.

These results confirm the importance of having VRS reference data that are not only distinguishable between subgroups according to sex, as has been the case thus far, but also according to different age cohorts. Without these data, changes in spinal posture that

physiologically occur over a healthy life span could be falsely diagnosed as pathologic, resulting in troubling uncertainty for the affected patients in clinical practice.

4.2. Specific Spine Parameters

Apart from a previous sub-analysis of 100 female participants from the present study cohort, which was published by our own research group [24], this is the first paper to present systematic reference data for every vertebral body in all three dimensions for both sexes and for three different age cohorts, which were derived using the VRS "Formetric III 4D" measuring device. As already described, in contrast to the currently common clinical beliefs, the physiological spinal posture in the transverse and the coronal planes was not found to be straight and symmetric with regard to rotation and lateral flexion [24]. Instead, a systematic rotation of the mid- and lower thoracic and lumbar vertebrae towards the right side was observed and supported by explorative data analyses. This rotation was found to be more pronounced in males than females and in young compared to middle-aged and old participants. A pre-existing vertebral rotation in healthy participants was also previously described based on CT and MRI measurements [34]. In patients with a diagnosed situs inversus totalis, the side of the vertebral rotation changed, respectively [35]. These results suggest that the VRS findings of the current study are clinically comprehensible and that internal organ arrangement might be a possible physiological cause of the observed asymmetric spinal posture.

In the coronal plane, a lateral flexion to the right side was found in the case of the upper thoracic vertebrae, while the underlying vertebrae showed a systematic lateral flexion to the left. Contrary to the results for the spinal rotation, visually, the lateral flexion in the upper thoracic vertebrae seemed to be more pronounced in the female compared to the male participants, whereas no sex-specific differences were detectable in the mid- and lower thoracic or the lumbar vertebral body positions. According to age-related differences, the younger group visually seemed to demonstrate less lateral flexion than the middle-aged and old participants, specifically in the thoracic spinal region. Whether or not this might be caused by posture adaptations induced by normal degenerative changes in the spine remains unclear. However, Kilshaw et al. [36], who analyzed the lumbar spine retrospectively based on abdominal radiographs and found that deformities such as lumbar scoliosis, lateral listhesis and osteoarthritis in the coronal plane started to occur after the age of 50 and steadily increased with age, previously described such an effect, albeit in a different spinal section.

No unexpected outcomes for the vertebral positions were detected in the sagittal plane parameters. The apex of the VRS-measured thoracic kyphosis, meaning the least tilted vertebrae, appeared around T8. This is in accordance with recently published findings derived from radiographic data. Here, the thoracic apex was located between T7 and T9 [37,38]. In the current study, the lumbar lordosis apex appeared between the second and the fourth lumbar vertebrae, depending on the analyzed subgroup. As already described, a statistically significant trend towards a difference between the female and male participants was found for the global parameter of "Lumbar Lordosis (ITL-ILS) (°)". This difference according to sex was also apparent among almost all the specific spine parameters, except for the two major curvature turning points (the most flexed (T1) and the most extended (L1) vertebral body). In the thoracic spine, males showed a greater curvature in the upper thoracic spine, and females showed greater curvature in the lower thoracic spine. The authors assume that this difference between females and males canceled each other out, which is why the sex difference did not manifest in the global variable of "Thoracic Kyphosis (ICT-ITL) (°)". Nevertheless, the global parameter of "Thoracic Kyphosis (ICT-ITL) (°)" revealed significant differences between the analyzed age cohorts caused by the significant age differences in the respective specific parameters of the upper thoracic spine. Sex differences in spinopelvic alignment and in per-level vertebral inclination have also been reported in healthy participants based on upright low-dose digital biplanar X-ray analyses [39]. Similar to the current study, more dorsally inclined vertebrae were found

in females than in males from T1 down to L2. In the current study, females showed more extended vertebral positions from T2 to L3 compared to their male counterparts. Even though the isolated raw values for vertebral inclination differed slightly between the two measurement approaches, the functional comparability of our results with those derived from X-ray analyses further supports the clinical importance of VRS as a non-invasive and simultaneously quick and easy assessment tool for spinal posture analysis in daily clinical routines.

However, despite the described functional agreement between the results based on the VRS and X-ray based measurements, the visual differences in the graphical data outputs between the analyzed subgroups could not be confirmed through statistical analyses for the specific spine parameters in the transverse or the coronal plane in the current study. One reason for this might be the large standard deviation identified in each of the analyzed variables. A normal spine anatomy also means that the results for the parameters in the transverse and the coronal planes are distribute naturally in a preferably narrow corridor reflecting an almost neutral spine position. No physiologically large differences are expected. Due to the high individuality displayed in the large standard deviation and those additional anatomical conditions, the analyzed sample of 201 healthy participants (and, partly, less than $n = 67$ in the respective subgroups) might have simply been too small to detect potential significant differences in the respective planes.

The fact that, in contrast, statistically significant trends in the possible differences between the analyzed subgroups were revealed for the parameters in the sagittal plane might be due to the presence of the two physiological major spinal curvatures, "thoracic kyphosis" and "lumbar lordosis". These anatomical conditions mean that there is a higher natural deviation from the neutral position throughout the whole vertebral column, making it easier to detect statistically significant deviations between the analyzed subgroups even in this "small" sample of 201 healthy participants.

The possibility that sagittal plane parameters will be suitable for detecting differences between subgroups and between different pathologies is in accordance with previously published research [40,41]. Artificial intelligence (AI)-driven analyses of VRS measurement results also found sagittal plane parameters to be one of the most important features with which to distinguish pathology-independent spinal posture data from healthy comparative datasets [41]. Similar results were found when dynamic VRS gait data were analyzed by AI-driven methods. Here, the parameters of the coronal and the sagittal planes were most relevant for the classifications between the sexes [40]. Whether or not sagittal spine parameters have the potential to systematically distinguish between physiological and pathological spinal postures and which parameters are specifically involved must be investigated further in the future. Nevertheless, the first results point in this direction.

4.3. Limitations

The manufacturer of the "Formetric III 4D" system recommends the use of reflective markers for spinal posture analysis only when the software is not able to identify the required visual landmarks (vertebra prominens (VP) and the two lumbar dimples (DM)) on its own. However, the use of three reflective markers for the landmarks is necessary for dynamic gait analysis. As this study is part of an overarching research project aiming to collect reference data for spinal posture in the habitual stance and when walking at four different walking speeds among the same healthy study cohort, it was necessary to mark all the participants with the three markers in order to render the stance and gait results comparable with each other. Software misinterpretations that arose in advance during the test measurements at the fast walking speeds, caused by the soft tissue and scapular motions of the participants' back surface, meant that the researchers decided to use two additional markers (~T3 and ~T12) to stabilize the systems' dynamic data analysis procedures. The researchers also decided to mark C7 and the PSIS instead of the VP and DM. This approach was chosen because marking C7 and the PSIS is recommended in cases where the VP and DM are not clearly identifiable on the surface of the participant's back.

In order to standardize the measuring procedure and to render the results as comparable to each other as possible, the marking of C7 and the PSIS was determined a priori for all the participants, even though this technique was definitely more prone to palpation bias [42,43]. Furthermore, only participants with a BMI of $\leq$30.0 kg/m^2 were included in the study due to data capture requirements. The procedures described enabled the collection of highly standardized data under controlled laboratory conditions. Nevertheless, the researchers are aware that this approach limits the external validity of the presented findings and, thus, their direct transferability to clinical practice.

The large number of parameters analyzed and the resulting high number of tested hypotheses also mean that the significant results have to be interpreted with caution. They are more suitable for showing trends in possible differences rather than real statistical significance. In this regard, it must also be mentioned that, retrospectively, the chosen sample size seemed to be too small to detect potential differences between the analyzed subgroups, especially for the specific spine parameters.

Finally, yet importantly, their radiation and contact-free nature mean that results derived from VRS measurements are calculated and based on mathematical algorithms. Even though their validity has been investigated in various publications, those studies mainly focused on comparisons between X-ray and VRS data captured from patients affected by different spinal pathologies (mainly scoliosis) [8,14,15,44,45]. For ethical reasons, no such comparative studies based on healthy participants are available. The results presented here, however, reveal a strong functional agreement with the results derived from clinically established measurement approaches, such as X-ray or MRI/CT scans, and VRS measurements [33,34,39]. This underlines the potential of VRS to serve as a non-invasive, quick and objective alternative for spinal posture analysis in clinical practice, especially when the therapeutic focus lies in function-orientated clinical outcomes and when pre-post measurements are required.

5. Conclusions

This study complements the existing VRS reference datasets for global spine parameters by adding normative values for different subgroups according to sex and age over an adult life span from 18 to 70 years. The closure of this gap, retrospectively, was found to be very important, because relevant changes over the life span in the isolated spine parameters became visible. Reference values for the specific spine parameters of every vertebral body from C7 to L4 in all three dimensions according to sex and age were presented and revealed visual but statistically non-significant differences between the analyzed subgroups. The sagittal plane parameters seem to have the greatest potential to detect differences between groups of participants. Whether or not those variations are possibly significant must be investigated in future studies by repeating the current project with an appropriate number of healthy participants.

The great variation in and individuality of the spinal posture displayed in the large standard deviation of the analyzed parameters, which was described previously by our research group using data derived from VRS measurements of asymptomatic female volunteers [24], were confirmed for the respective subgroups in the current study. Most importantly, and against widespread clinical expectations, the healthy human spine was found to be systematically asymmetric in the transverse and the coronal planes during upright habitual standing. There needs to be discussion in the therapeutic setting about whether approximations to an almost symmetrical spine in the respective planes are biomechanically desirable in any way [24].

Author Contributions: Conceptualization, J.H. and U.B.; methodology, J.H. and U.B.; software, J.K., C.W., R.W. and I.S.; validation, J.H., J.K., C.W., R.W. and I.S.; formal analysis, J.H., J.K., C.W., R.W. and I.S.; investigation, J.H.; resources, P.D. and U.B.; data curation, J.H., J.K., C.W., R.W. and I.S.; writing—original draft preparation, J.H.; writing—review and editing, J.K., C.W., R.W., I.S., P.D. and U.B.; visualization, J.H., J.K. and C.W.; supervision, J.K., P.D. and U.B.; project administration, J.K., P.D. and U.B. All authors have read and agreed to the published version of the manuscript.

Funding: This research received no external funding.

Institutional Review Board Statement: The study was conducted in accordance with the Declaration of Helsinki and was approved by the responsible ethics committee of the Rhineland-Palatinate Medical Association. The study is registered with the World Health Organization (WHO) (INT: DRKS00010834).

Informed Consent Statement: Informed consent was obtained from all subjects involved in the study.

Data Availability Statement: Due to ethical and privacy reasons, the data presented in this study are not publicly available.

Acknowledgments: The authors would like to express their gratitude to all the participants for their time and interest in participating in this study. Our colleagues are also acknowledged for their professional expertise and contributions to this project and their strong support during the participant recruitment process. Special thanks also go to Amira Basic and Kjell Heitmann (DIERS Company) for their technical support and assistance.

Conflicts of Interest: The authors declare no conflict of interest. Technical assistance was provided by staff members of the DIERS Company in preparation for the statistical data analysis process; however, there was no external influence on the design of the study; the collection, analysis, or interpretation of the data; the writing of the manuscript; or the decision to publish the results.

References

1. Dindorf, C.; Konradi, J.; Wolf, C.; Taetz, B.; Bleser, G.; Huthwelker, J.; Werthmann, F.; Drees, P.; Fröhlich, M.; Betz, U. Machine learning techniques demonstrating individual movement patterns of the vertebral column: The fingerprint of spinal motion. *Comput. Methods Biomech. Biomed. Eng.* **2021**, *25*, 821–831. [CrossRef] [PubMed]
2. Bundesärztekammer; Bundesvereinigung, K.; der Wissenschaftlichen, A.; Fachgesellschaften, M. *Nationale VersorgungsLeitlinie Nicht-spezifischer Kreuzschmerz—Langfassung*, 2nd ed.; Version 1; 2017; Available online: http://www.leitlinien.de/themen/kreuzschmerz (accessed on 11 December 2022). [CrossRef]
3. Fedorak, C.; Ashworth, N.; Marshall, J.; Paull, H. Reliability of the visual assessment of cervical and lumbar lordosis: How good are we? *Spine* **2003**, *28*, 1857–1859. [CrossRef] [PubMed]
4. Takatalo, J.; Ylinen, J.; Pienimäki, T.; Häkkinen, A. Intra- and inter-rater reliability of thoracic spine mobility and posture assessments in subjects with thoracic spine pain. *BMC Musculoskelet. Disord.* **2020**, *21*, 529. [CrossRef] [PubMed]
5. Mangone, M.; Paoloni, M.; Procopio, S.; Venditto, T.; Zucchi, B.; Santilli, V.; Paolucci, T.; Agostini, F.; Bernetti, A. Sagittal spinal alignment in patients with ankylosing spondylitis by rasterstereographic back shape analysis: An observational retrospective study. *Eur. J. Phys. Rehabil. Med.* **2020**, *56*, 191–196. [CrossRef] [PubMed]
6. Applebaum, A.; Ference, R.; Cho, W. Evaluating the role of surface topography in the surveillance of scoliosis. *Spine Deform.* **2020**, *8*, 397–404. [CrossRef] [PubMed]
7. Betsch, M.; Wild, M.; Rath, B.; Tingart, M.; Schulze, A.; Quack, V. Radiation-free diagnosis of scoliosis: An overview of the surface and spine topography. *Orthopade* **2015**, *44*, 845–851. [CrossRef] [PubMed]
8. Krott, N.L.; Wild, M.; Betsch, M. Meta-analysis of the validity and reliability of rasterstereographic measurements of spinal posture. *Eur. Spine J.* **2020**, *29*, 2392–2401. [CrossRef]
9. Drerup, B.; Hierholzer, E. Evaluation of frontal radiographs of scoliotic spines—Part I measurement of position and orientation of vertebrae and assessment of clinical shape parameters. *J. Biomech.* **1992**, *25*, 1357–1362. [CrossRef]
10. Drerup, B.; Hierholzer, E. Evaluation of frontal radiographs of scoliotic spines—Part II: Relations between lateral deviation, lateral tilt and axial rotation of vertebrae. *J. Biomech.* **1992**, *25*, 1443–1450. [CrossRef]
11. Drerup, B.; Hierholzer, E. Back shape measurement using video rasterstereography and three-dimensional reconstruction of spinal shape. *Clin. Biomech.* **1994**, *9*, 28–36. [CrossRef]
12. Drerup, B.; Ellger, B.; Meyer zu Bentrup, F.M.; Hierholzer, E. Functional rasterstereographic images. A new method for biomechanical analysis of skeletal geometry. *Orthopade* **2001**, *30*, 242–250. [CrossRef] [PubMed]
13. Drerup, B. Rasterstereographic measurement of scoliotic deformity. *Scoliosis* **2014**, *9*, 22. [CrossRef] [PubMed]
14. Mohokum, M.; Mendoza, S.; Udo, W.; Sitter, H.; Paletta, J.R.; Skwara, A. Reproducibility of rasterstereography for kyphotic and lordotic angles, trunk length, and trunk inclination: A reliability study. *Spine* **2010**, *35*, 1353–1358. [PubMed]
15. Mohokum, M.; Schülein, S.; Skwara, A. The validity of rasterstereography: A systematic review. *Orthop. Rev.* **2015**, *7*, 68–73. [CrossRef]
16. Schulte, T.L.; Hierholzer, E.; Boerke, A.; Lerner, T.; Liljenqvist, U.; Bullmann, V.; Hackenberg, L. Raster stereography versus radiography in the long-term follow-up of idiopathic scoliosis. *J. Spinal Disord Tech.* **2008**, *21*, 23–28. [CrossRef]

17. Tabard-Fougere, A.; Bonnefoy-Mazure, A.; Hanquinet, S.; Lascombes, P.; Armand, S.; Dayer, R. Validity and Reliability of Spine Rasterstereography in Patients With Adolescent Idiopathic Scoliosis. *Spine* **2017**, *42*, 98–105. [CrossRef]
18. Furian, T.C.; Rapp, W.; Eckert, S.; Wild, M.; Betsch, M. Spinal posture and pelvic position in three hundred forty-five elementary school children: A rasterstereographic pilot study. *Orthop. Rev.* **2013**, *5*, e7. [CrossRef]
19. Michalik, R.; Hamm, J.; Quack, V.; Eschweiler, J.; Gatz, M.; Betsch, M. Dynamic spinal posture and pelvic position analysis using a rasterstereographic device. *J. Orthop. Surg. Res.* **2020**, *15*, 389. [CrossRef]
20. Schröder, J.; Stiller, T.; Mattes, K. Reference data for spine shape analysis. Approaching a majority norm and deviations for unspecific low back pain. *Man. Med.* **2011**, *49*, 161–166. [CrossRef]
21. Schröder, J.; Braumann, K.M.; Reer, R. Wirbelsäulenform- und Funktionsprofile. *Orthopäde* **2014**, *43*, 841–849. [CrossRef]
22. Degenhardt, B.F.; Starks, Z.; Bhatia, S.; Franklin, G.-A. Appraisal of the DIERS method for calculating postural measurements: An observational study. *Scoliosis Spinal Disord.* **2017**, *12*, 28. [CrossRef] [PubMed]
23. Degenhardt, B.F.; Starks, Z.; Bhatia, S. Reliability of the DIERS Formetric 4D Spine Shape Parameters in Adults without Postural Deformities. *Biomed. Res. Int.* **2020**, *2020*, 1796247. [CrossRef] [PubMed]
24. Wolf, C.; Betz, U.; Huthwelker, J.; Konradi, J.; Westphal, R.S.; Cerpa, M.; Lenke, L.; Drees, P. Evaluation of 3D vertebral and pelvic position by surface topography in asymptomatic females: Presentation of normative reference data. *J. Orthop. Surg. Res.* **2021**, *16*, 703. [CrossRef] [PubMed]
25. Bischoff, H.A.; Stahelin, H.B.; Monsch, A.U.; Iversen, M.D.; Weyh, A.; von Dechend, M.; Akos, R.; Conzelmann, M.; Dick, W.; Theiler, R. Identifying a cut-off point for normal mobility: A comparison of the timed 'up and go' test in community-dwelling and institutionalised elderly women. *Age Ageing* **2003**, *32*, 315–320. [CrossRef]
26. Bohannon, R.W.; Wang, Y.C.; Gershon, R.C. Two-minute walk test performance by adults 18 to 85 years: Normative values, reliability, and responsiveness. *Arch. Phys. Med. Rehabil.* **2015**, *96*, 472–477. [CrossRef]
27. Myklebust, M.; Magnussen, L.; Inger Strand, L. Back Performance Scale scores in people without back pain: Normative data. *Adv. Physiother.* **2009**, *9*, 2–9. [CrossRef]
28. Perry, J.; Burnfield, J.M. *Gait Analysis—Normal and Pathological Function*, 2nd ed.; SLACK Incorporated: Thorofare, NJ, USA, 2010.
29. Betsch, M.; Michalik, R.; Graber, M.; Wild, M.; Krauspe, R.; Zilkens, C. Influence of leg length inequalities on pelvis and spine in patients with total hip arthroplasty. *PLoS ONE* **2019**, *14*, e0221695. [CrossRef]
30. Schroeder, J.; Schaar, H.; Mattes, K. Spinal alignment in low back pain patients and age-related side effects: A multivariate cross-sectional analysis of video rasterstereography back shape reconstruction data. *Eur. Spine J.* **2013**, *22*, 1979–1985. [CrossRef]
31. Schulte, T.L.; Liljenqvist, U.; Hierholzer, E.; Bullmann, V.; Halm, H.F.; Lauber, S.; Hackenberg, L. Spontaneous correction and derotation of secondary curves after selective anterior fusion of idiopathic scoliosis. *Spine* **2006**, *31*, 315–321. [CrossRef]
32. Arshad, R.; Pan, F.; Reitmaier, S.; Schmidt, H. Effect of age and sex on lumbar lordosis and the range of motion. A systematic review and meta-analysis. *J. Biomech.* **2019**, *82*, 1–19. [CrossRef]
33. Zappalá, M.; Lightbourne, S.; Heneghan, N.R. The relationship between thoracic kyphosis and age, and normative values across age groups: A systematic review of healthy adults. *J. Orthop. Surg. Res.* **2021**, *16*, 447. [CrossRef] [PubMed]
34. Kouwenhoven, J.W.; Vincken, K.L.; Bartels, L.W.; Castelein, R.M. Analysis of preexistent vertebral rotation in the normal spine. *Spine* **2006**, *31*, 1467–1472. [CrossRef] [PubMed]
35. Kouwenhoven, J.W.; Bartels, L.W.; Vincken, K.L.; Viergever, M.A.; Verbout, A.J.; Delhaas, T.; Castelein, R.M. The relation between organ anatomy and pre-existent vertebral rotation in the normal spine: Magnetic resonance imaging study in humans with situs inversus totalis. *Spine* **2007**, *32*, 1123–1128. [CrossRef] [PubMed]
36. Kilshaw, M.; Baker, R.P.; Gardner, R.; Charosky, S.; Harding, I. Abnormalities of the lumbar spine in the coronal plane on plain abdominal radiographs. *Eur. Spine. J.* **2011**, *20*, 429–433. [CrossRef] [PubMed]
37. Sebaaly, A.; Silvestre, C.; Rizkallah, M.; Grobost, P.; Chevillotte, T.; Kharrat, K.; Roussouly, P. Revisiting thoracic kyphosis: A normative description of the thoracic sagittal curve in an asymptomatic population. *Eur. Spine J.* **2021**, *30*, 1184–1189. [CrossRef] [PubMed]
38. Lafage, R.; Steinberger, J.; Pesenti, S.; Assi, A.; Elysee, J.C.; Iyer, S.; Lenke, L.G.; Schwab, F.J.; Kim, H.J.; Lafage, V. Understanding Thoracic Spine Morphology, Shape, and Proportionality. *Spine* **2020**, *45*, 149–157. [CrossRef]
39. Janssen, M.M.; Drevelle, X.; Humbert, L.; Skalli, W.; Castelein, R.M. Differences in male and female spino-pelvic alignment in asymptomatic young adults: A three-dimensional analysis using upright low-dose digital biplanar X-rays. *Spine* **2009**, *34*, E826–E832. [CrossRef]
40. Dindorf, C.; Konradi, J.; Wolf, C.; Taetz, B.; Bleser, G.; Huthwelker, J.; Drees, P.; Fröhlich, M.; Betz, U. General method for automated feature extraction and selection and its application for gender classification and biomechanical knowledge discovery of sex differences in spinal posture during stance and gait. *Comput. Methods Biomech. Biomed. Eng.* **2020**, *24*, 299–307. [CrossRef]
41. Dindorf, C.; Konradi, J.; Wolf, C.; Taetz, B.; Bleser, G.; Huthwelker, J.; Werthmann, F.; Bartaguiz, E.; Kniepert, J.; Drees, P.; et al. Classification and Automated Interpretation of Spinal Posture Data Using a Pathology-Independent Classifier and Explainable Artificial Intelligence (XAI). *Sensors* **2021**, *21*, 6323. [CrossRef]
42. Cooperstein, R.; Hickey, M. The reliability of palpating the posterior superior iliac spine: A systematic review. *J. Can. Chiropr. Assoc.* **2016**, *60*, 36–46.

43. Póvoa, L.C.; Ferreira, A.P.A.; Zanier, J.F.C.; Silva, J.G. Accuracy of Motion Palpation Flexion-Extension Test in Identifying the Seventh Cervical Spinal Process. *J. Chiropr. Med.* **2018**, *17*, 22–29. [CrossRef] [PubMed]
44. Schülein, S.; Mendoza, S.; Malzkorn, R.; Harms, J.; Skwara, A. Rasterstereographic Evaluation of Interobserver and Intraobserver Reliability in Postsurgical Adolescent Idiopathic Scoliosis Patients. *J. Spinal. Disord. Tech.* **2013**, *26*, E143–E149. [CrossRef] [PubMed]
45. Tabard-Fougere, A.; Bonnefoy-Mazure, A.; Dhouib, A.; Valaikaite, R.; Armand, S.; Dayer, R. Radiation-free measurement tools to evaluate sagittal parameters in AIS patients: A reliability and validity study. *Eur. Spine J.* **2019**, *28*, 536–543. [CrossRef] [PubMed]

2.2 Reference values and functional descriptions of transverse plane spinal dynamics during gait based on surface topography

Human Movement Science 88 (2023) 103054

Contents lists available at ScienceDirect

Human Movement Science

journal homepage: www.elsevier.com/locate/humov

Reference values and functional descriptions of transverse plane spinal dynamics during gait based on surface topography

Janine Huthwelker [a], Jürgen Konradi [a], Claudia Wolf [a], Ruben Westphal [b], Irene Schmidtmann [b], Patric Schubert [c], Philipp Drees [d], Ulrich Betz [a,*]

[a] Institute of Physical Therapy, Prevention and Rehabilitation, University Medical Center of the Johannes Gutenberg University Mainz, Langenbeckstrasse 1, D-55131 Mainz, Germany
[b] Institute of Medical Biostatistics, Epidemiology and Informatics, University Medical Center of the Johannes Gutenberg University Mainz, Obere Zahlbacher Straße 69, D-55131 Mainz, Germany
[c] Institute of Complex Health Sciences, Hochschule Fresenius, University of Applied Sciences, Limburgerstr. 2, D-65510 Idstein, Germany
[d] Department of Orthopedics and Trauma Surgery, University Medical Center of the Johannes Gutenberg University Mainz, Langenbeckstrasse 1, D-55131 Mainz, Germany

ARTICLE INFO

Keywords:
Videorasterstereography
Gait analysis
Motion analysis
Normative values
Healthy human spine

ABSTRACT

Spinal dynamics during gait have been of interest in research for many decades. Based on respective previous investigations, the pelvis is generally expected to be maximally forward rotated on the side of the reference leg at the beginning of each gait cycle and to reach its maximum counterrotation approximately at the end of the reference leg's stance phase. The pelvic–upper-thoracic-spine coordination converges towards an anti-phase movement pattern in high velocities during ambulation. The vertebral bodies around the seventh thoracic vertebra are considered to be an area of transition during human ambulation where no or at least little rotary motion can be observed. The respective cranial and caudal vertebrae meanwhile are expected to rotate conversely around this spinal point of intersection. However, these previous assumptions are based on scarce existing research, whereby only isolated vertebrae have been analyzed contemporaneously. Due to huge methodological differences in data capturing approaches, the results are additionally hardly comparable to each other and involved measurement procedures are often not implementable in clinical routines. Furthermore, none of the above-mentioned methods provided reference data for spinal motion during gait based on an appropriate number of healthy participants. Hence, the aim of this study was to present such reference data for spinal rotary motion of every vertebral body from C7 down to L4 and the pelvis derived from surface topographic back shape analyses in a cohort of 201 healthy participants walking on a treadmill at a given walking speed of 5 km/h. Additionally, the spine's functional movement behavior during gait should be described in the transverse plane based on data derived from this noninvasive, clinically suitable measurement approach and, in conclusion, the results shall be compared against those of previous research findings derived from other measurement techniques. Contrary to the previous functional understanding, the area of the mid-thoracic spine was found to demonstrate the largest amplitude of rotary motion of all investigated vertebrae and revealed an approximately counterrotated movement behavior compared to the rotary motion of the pelvis. In both directions, spinal rotation during gait seemed to be initiated by the pelvis. The overlying vertebrae followed in succession in the sense of an ongoing movement. Therefore, the

* Corresponding author.
E-mail address: Ulrich.Betz@unimedizin-mainz.de (U. Betz).

https://doi.org/10.1016/j.humov.2022.103054
Received 10 June 2022; Received in revised form 30 November 2022; Accepted 26 December 2022
Available online 6 January 2023

point of intersection was not statically located in a specific anatomical section of the spine. Instead, it was found to be dynamic, ascending from one vertebra to the next from caudal to cranial in dependence of the pelvis's rotation initiation.

1. Introduction

Back pain is still a health problem of outstanding medical, epidemiological and economical importance (Raspe, 2012) and asymmetrical, respectively irregular movement patterns or changes in the pelvic–thorax coordination during gait are associated with low-back pain disorders (Kakushima, Miyamoto, & Shimizu, 2003; Lamoth et al., 2002; Vogt, Pfeifer, Portscher, & Banzer, 2001). However, even for the healthy population there is no proper understanding of the precise motion pattern of each individual vertebral body during gait. So far, the literature only provides a rough functional framework whose details remain unclear. The pelvis is generally expected to reach its maximally forward rotated position on the side of the reference leg at the beginning of each gait cycle (initial contact) and to reach its maximum counterrotation at the end of the reference leg's stance phase (terminal stance) (Perry & Burnfield, 2010). The pelvis–thorax coordination (measured between the pelvis and the anatomical height of the shoulders) evolves from an in-phase towards an almost anti-phase movement pattern with increasing velocity during ambulation (1.4 km/h – 5.4 km/h) (Lamoth, Beek, & Meijer, 2002). Additionally, an early invasive measurement approach, using Steinmann pins and a relative-rotation transducer, found the seventh thoracic vertebra to be an area of transition during human ambulation, where no, or at least little, rotary motion can be observed (Gregersen & Lucas, 1967). The pelvis and the lumbar spine were described to be forwardly rotated at heel strike in terms of a functional unit. Further up, the rotation of the lower thoracic spine diminishes gradually until zero degrees at the seventh thoracic vertebra. The counterrotation of the upper-thoracic spine gradually increased from the seventh thoracic vertebra upwards and reached its maximum at the first thoracic vertebra. Needham et al. (Needham, Naemi, Healy, & Chockalingam, 2016) investigated three isolated vertebrae using an optoelectronic motion capturing device (T3, T8 and L3) and also found the mid-thoracic vertebra to be the one with the least rotational movement. These findings correspond with commonly used and widely accepted visual observation criteria in clinical gait analysis: In functional kinetics, for example, the "hypothetical standard" for human gait also expects the "frontotransverse diameter of the thorax" (~T7) to be dynamically stabilized rectangular to the direction of movement (Suppé, 2014; Suppé & Bongarz, 2013). Those findings support the assumption that in healthy individuals the vertebrae below the mid-thoracic spine (~T7) are expected to gradually increase their rotation downwards until the maximum rotation of the pelvis is achieved. In contrast, the vertebrae above ~T7 are expected to gradually increase their rotation in the opposite direction to enable and facilitate the typical counterrotation of the shoulder-girdle during gait.

Challenging results of this presumption came from Bruijn, Meijer, van Dieen, Kingma, and Lamoth (2008), who analyzed transverse plane pelvis and thorax rotations in relation to movements of the upper leg. Among others, they measured three-dimensional trunk movements by a 3D-cluster of infrared LEDs at the anatomic level of T6. Thereby the authors revealed that with increasing walking speed (2.0 km/h – 5.2 km/h), the pelvis–thorax coordination shifted from in-phase to out of phase with increasing gait velocity. As T6 represented thorax rotations, these findings provided initial indications that the vertebral bodies of the mid-thoracic spine might possibly not be the described area of transition during human gait where no or at least only little rotary motion occurs.

Nevertheless, based on huge methodological differences the results of previous research are hardly comparable to each other and, to the authors' knowledge, there are currently no reference data addressing the three-dimensional movement behavior of every single vertebra of the healthy human spine during gait in relation to a standardized gait cycle (SGC) available. So far, either only isolated/multiple spinal vertebrae have been marked and analyzed (Ceccato, de Seze, Azevedo, & Cazalets, 2009; D'Amico, D'Amico, Paniccia, Roncoletta, & Vallasciani, 2010; D'Amico, Kinel, D'Amico, & Roncoletta, 2021; Konz et al., 2006; Needham, Naemi, et al., 2016) or the vertebral column has been subdivided into large anatomic sections, respectively encompassing several vertebrae ("lumbar spine," "thorax," "trunk," etc.), which were regarded as almost rigid bodies in themselves and whose three-dimensional movement behavior during gait had then been described in multiple planes (Crosbie, Vachalathiti, & Smith, 1997; Feipel, De Mesmaeker, Klein, & Rooze, 2001; MacWilliams et al., 2013; Needham, Stebbins, & Chockalingam, 2016; Perry & Burnfield, 2010).

Additionally, invasive and noninvasive measurement approaches have to be distinguished from each other. MacWilliams et al. (2013) analyzed three-dimensional spinal movements during gait by inserting bone pins into the spinal process of each lumbar vertebra and attaching reflective markers laterally on the protruding pins. This procedure can theoretically be considered as a gold standard for motion analysis of spinal bony structures (Needham, Stebbins, & Chockalingam, 2016). However, by reasons of the surgical intervention and the required radiation exposure to control for the correct position of the pins, this approach is, just like the invasive procedure from Gregersen and Lucas (1967), inappropriate for use as a routine assessment in clinical as well as in scientific practice. Furthermore, the results have to be interpreted with caution because the participants' movement behavior might have been influenced by pain- or fear-induced inhibition of habitual movement patterns due to the surgical interventions.

In contrast, noninvasive reflective marker-based systems attached on the skin's surface, which are generally accepted to be the gold standard for three-dimensional analyses of human movements in clinical as well as in scientific practice (Needham, Stebbins, & Chockalingam, 2016), contain several limitations that have specifically been described for applications in the field of spinal motion analysis, and thereby particularly for data capturing in the transverse plane. These limitations include that for data capturing in the transverse plane each single vertebra of interest needs to be marked with three noncollinear markers (or a 3D cluster), respectively (Konz et al., 2006; Needham, Stebbins, & Chockalingam, 2016). Due to the small anatomic size of functional spinal units and the large number of required markers/3D-clusters to analyze every single vertebral body, the usability of marker-based technologies is limited

(Konz et al., 2006). Additionally, a large number of anatomic landmarks that have to be palpated and marked raise further difficulties (Chockalingam, Dangerfield, Giakas, & Cochrane, 2002) and the use of numerous 3D-clusters, even though they are from lightweight materials, is vulnerable to perturbations from impact forces created during walking (Needham, Stebbins, & Chockalingam, 2016). Such perturbations might possibly add up with other described and known effects of soft-tissue artifacts derived from marker-based motion analysis systems (Leardini, Chiari, Della Croce, & Cappozzo, 2005).

The ability, however, to further investigate spinal motion during gait by use of a suitable measurement tool able to capture three-dimensional motion of all vertebral bodies contemporaneously without usage of multiple markers, extensive preparation or the need for invasive or radiation-based measurement approaches would be of great value for the transferability of results into clinical practice as well as for future research. It could gain further knowledge of the healthy spine's functional movement behavior during gait and of the effects that different pathologies might possibly have on those movement patterns.

Surface topography (ST) might be just such a noninvasive and radiation-free alternative. It is based upon a stereophotogrammetric surface measurement approach, considers the Turner–Smith model (Turner-Smith, 1988; Turner-Smith, Harris, Houghton, & Jefferson, 1988), as well as the models of Drerup and Hierholzer (Drerup, 1993; Hierholzer, 1993) to not only analyze the participants' back surface, but also to precisely estimate every underlying vertebral body's position (C7–L4) and the pelvis in a virtually constructed three-dimensional model of the human spine (Drerup, Ellger, Meyer Zu Bentrup, & Hierholzer, 2001; Drerup & Hierholzer, 1994). During the last decades, ST was only applicable for static assessments of spinal posture and was predominantly used for the monitoring of progression in adolescent idiopathic scoliosis (Liljenqvist, Halm, Hierholzer, Drerup, & Weiland, 1998; Schulte et al., 2008) and recently also for pathology independent classifications (Dindorf et al., 2021a). In the static context, the system has been investigated in a series of studies and has proven to be valid and highly reliable in the estimation of segment-related spinal posture based on back surface information when compared with the clinical gold standard (x-ray imaging) (Krott, Wild, & Betsch, 2020; Mohokum et al., 2010; Mohokum, Schülein, & Skwara, 2015).

Meanwhile, ST is also applicable for the evaluation of spinal motion during gait due to technical and mathematical development. Its validity in marker detection and reproducibility in dynamic assessments has already been demonstrated (Betsch et al., 2011; Betsch et al., 2013; Gipsman, Rauschert, Daneshvar, & Knott, 2014). However, even though exploratory artificial intelligence (AI) -driven analyses were used to map gender differences (Dindorf et al., 2020) and to identify individuals based on dynamic ST data (Dindorf et al., 2021b), the dynamic ST measurement approach is still predominantly used for evaluations of global spine parameters (Gipsman et al., 2014; Michalik et al., 2019; Michalik et al., 2020). To the authors' knowledge, only one further article, which mainly focused on comprehensive visualization tools to facilitate data interpretation of ST measurements, presented data of isolated spinal movements of individual vertebrae in temporal relation to the gait cycle based on a small sample of 12 healthy participants (Haimerl et al., 2022).

Hence, the aim of this study was to present reference data for rotary spinal motion of every vertebral body from C7 down to L4 and the pelvis, derived from ST back shape analyses in a cohort of 201 healthy participants walking on a treadmill at a given walking speed of 5 km/h. Additionally, the spine's functional movement behavior during gait should be described in the transverse plane.

2. Methods

The present investigation followed the design of a prospective, explorative, cross-sectional study. Participants were included if they were aged 18 to 70 years, were free of pain at the moment of data collection and had no history of surgery or fracture between the spinal segments of C7 and the pelvis. They had no medical or therapeutic treatment due to spinal or pelvic girdle complaints (C7-pelvis) within the last 12 months and no medical or therapeutic treatment due to musculoskeletal problems (musculoskeletal system except C7-pelvis) within the last 6 months prior to the investigation. All participants had a body mass index (BMI) of $\leq$30.0 kg/m^2 (due to data capturing requirements), demonstrated an adequate gait stability (Timed-up-and-Go test (Bischoff et al., 2003)), an age- and sex-accorded walking speed (Two-Minute Walk test (Bohannon, Wang, & Gershon, 2015)) and spinal function (Back Performance Scale (Myklebust, Magnussen, & Inger Strand, 2009)) as well as an appropriate joint mobility to theoretically be able to perform a physiological gait pattern (Perry & Burnfield, 2010). The study was approved by the responsible ethics committee at the Rhineland-Palatinate Medical Association in Germany and is registered with the World Health Organization (WHO) (INT: DRKS00010834).

Based on a statistical sample size calculation, 201 healthy participants (sex ratio 2/3 to 1/3) were included who gave their informed consent prior to participation. Further details of participants' biometric characteristics are presented in Table 1. The sample size of n = 201 participants has been chosen to ensure sufficient accuracy for the limits of 95% reference ranges. It was planned to determine 95%

Table 1
Biometric characteristics of the included participants (n = 201).

Characteristics	Participants (n = 201)
Age (years):	
mean (±SD)	41.3 years (±13.4 years)
range	18–70 years
Sex (n):	
female (%)	n = 132 (65.7%)
male (%)	n = 69 (34.3%)
BMI (kg/m^2):	
mean (±SD)	23.5 kg/m^2 (±2.8 kg/m^2)
range	17.5–29.9 kg/m^2

reference ranges for all clinically relevant spinal parameters within each of the three planned age cohorts and to limit those reference ranges by 2.5% and 97.5% percentile curves. To ensure the reference range's width is not too large in direct proportion to the width of the confidence interval, a sample size of 66–67 participants per age cohort (young age cohort (18–30 years), middle age cohort (31–50 years) and old age cohort (51–70 years)) has been chosen, which resulted in a respective width-proportion of 0.175 (Troendle & Yu, 2003).

Data were captured using the ST DIERS formetric III 4D™ measuring device (software versions DICAM 3.7.1.7 for data collection and DICAM v3.5.0Beta11 for data export). The measurement approach is based on the principle of triangulation (Drerup, 2014). A slide projector is used as the optical equivalent to an inverse camera and projects horizontal and parallel lines on the unclothed back, while the participants are walking on a treadmill at a predefined distance from the measuring device. An additional camera system contemporaneously records the transformed line pattern (due to the participant's individual back surface curvatures) with a frequency of 60 Hz. By means of a software integrated algorithm, a three-dimensional scatter plot is created, which is comparable to a virtual plaster cast of the participant's individual back surface (consisting of up to 150,000 individual data points, depending on body size). Based on a clinically validated correlational model, the measuring system estimates the three-dimensional position of the underlying spinal segments continuously based on back surface information (Drerup, 2014; Drerup et al., 2001; Drerup & Hierholzer, 1994) (Fig. 1).

With a frequency of 100 Hz, a synchronized, treadmill-integrated foot pressure measuring system (Zebris FDM) enabled the automatic detection of initial and terminal contacts of the feet, required for later gait cycles analyses.

In contrast to static measurements, scattered reflective markers were required for dynamic analyses. For this reason, all participants were marked with seven reflective markers prior to data capturing (on the spinal process of C7, the spinous processes between the medial parts of the spinae scapulae (~T3) and the thoracolumbar transitions (~T12), the left and right posterior superior iliac spine (PSIS) and on both acromia). Palpation and marker attachments were always performed by the same investigator (physical therapist) following a standardized protocol for best possible control for potential palpation bias. To verify the correct placement of markers, a static control scan of the participant's back surface has been performed prior to data collection. In case of clinically inconclusive measurement results, marker placements had been checked, palpated again and corrected if necessary. Once the final position of markers was fixed, they were not changed for the duration of data collection.

To become familiar with the treadmill and the measuring environment, all participants completed a standardized warm-up procedure. They were asked to walk on the treadmill without using the handrail at a given walking speed of 3.5 km/h for 3 min. Afterwards the velocity was slowed down to 2 km/h and accelerated every 30 s by 1 km/h until the highest predefined walking speed (5 km/h) was reached and maintained for further 30 s.

During data collection, participants were barefoot and only wore short sports pants; the upper body was bare due to metrological reasons. Participants with long hair were asked to put their hair up, to allow the measurement system to detect the neck contour and the C7 marker. After a static scan in an upright standing position with eyes looking at a standardized point ~2 m away and 20 cm below each individual's body height, the three-dimensional vertebral body-related movement behavior was captured at four gait velocities (2 km/h, 3 km/h, 4 km/h and 5 km/h) in randomized order from every participant with the same standardization of viewing direction. Three complete gait cycles, starting with initial contact of the right foot, were recorded subsequently for a familiarization period of two minutes walking at the respective walking speed. Participants were not explicitly informed about the start of data recording after the familiarization period to ensure a preferably habitual gait performance.

In case of directly apparent software misinterpretations or other inconsistent, clinically not comprehensible measuring artifacts in evidence of the data output, the respective measurement has been repeated. After completion of the data collection phase, the investigator and an additional technician, who was highly familiar with the software and the measuring system, inspected all videos and the graphical data output visually for reasons of quality assurance, to check for further abnormal spinal movements or other measuring artifacts and to correct them if necessary.

Using a data export interface with the DICAM v3.5.0Beta11 software that was developed in close collaboration with the

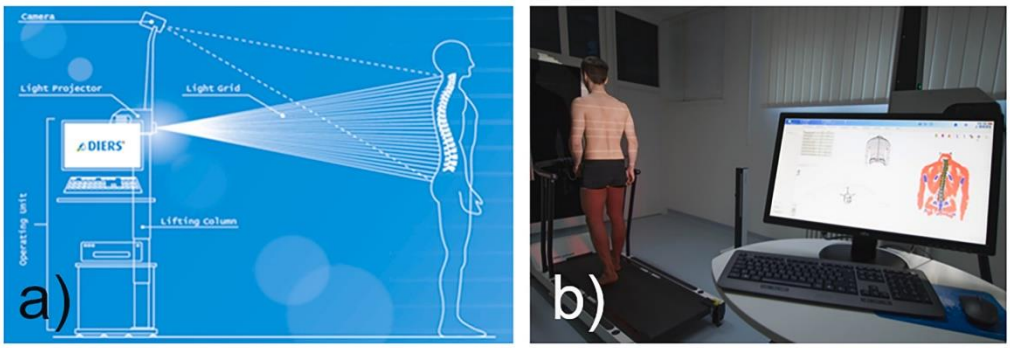

Fig. 1. a) Schematic illustration of the ST measurement device; b) ST measurement of a participant.

Table 2
Number of shifted values on the SGC-axis and the respective formula used.

	C7	T1	T2	T3	T4	T5	T6	T7	T8	T9	T10	T11	T12	L1	L2	L3	L4	Pel
Formula:	93	83	76	75	74	82	83	86	87	80	74	67	54	37	15	8	3	4
if value ≤ cut-off value, then + 101	(29)	(31)	(13)	(12)	(10)	(9)	(8)	(9)	(9)	(10)	(10)	(10)	(16)	(18)	(7)	(9)	(14)	(16)
Formula:	0	3	2	0	0	0	0	0	0	0	0	0	0	1	3	6	16	37
if value > cutoff value, then − 101		(96)	(96)											(95)	(96)	(96)	(88)	(91)

Note. Cutoff values are presented in brackets ().

manufacturing company of the Formetric®-System (DIERS International GmbH) it was possible to export ST vertebral body-related raw data in all three dimensions, respectively, and in temporal relation to the actual phase of the gait cycle as .csv files from the DICAM software.

For data preprocessing, the Statistical Analysis System (SAS version 9.4) was used to standardize the data by transforming time stamps of measurements from seconds to the completed percentage of each individual gait cycle and averaging the results over all three recorded gait cycles. Due to the application of interpolating splines, smoothed and averaged data curves of measured rotation over gait cycle percentages were obtained for each individual vertebra and the pelvis. A regression model was used for interpolation of the individual's respective value for a scale reaching from 0 to 100 as a percentage (standardized gait cycle (SGC)). This allowed for the comparison of various data points of interest, irrespective of the individual's scale of the gait cycle. For the following descriptive analyses, the SGC of the right reference leg was evaluated at all integer percentage values between 0% and 100%, making it possible to compare the segment-related spinal movements between different individuals (Betz et al., 2018). Repositories, containing the respective SAS and SPSS scripts are accessible (Konradi, 2022a, 2022b, 2022c, 2022d; Schmidtmann & Konradi, 2022; Westphal & Konradi, 2022).

Because of the cyclical nature of gait cycle data, the distribution of each parameter of interest within the cycle had to be taken into account for further statistical analyses. This meant that for parameters that were distributed around the beginning and end of the gait cycle, the timescale was shifted in order to yield continuous distributions of these parameters. This was necessary, for example, for calculations of mean times within the gait cycle, e.g., in a situation where half the rotation maxima lay between 90% and 100% and the other half lay between 0% and 10%. The shift was done manually for each parameter and according to predefined rules. These contained that the largest gap between two different data points within the SGC data sets was defined for every analyzed vertebra and the pelvis and for both directions of movement (left and right rotation). Once the largest gap was found (at least $\geq$10 percentage values), it was used to divide the respective set of data into two groups. Depending on whether the majority of data points of the larger group were located within the first (0%–50%) or the second half (50%–100%) of the SGC, the data points of the smaller group were shifted by either adding or subtracting 101 percentage values on the x-axis to move them respectively to the end or to the beginning of the SGC. The chosen approach was deemed more efficient and reliable than implementing additional cyclical data analysis methods.

Afterwards, 95% prediction ellipses, mean values and the 2.5% and 97.5% percentiles were calculated for the respective sets of data. To enable a better traceability of the chosen approach, the x-axis (SGC) had been adjusted accordingly for the relevant graphical presentations (reaching now from −20% to 140%). Additionally, the number of affected values that had been shifted was indicated for the respective vertebrae and for both directions of movement (Table 2). Descriptive data analysis was performed using Statistical Package of the Social Sciences (SPSS version 23) and Microsoft Excel (version 2016).

To give a comprehensive overview across one dimension of movement, the following analyses and presentations of results will solely focus on vertebral body-related motion data from the transverse plane, as, on the one hand, this turned out to be the most difficult one to measure with the current commonly used motion capturing devices. On the other hand, ST transverse plane analyses

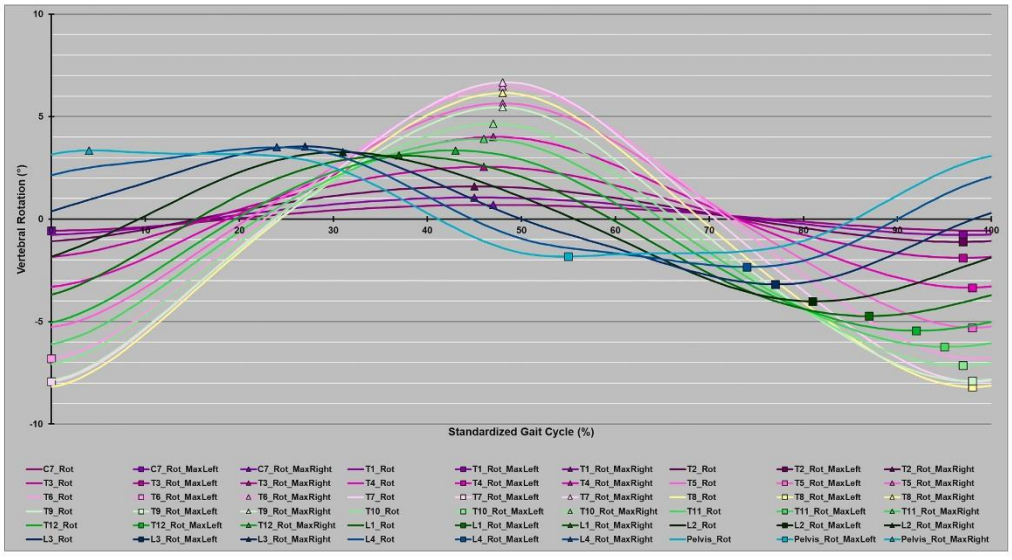

Fig. 2. Mean rotation curves of all investigated vertebrae and the pelvis within one SGC.
Note. Mean rotation curves are marked with their respective maximum of left (▲) and right (■) -side rotation (y-axis (−10°/+10°); x-axis (0%–100%)).

demonstrated the lowest standard error of the mean and therewith higher accuracy compared to the two other planes of movement for dynamic analyses in previous research (Gipsman et al., 2014). Additionally, evaluations will solely concentrate on data derived from a gait velocity of 5 km/h. Future analyses, however, will also address the remaining two axes of motion and the remaining measured gait velocities (2 km/h, 3 km/h and 4 km/h). Furthermore, subgroup analyses will look for possible differences in spinal motion patterns between male and female participants as well as between participants of different age cohorts within the presented study population. In addition, reference values for static spinal posture have recently been published based on the present set of data for the above-described subgroups as well (Huthwelker et al., 2022).

3. Results

For a gait velocity of 5 km/h, the mean curves of all investigated vertebrae and their respective maximum values of right- and left-side vertebral rotation within the SGC derived from 201 healthy participants are presented in Fig. 2. Fig. 3 shows the same data, but presents the averaged rotation of every investigated vertebra and the pelvis in anatomical order from cranial to caudal in a single SGC, respectively, in the style of the visualization approach from Haimerl et al. (2022).

For better interpretability and to address inter-individual variances, Fig. 4 and Video 1 show the isolated mean curve progressions of every investigated vertebra and the pelvis, complemented by the 2.5% and 97.5% percentile curves (for numerical displays see Table 3).

The graphical data output revealed almost sinusoidal curve oscillations for rotary spinal motion in all anatomic heights. Only one maximum for right- and left-side vertebral rotation can be seen within the SGC over all investigated vertebrae and for the pelvis itself. The mean curves, however, did not oscillate completely uniformly around 0° but were instead slightly shifted towards a negative (right side) vertebral rotation (Figs. 2 and 3; Video 1; Table 3).

In the cervicothoracic region, very little rotary motion was observed and maximum values could hardly be defined. Beginning with the third thoracic vertebra, the rotary amplitude of the respective oscillations started to increase and reached its largest extent around the mid-thoracic spine (T7 and T8). Afterwards, the extent of the rotary movement amplitude diminished again for the lower-lying vertebrae and for the pelvis itself. For the mid- and lower-thoracic spine the respective curves' apexes were clearly identifiable. The vertebrae of the lumbopelvic region, however, demonstrated a plateau formation for both sides of rotary curve progressions, making it more difficult to explicitly identify the respective curves' extreme values.

When looking at the time course of appearances of the movement curves' vertices, it can be seen that the pelvis reached its curve maximum almost at the beginning of the SGC (4%), as the first of all investigated structures. The overlying vertebrae until the lumbothoracic transition (L4–T12) followed in succession. The mid-thoracic vertebrae (T11–T3) achieved their maximum values almost simultaneously around 46%–48% of the SGC. For vertebral rotations to the other side, a comparable pattern could be observed (Figs. 2 and 4; Video 1; Table 3).

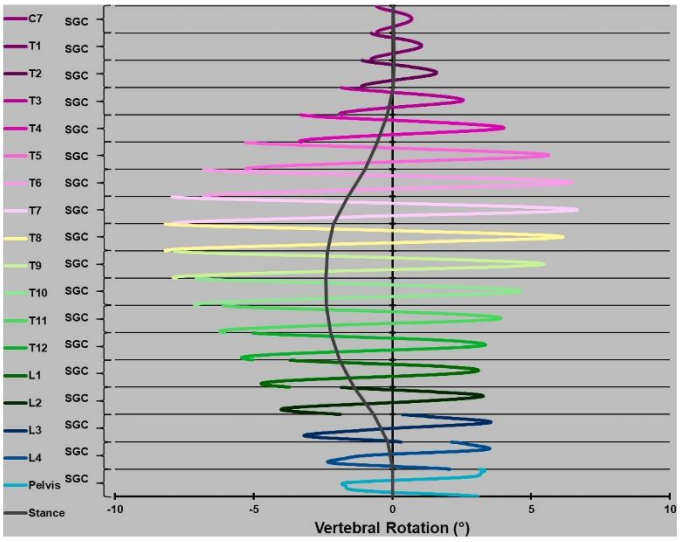

Fig. 3. Mean rotation curves of all investigated vertebrae and the pelvis within a single SGC respectively.
Note. Data is presented in the style of the visualization approach from Haimerl et al. (2022). The mean transverse plane results for spinal posture during stance are additionally presented. In contrast to dynamic results from gait analyses, the DIERS system provides static results from posture analyses for each vertebral structure during stance measurements in relation to a neutral pelvic position (Wolf et al., 2021).

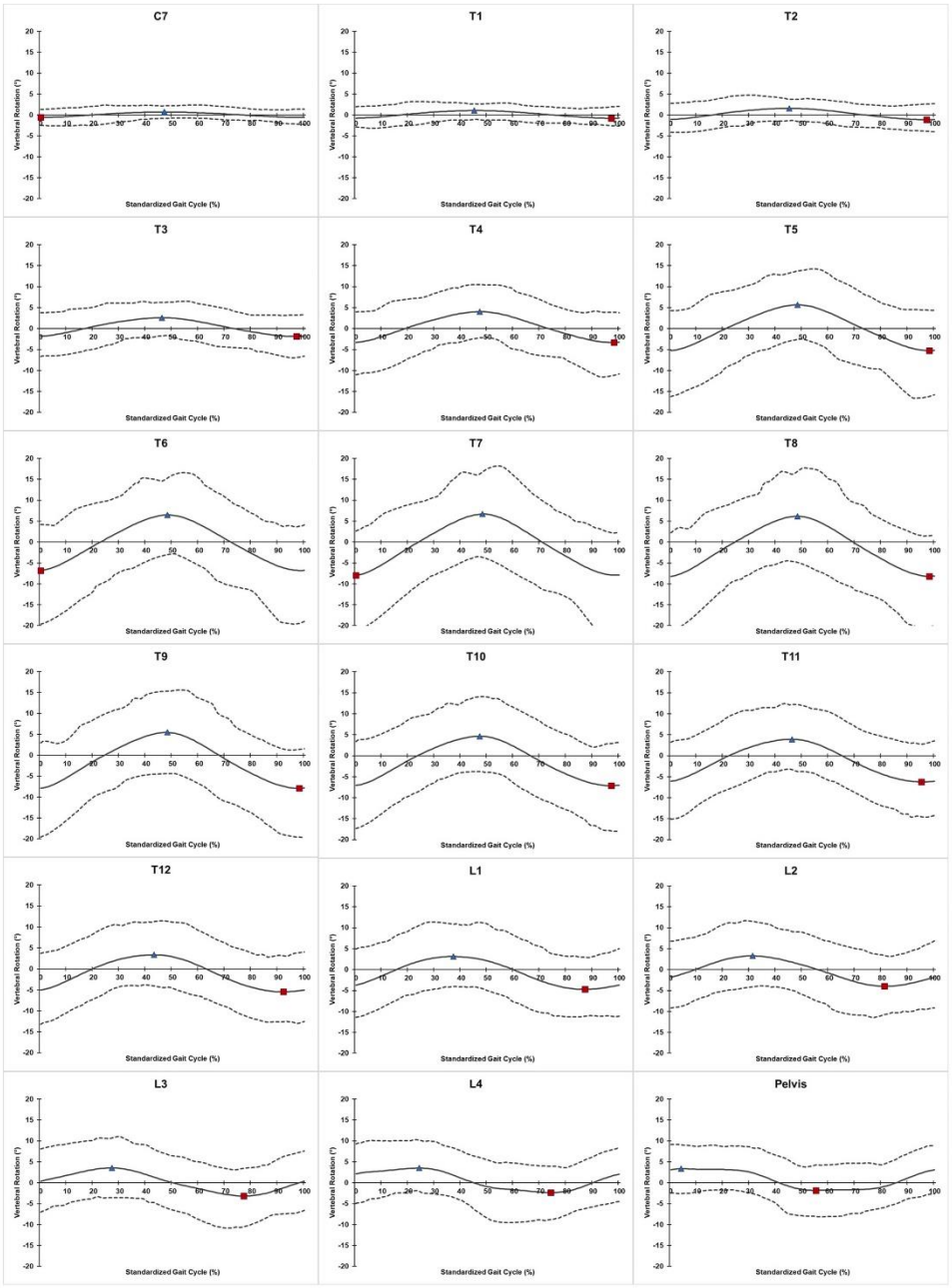

Fig. 4. Mean rotation curves and their respective 2.5% and 97.5% percentile curves of every vertebra and the pelvis (C7–L4; pelvis) within the SGC. *Note.* Vertebral rotation (°) is represented on the y-axis (range: −25°/+25°), the time progression of the SGC is represented on the x-axis (0–100%). Mean rotation curves are covered by their respective 2.5% and 97.5% percentile curves. The mean's maximum vertebral rotation values to the left (▲) and to the right (■) side are highlighted.

Table 3
Maximum values of the mean curves across the SGC with their respective 2.5% and 97.5% percentiles and the associated time of appearance within the SGC.

	Time within SGC (%)	Max of Mean Rot Right (°)	2.5% Pctl (°)	97.5% Pctl (°)	Time within SGC (%)	Max of Mean Rot Left (°)	2.5% Pctl (°)	97.5% Pctl (°)	Range of Rotary motion (°)
C7	0	−0.6	−2.5	1.3	47	0.7	−0.8	2.3	1.3
T1	97	−0.8	−2.6	2.0	45	1.1	−1.1	2.7	1.8
T2	97	−1.1	−3.9	2.6	45	1.6	−1.3	3.8	2.7
T3	97	−1.9	−6.9	3.2	46	2.6	−1.7	6.2	4.4
T4	98	−3.3	−11.1	3.9	47	4.0	−2.2	10.5	7.4
T5	98	−5.3	−16.2	4.4	48	5.7	−2.6	13.7	10.9
T6	0	−6.8	−19.7	4.1	48	6.5	−3.0	15.3	13.3
T7	0	−7.9	−21.3	2.6	48	6.7	−3.7	16.7	14.6
T8	98	−8.2	−20.3	1.5	48	6.2	−4.9	16.9	14.4
T9	98	−7.9	−19.6	1.4	48	5.5	−4.4	15.3	13.4
T10	97	−7.1	−17.9	2.9	47	4.6	−3.8	14.1	11.8
T11	95	−6.2	−14.5	2.7	46	3.9	−3.3	12.2	10.2
T12	92	−5.4	−12.6	3.2	43	3.3	−4.1	11.3	8.8
L1	87	−4.7	−11.1	3.0	37	3.1	−4.1	10.8	7.8
L2	81	−4.0	−10.8	3.4	31	3.3	−4.1	11.5	7.3
L3	77	−3.2	−10.5	3.5	27	3.5	−3.6	10.7	6.7
L4	74	−2.3	−8.8	4.0	24	3.5	−2.0	10.2	5.8
Pelvis	55	−1.8	−8.1	4.2	4	3.3	−2.6	9.1	5.2

Due to these findings, the point of intersection (PoI), meaning the area of transition where the vertebral rotation changes its direction (from right- to left-side vertebral rotation and vice versa) and around which the spinal screwing occurs, was not found to be static around the area of the mid-thoracic spine (Fig. 5; Video 2).

At the beginning of the SGC, the PoI was located between the 3rd and the 2nd lumbar vertebra (Figs. 2 and 5; Video 2). With the progression of the SGC over time, it moved upwards in its anatomic localization from one vertebra to the next until the anatomic height of T9/T10. Afterwards a time interval occurs, in which all vertebrae were rotated into the same direction and where no PoI could be observed (Figs. 2 and 5; Video 2). Initiated by the pelvis's change of rotary motion to the opposite direction, all other vertebrae

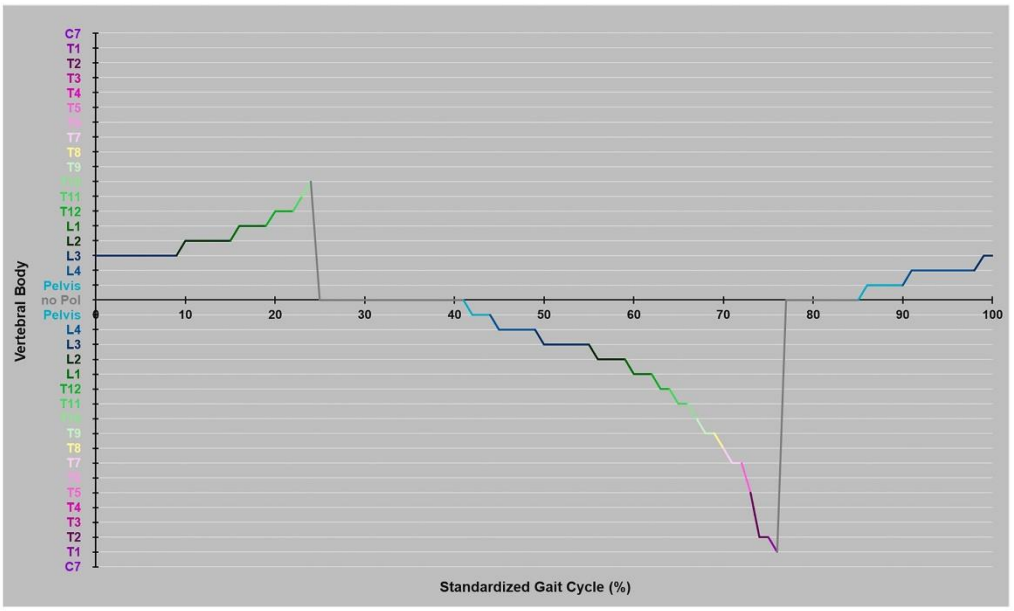

Fig. 5. Progression of the PoI within the SGC.
Note. As the PoI always occurs between two adjacent vertebrae, the respective caudal vertebra is marked as the PoI in this figure.

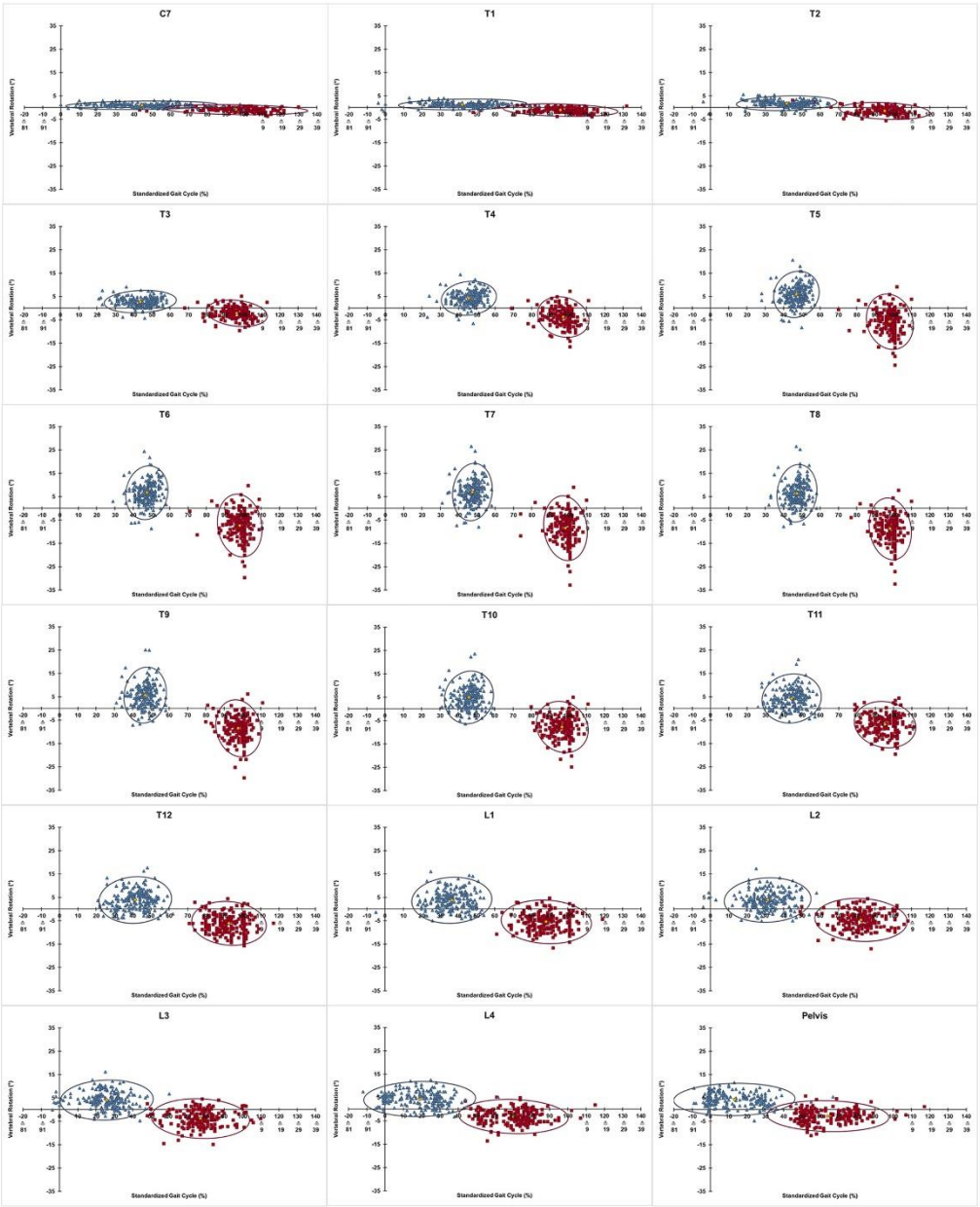

Fig. 6. Distribution of individual values (n = 201) for maximum vertebral rotation to the right (■; red) and to the left side (▲; blue) for all investigated vertebrae and the pelvis.
Note. Rotary vertebral motion (°) is represented on the y-axis (range: −35°/+35°), the time of occurrence within the SGC is represented on the x-axis (range: -20%/+140%). Scatter plots are covered by the 95% prediction ellipses for right- and left-side vertebral rotation, respectively. The center of the ellipses are marked (●; yellow). (For interpretation of the references to colour in this figure legend, the reader is referred to the web version of this article.)

followed in succession. The period of no PoI ended at that moment when the extent of rotary motion of the pelvis crossed the neutral position (0° of rotary motion on the y-axis) at around 42% of the SGC (Figs. 2 and 5; Video 2; Table 3). At this moment, the PoI appeared caudal, between the pelvis and the 4th lumbar vertebra and again started to increase gradually, vertebra by vertebra until all investigated structures were rotated into the same direction again and no PoI can be located. Even before all vertebral bodies have crossed the neutral rotary position, the pelvis had already started to initiate the next change of rotary direction and crossed the x-axis at around 86% of the SGC (Figs. 2 and 5; Video 2). In consequence, the PoI appeared caudal again between the pelvis and the 4th lumbar vertebra. As before, it increased slightly until the anatomic level of L3/L2 was achieved at the end of the SGC.

Even though mean results of the entire group demonstrated those very systematic spinal movement patterns, individual observations revealed large inter-individual differences in vertebral movement habits during gait. Fig. 6 and Video 3 present the distribution of individual rotational maximum values of all 201 participating subjects within the SGC. The presented scatter plots of individual values are framed by their respective 95% prediction ellipses, meaning that with a probability of 95% the ellipse is able to cover a respective future observation (Schubert & Kirchner, 2014). The pelvis and the lower lumbar vertebrae demonstrate that, compared to their considerable homogeneous distribution on the y-axis (range of vertebral rotation), the temporal occurrence of individual maximum values spreads widely on the x-axis (% SGC), which is also visible in the ratio of the ellipses length to its width. In contrast, the mid- and lower-thoracic vertebrae demonstrate the almost opposite movement behavior. They provide quite homogeneous patterns for timely occurrence of the individual maximum values within the SGC. The distribution of values on the y-axis, however, revealed quite heterogeneous results. The area of the prediction ellipse, which is defined to be the product of its principal axes with pi (Schubert & Kirchner, 2014), tends to increase from the cranial to the caudal structures, indicating in general a more heterogeneous movement behavior of the caudal compared to the cranial vertebrae (Fig. 6; Video 3; Table 4). The mean values and their respective 2.5% and 97.5% percentiles for temporal occurrence of right- and left-side maximum rotation within the SGC and the corresponding rotation values are presented in Table 5.

4. Discussion

The aim of this study was to present reference data for rotary spinal motion of every vertebral body from C7 down to L4 and the pelvis derived from ST back shape analyses in a cohort of 201 healthy participants walking on a treadmill at a given walking speed of 5 km/h. Additionally, the spine's functional movement behavior during gait should be described in the transverse plane.

The vertebrae of the cervicothoracic region demonstrated no notable range of rotary motion (rRoM) (rRoM C7 = 1.3°, rRoM T1 = 1.8°, rRoM T2 = 2.7°). Additionally, the respective prediction ellipse areas were also relatively small, indicating more homogeneous movement patterns compared to those of the underlying spinal structures. This was expected because, in general, the human body seems to be striving to stabilize the head during walking (Kavanagh, Barrett, & Morrison, 2006). The standardization of viewing direction on a fixed point at a predefined height and distance from the walking participant might also have contributed to this outcome.

Based on the made observations of the underlying vertebrae, however, the current results challenge the existing functional understanding of vertebral body-related rotary motion of the healthy spine during gait. So far, the mid-thoracic spine (~T7) was mostly expected to be dynamically stabilized, demonstrating no or rather little rotary motion during ambulation in healthy participants at all

Table 4
Numerical presentation of the 95% prediction ellipses for maximum values of right- and left-side vertebral rotation.

	Maximum of right-side vertebral rotation					Maximum of left-side vertebral rotation				
	Center of the ellipse		Length of the ellipse	Width of the ellipse	Area of the ellipse	Center of the ellipse		Length of the ellipse	Width of the ellipse	Area of the ellipse
	SGC-axis	Rotation-axis				SGC-axis	Rotation-axis			
C7	95.8	−0.9	39.3	2.1	258.1	44.2	1.0	41.6	1.8	238.4
T1	95.8	−1.1	31.3	2.6	254.7	42.0	1.4	35.0	2.3	254.2
T2	95.3	−1.4	24.6	3.6	276.7	41.7	1.9	27.5	3.2	272.9
T3	96.5	−2.2	16.7	5.6	292.0	43.7	2.8	19.7	4.8	296.2
T4	97.3	−3.7	14.2	8.5	379.2	45.6	4.3	15.1	7.2	341.4
T5	98.1	−5.8	13.2	11.4	472.5	47.0	5.9	12.6	9.8	386.3
T6	98.3	−7.4	13.8	11.8	513.2	47.5	6.8	12.0	10.9	413.9
T7	98.5	−8.5	14.1	11.7	516.7	47.6	7.0	12.5	10.7	417.1
T8	98.3	−8.8	13.5	11.2	475.1	47.3	6.4	12.5	10.7	419.6
T9	97.8	−8.5	13.1	11.5	470.8	46.8	5.8	12.4	11.2	435.8
T10	96.9	−7.7	14.3	10.8	484.4	45.9	5.0	13.5	11.2	473.1
T11	95.4	−6.9	16.9	9.8	521.9	44.3	4.3	16.2	10.5	533.3
T12	92.6	−6.1	20.5	9.3	598.7	41.5	3.9	19.9	10.0	623.2
L1	88.2	−5.5	24.6	9.3	720.6	36.6	3.8	22.0	9.9	679.4
L2	82.4	−4.7	25.3	9.2	731.8	31.3	3.9	23.7	9.5	706.9
L3	77.1	−3.8	26.9	8.4	712.9	25.8	4.1	25.5	8.5	682.6
L4	70.2	−3.1	29.9	7.3	688.3	19.0	4.3	30.7	7.5	725.2
Pelvis	64.3	−2.8	33.4	6.6	696.4	13.2	4.3	33.2	6.9	718.3

Note. Ellipses are described based on their length, width and area.

Table 5
Mean values and their respective 2.5% and 97.5% percentiles for temporal occurrence (Mean Max Rot (% SGC)) and the corresponding rotational deflection (Mean Max Rot (° Rot) of right and left side maximum vertebral rotation values.

	Right-side vertebral rotation						Left-side vertebral rotation					
	Mean Max Rot Right (% SGC)	2.5% Pctl (% SGC)	97.5% Pctl (% SGC)	Mean Max Rot Right (° Rot)	2.5% Pctl (° Rot)	97.5% Pctl (° Rot)	Mean Max Rot Left (% SGC)	2.5% Pctl (% SGC)	97.5% Pctl (% SGC)	Mean Max Rot Left (° Rot)	2.5% Pctl (° Rot)	97.5% Pctl (° Rot)
C7	95.8	48.2	120.0	−0.9	−2.7	0.6	44.2	10.1	80.9	1.0	−0.4	2.9
T1	95.8	55.4	115.9	−1.1	−3.2	1.0	42.0	13.0	67.0	1.4	−0.8	3.4
T2	95.3	71.1	109.0	−1.4	−4.4	1.7	41.7	18.1	59.0	1.9	−1.2	4.8
T3	96.5	79.1	106.0	−2.2	−7.4	2.9	43.7	23.2	56.0	2.8	−1.6	7.2
T4	97.3	83.1	105.0	−3.7	−11.7	3.2	45.6	33.0	56.0	4.3	−2.0	10.5
T5	98.1	85.1	106.0	−5.8	−16.6	3.7	47.0	35.1	56.0	5.9	−2.5	14.2
T6	98.3	87.0	106.0	−7.4	−19.8	3.3	47.5	36.1	56.0	6.8	−2.8	16.6
T7	98.5	87.1	106.0	−8.5	−21.3	2.1	47.6	38.0	55.0	7.0	−3.3	18.3
T8	98.3	87.1	106.0	−8.8	−21.0	1.3	47.3	37.0	55.0	6.4	−4.4	17.9
T9	97.8	84.1	106.0	−8.5	−19.8	1.2	46.8	34.1	55.0	5.8	−4.3	17.0
T10	96.9	83.0	106.0	−7.7	−18.1	1.9	45.9	33.0	55.0	5.0	−3.8	14.7
T11	95.4	80.1	107.0	−6.9	−15.2	1.8	44.3	29.1	57.0	4.3	−2.5	13.2
T12	92.6	77.1	107.0	−6.1	−13.6	2.0	41.5	24.0	56.0	3.9	−3.3	12.8
L1	88.2	69.0	105.0	−5.5	−12.1	2.3	36.6	19.1	52.0	3.8	−3.2	12.1
L2	82.4	59.0	102.0	−4.7	−11.8	2.9	31.3	12.1	50.0	3.9	−3.6	11.8
L3	77.1	51.1	102.0	−3.8	−10.9	2.4	25.8	−2.0	46.9	4.1	−2.8	11.3
L4	70.2	48.1	94.9	−3.1	−9.8	2.4	19.0	−3.0	39.0	4.3	−1.8	10.5
Pelvis	64.3	46.1	89.0	−2.8	−8.1	2.0	13.2	−4.0	37.9	4.3	−0.9	9.5

(Gregersen & Lucas, 1967; Needham, Naemi, et al., 2016; Suppé & Bongarz, 2013). The vertebrae above, respectively, the vertebrae and the pelvis below tended to be almost counterrotated depending on walking speed (Gregersen & Lucas, 1967; Lamoth, Beek, & Meijer, 2002). ST back shape analyses however, found the pelvis to be forwardly rotated on the side of the reference leg, reaching its curve maximum as the first of all investigated anatomic structures within the SGC (rRoM Pelvis = 5.2°). The maxima of the overlying lumbar vertebrae followed in succession. Instead of being adjusted in an almost neutral position, the vertebrae of the mid-thoracic spine were almost maximally counterrotated at the beginning of the SGC. Approximately halfway through the gait cycle the directions of maximum rotary movement reversed. Of all thoracic vertebrae, T7 and T8 demonstrated the largest amplitude of rotary motion during gait at a continuous velocity of 5 km/h (rRoM T7 = 14.6°, rRoM T8 = 14.4°). In addition, the largest rotary opposition was also found between the pelvis and T7/T8. Furthermore, the thoracic spine turned out to rotate in terms of a functional unit whereby all included vertebrae almost contemporaneously rotated into the same direction by the same period only with different amplitudes for the rotary RoM. Conversely, the segments of the pelvis and the lumbar spine seem to rotate successively but with almost identical rotary motion amplitudes.

Contrary to previous assumptions, the analysis of the present data additionally indicates that the mid-thoracic spine (~T7) might possibly not be an almost static point of intersection (PoI) where the direction of rotary motion changes from one side to the other and around which the spinal screwing occurs during ambulation. It rather looks as if the PoI seems to be dynamic in its anatomic localization during the course of the SGC, following a systematic and relatively constant from-caudal-to-cranial oscillation pattern (Fig. 5; Video 2). It may be conjectured that a dynamical PoI is a consequence of the human body increasing the degrees of freedom and simultaneously minimizing leverages to address the ability to be more resilient towards internal and external perturbations during the complex motion pattern of gait.

Comparable to the presented mean curves (specifically to those representing the rotary motion of the thoracic vertebrae), which oscillated not completely uniformly around the x-axis (0° of rotation) and which were slightly shifted downwards on the y-axis (Figs. 2, 3 and 4; Video 1), the course of the PoI revealed two different progressions within the SGC that showed an uneven increase of its anatomic localization between the first and the second rise (Fig. 5; Video 2). This phenomenon might be caused by the fact that the normal, non-scoliotic spine also demonstrates a pre-existing pattern of vertebral rotation, especially in the thoracic segments in consequence of internal organ anatomy and location (Kouwenhoven et al., 2007; Kouwenhoven, Vincken, Bartels, & Castelein, 2006). This predominant rotation was verifiable in static ST analyses of 100 female participants from the study cohort described within this paper as well (Wolf et al., 2021) and is also present in all 201 participants (stance graph in Fig. 3) (Huthwelker et al., 2022). However, as data of the current project were not normalized for the individual's habitual stance, this pre-existing rotation might have influenced the slightly asymmetrical rotary movement behavior between left and right vertebral rotation and therewith might also have affected the uneven progression of the PoI between left and right vertebral rotation. These findings seem to indicate that every individual walks systematically "around" his or her personal spinal posture, but future research needs to address this topic in more detail. Nevertheless, the described findings of a dynamic PoI that starts caudal and systematically rises upwards, reveals that the pelvis plays a very important role in transverse plane spinal motion during gait. It appears to actually initiate spinal rotary motion, while the overlying vertebrae "only" seem to follow the pelvis's movement in succession. Whether this pattern is dependent on gender, age or other contributing factors like walking speed will be analyzed and discussed elsewhere in further publications on this topic. Future analyses will also have to answer the question of whether the PoI's progression might differ between patient groups suffering from different

musculoskeletal pathologies, and in this case, whether its progression might be a reliable indicator to differentiate between physiological and pathological spinal movement patterns in the future.

The current study also found that rotary movement patterns during ambulation turned out to be much more individual than primarily expected, and that this heterogeneity increased from the cranial to the caudal spinal structures. This phenomenon could be observed, even though all participants were free of pain and healthy with regard to the musculoskeletal system, the procedure of data capturing was strictly standardized, and walking speed could be perfectly controlled for. These findings are in accordance with results of previous research regarding the individuality of gait patterns of the pelvic-leg region. Previous authors found that movement patterns of the lower extremity are quite individual and could differ so strongly from one subject to another that the respective gait characteristics can be used to recognize an individual reliably (Horst et al., 2016; Horst, Lapuschkin, Samek, Muller, & Schollhorn, 2019; Schöllhorn, Nigg, Stefanyshyn, & Liu, 2002). Additionally, it could be shown that those individual gait characteristics were persistent over years (Horst, Mildner, & Schollhorn, 2017). Whether this is also the case for movement patterns of the spine needs to be further investigated. Initial results using AI, however, indicate in this direction (Dindorf et al., 2021b).

Due to huge methodological differences in data capturing approaches, and different ways for data preparation in previous research investigating spinal dynamics during gait by using other measurement techniques, direct comparisons between previous findings and the results of the current study are hardly possible. To the authors' knowledge, this is additionally the first study presenting reference data for rotary spinal motion from all vertebrae (C7 to L4 and the pelvis) derived from healthy participants and in temporal relation to a standardized gait cycle using an ST measurement approach. Indeed, two further research groups previously used ST on healthy participants as well, but either focused on the presentation of global spine parameters (Michalik et al., 2020) or on the development of comprehensive new visualization tools (Haimerl et al., 2022). Even though Haimerl et al. (2022) did not present mean values for respective vertebral rotations of their study cohort, data visualizations of axial rotation revealed quite comparable movement patterns. The authors found the vertebral bodies to not oscillate even around 0°. Additionally, the vertebrae of the mid-thoracic spine seem to present the largest range of rotary motion, comparable to the results of the current study. Nevertheless, it has to be considered that individual data were presented from only 12 participants and for a walking speed of 3 km/h (Haimerl et al., 2022), which is why direct comparisons with results of the current study have to be interpreted with caution. For this reason, future research will have to evaluate the results presented herein and compare them in detail against prospective research findings.

4.1. Limitations

The presented study had several limitations. Thereby a distinction must be made between different methodological causes and limitations derived from the measurement method itself.

4.1.1. Methodological limitations

All participants included in the study were healthy, free of pain and did not show any functional abnormalities in relation to the inclusion criteria described. However, spinal health was not further verified by radiographic images due to ethical reasons. For this reason, the existence of small spinal deformities or other asymptomatic degenerative adaptations cannot be excluded.

Additionally, it has to be considered that the researchers decided to use two more markers (~T3 and ~ T12) than officially recommended by the manufacturer. This was to minimize systematic software misinterpretations for positions of individual vertebral bodies at the respective anatomical heights that frequently occurred during test measurements at fast walking speeds due to soft tissue motion on the participants' back surface. Additionally, C7 and the PSIS were palpated and marked instead of the recommended, visually identifiable landmarks (vertebra prominens and lumbar dimples). This approach was used because the recommended visual landmarks were not always identifiable on every participant's back surface. In such cases, the manufacturer recommends palpating and marking the respective anatomic landmarks anyway. As the researchers strived to standardize the measuring procedure as much as possible, they decided to mark the anatomic structures a priori for all participants. Nevertheless, the chosen approach was definitely more prone to palpation bias (Cooperstein & Hickey, 2016; Póvoa, Ferreira, Zanier, & Silva, 2018) and limits the external validity of the presented findings. Additionally, the divergent marking of landmarks might have influenced reconstructions of the virtual spinal model and consequently might have had an effect on the generated outcome for spinal rotary motion.

A further attempt to standardize the data capturing procedure as much as possible within the current study was the decision to analyze the participants' spinal motion based on predefined walking speeds. The researchers are aware that individual anthropometrics have an influence on biomechanical gait parameters (McKay et al., 2017) and that normal differences in comfortable gait speeds according to sex, age and height (Bohannon, 1997) have not taken into account. This has to be considered when transferring the here presented results into clinical practice.

The age of the participants included in this study ranged from 18 to 70 years. As age-related changes in spinal and lower limb movement patterns are known during gait (Crawford, Gizzi, Dieterich, Ni Mhuiris, & Falla, 2018), the wide age-range might have possibly contributed to the high inter-individual variance of gait patterns that occurred in the presented results. Further planned publications will analyze the available data with regard to sex, different age cohorts and different walking speeds (2 km/h, 3 km/h, 4 km/h and 5 km/h) to provide further clarity on the possible impact that those contributing factors might have had on individual gait performances.

Even though no explorative statistical analyses have been performed, multiple descriptive analyses of the same data set limits its statistical significance as the data are correlated. This has to be considered when the presented results are consulted in clinical practice.

A further weakness of the presented study is that the authors missed to capture the required number of performed manual data corrections. The lack of this information limits the interpretability of the results in a wider context and has to be considered when

results shall be transferred into clinical practice.

Furthermore, during a short period of time (16–24% of the SGC) more than one PoI was apparent in the available set of data (Video 2). As the additional PoIs were located in the upper-thoracic spine, where only very little rotary motion was observed anyway, and because they were only apparent for a very short time, the authors waived picturing these additional data for reasons of a better interpretability of the graphical PoI visualization.

4.1.2. Limitations that arised from the measurement method itself

To date, it is not possible to properly validate the dynamic ST measurement approach due to the absence of a suitable clinical gold standard for spinal motion analysis to compare it against. Therefore, the results from dynamic ST analyses still derive from optical back shape recordings via a mathematical algorithm that was originally developed and validated for static measurements. Additionally, arising soft tissue artifacts caused by scapula motion on the thorax, back muscle activation, general skin displacements or skin stretching over the spinal processes during motion might have had an influence on the measured data that also has to be considered when interpreting and using the presented results for clinical or scientific practice.

Furthermore, only participants with a BMI $\leq$30.0 kg/m^2 were included in the study. This approach was chosen, due to data capturing requirements, knowing that this further limits the external validity of the presented outcome.

An additional point for consideration is that for ST measurements, it is required to hold the distance between the measuring device and the walking participant approximately constant during the time of data recording. This is why participants had to walk on a treadmill for data capturing within this study. Whether this is equal to walking overground or not, has been a much debated research question for many years. In this context, a recent systematic review found that while some biomechanical parameters are largely comparable between treadmill and overground walking, others were significantly different from each other (Semaan et al., 2022). Nevertheless, the laboratory conditions themselves will definitely have had an influence on the participants' gait performance compared to daily life walking, regardless of whether the participants were analyzed on a treadmill or on any other surface.

Last but not least, it is necessary to question whether three recorded gait cycles are representative of an individual's habitual gait performance. This approach has been chosen due to a high amount of data generated with the ST measuring device on the one hand, and indeed generous but still limited data storage capacities on the other. However, as already published ST measurement results indicated, spinal movement patterns, derived from identical three-gait-cycle ST analyses seem to be quite constant and reproducible over time (Dindorf et al., 2021b), the results of this approach seem nevertheless meaningful and suitable.

4.2. Outlook for future research

To the authors' knowledge, this is the first presentation of reference data of vertebral body-related rotary movement behavior of the healthy human spine during gait, collected with an ST measurement device. Future analyses of the current set of data will have to provide further information on spinal movement behavior in the remaining axes of motion (frontal and sagittal) and for the additionally measured gait velocities (2 km/h, 3 km/h and 4 km/h), which will be presented in further publications. Furthermore, the questions of whether the variety of spinal movement patterns is intra-individually consistent and whether it is affected by an individual's physical constitution, sex, anthropometric characteristics, age, walking speed or by other contributing factors will have to be addressed.

Additionally, future research will have to develop characteristic parameters to describe specific spinal gait patterns based on ST data. Those parameters should be able to differentiate between physiological and pathological movement patterns. AI methods might be able to further facilitate this process (Horst et al., 2019) and have already been used with promising results on the presented data set so far (Dindorf et al., 2020; Dindorf et al., 2021b).

Supplementary data to this article can be found online at https://doi.org/10.1016/j.humov.2022.103054.

Funding sources

The research did not receive any specific grant from funding agencies in the public, commercial, or not-for-profit sectors.

There was various technical assistance by staff members of the DIERS Company in preparation prior to the statistical data analysis process. However, there was no external influence on the study design, in the collection, statistical analysis and interpretation of data, in the writing of the manuscript, and in the decision to submit the manuscript for publication.

CRediT authorship contribution statement

Janine Huthwelker: Conceptualization, Methodology, Validation, Formal analysis, Investigation, Data curation, Writing – original draft, Visualization. **Jürgen Konradi:** Software, Validation, Formal analysis, Data curation, Writing – review & editing, Visualization, Supervision, Project administration. **Claudia Wolf:** Software, Validation, Formal analysis, Data curation, Writing – review & editing. **Ruben Westphal:** Software, Validation, Formal analysis, Data curation, Writing – review & editing. **Irene Schmidtmann:** Software, Validation, Formal analysis, Data curation, Writing – review & editing. **Patric Schubert:** Validation, Formal analysis, Data curation, Writing – review & editing, Visualization. **Philipp Drees:** Resources, Writing – review & editing, Supervision, Project administration. **Ulrich Betz:** Conceptualization, Methodology, Validation, Resources, Writing – review & editing, Supervision, Project administration.

Declaration of Competing Interest

None.

Data availability

The authors do not have permission to share data.

Acknowledgements

First and foremost we would like to thank all participants for their interest and their time to participate in this project. Our colleagues are acknowledged for their immense support within the participant recruitment process and for their professional expertise and contributions to this project. Special thanks also to Amira Basic and Kjell Heitmann (DIERS Company) for their technical support and assistance.

References

Betsch, M., Wild, M., Johnstone, B., Jungbluth, P., Hakimi, M., Kuhlmann, B., & Rapp, W. (2013). Evaluation of a novel spine and surface topography system for dynamic spinal curvature analysis during gait. *PLoS One, 8*(7), Article e70581. https://doi.org/10.1371/journal.pone.0070581

Betsch, M., Wild, M., Jungbluth, P., Hakimi, M., Windolf, J., Haex, B., … Rapp, W. (2011, Jun). Reliability and validity of 4D rasterstereography under dynamic conditions. *Computers in Biology and Medicine, 41*(6), 308–312. https://doi.org/10.1016/j.compbiomed.2011.03.008

Betz, U., Konradi, J., Huthwelker, J., Wolf, C., Diers, H., Heitmann, K., Westphal, R., & Drees, P. (2018). *Quantitative and qualitative parameters to characterize segmental spine movement during gait World Congress of Biomechanics, Dublin, Ireland,* 2018.07.08-12.

Bischoff, H. A., Stahelin, H. B., Monsch, A. U., Iversen, M. D., Weyh, A., von Dechend, M., … Theiler, R. (2003, May). Identifying a cut-off point for normal mobility: A comparison of the timed "up and go" test in community-dwelling and institutionalised elderly women. *Age and Ageing, 32*(3), 315–320. https://doi.org/10.1093/ageing/32.3.315

Bohannon, R. W. (1997, Jan). Comfortable and maximum walking speed of adults aged 20-79 years: Reference values and determinants. *Age and Ageing, 26*(1), 15–19. https://doi.org/10.1093/ageing/26.1.15

Bohannon, R. W., Wang, Y. C., & Gershon, R. C. (2015, Mar). Two-minute walk test performance by adults 18 to 85 years: Normative values, reliability, and responsiveness. *Archives of Physical Medicine and Rehabilitation, 96*(3), 472–477. https://doi.org/10.1016/j.apmr.2014.10.006

Bruijn, S. M., Meijer, O. G., van Dieen, J. H., Kingma, I., & Lamoth, C. J. (2008, Apr). Coordination of leg swing, thorax rotations, and pelvis rotations during gait: The organisation of total body angular momentum. *Gait & Posture, 27*(3), 455–462. https://doi.org/10.1016/j.gaitpost.2007.05.017

Ceccato, J. C., de Seze, M., Azevedo, C., & Cazalets, J. R. (2009, Dec 7). Comparison of trunk activity during gait initiation and walking in humans. *PLoS One, 4*(12), Article e8193. https://doi.org/10.1371/journal.pone.0008193

Chockalingam, N., Dangerfield, P. H., Giakas, G., & Cochrane, T. (2002). Study of marker placements in the back for opto-electronic motion analysis. *Studies in Health Technology and Informatics, 88*, 105–109.

Cooperstein, R., & Hickey, M. (2016, Mar). The reliability of palpating the posterior superior iliac spine: A systematic review. *The. Journal of the Canadian Chiropractic Association, 60*(1), 36–46.

Crawford, R., Gizzi, L., Dieterich, A., Ni Mhuiris, Á., & Falla, D. (2018). Age-related changes in trunk muscle activity and spinal and lower limb kinematics during gait. *PLoS One, 13*(11), Article e0206514. https://doi.org/10.1371/journal.pone.0206514

Crosbie, J., Vachalathiti, R., & Smith, R. (1997). Patterns of spinal motion during walking. *Gait & Posture, 5*(1), 6–12.

D'Amico, M., D'Amico, G., Paniccia, M., Roncoletta, P., & Vallasciani, M. (2010). An integrated procedure for spine and full skeleton multi-sensor biomechanical analysis & averaging in posture gait and cyclic movement tasks. *Studies in Health Technology and Informatics, 158*, 118–126.

D'Amico, M., Kinel, E., D'Amico, G., & Roncoletta, P. (2021, Jun 7). A self-contained 3D biomechanical analysis lab for complete automatic spine and full skeleton assessment of posture, gait and run. *Sensors (Basel), 21*(11). https://doi.org/10.3390/s21113930

Dindorf, C., Konradi, J., Wolf, C., Taetz, B., Bleser, G., Huthwelker, J., … Betz, U. (2020). General method for automated feature extraction and selection and its application for gender classification and biomechanical knowledge discovery of sex differences in spinal posture during stance and gait. *Computer Methods in Biomechanics and Biomedical Engineering, 24*(3), 1–9. https://doi.org/10.1080/10255842.2020.1828375

Dindorf, C., Konradi, J., Wolf, C., Taetz, B., Bleser, G., Huthwelker, J., … Fröhlich, M. (2021a). Classification and automated interpretation of spinal posture data using a pathology-independent classifier and explainable artificial intelligence (XAI). *Sensors, 21*(18). https://doi.org/10.3390/s21186323

Dindorf, C., Konradi, J., Wolf, C., Taetz, B., Bleser, G., Huthwelker, J., … Betz, U. (2021b). Machine learning techniques demonstrating individual movement patterns of the vertebral column: The fingerprint of spinal motion. *Computer Methods in Biomechanics and Biomedical Engineering, 1-11*. https://doi.org/10.1080/10255842.2021.1981884

Drerup, B. (1993). *[The shape of the scoliotic spine. Measurement and mathematical analysis of standard radiographs]. G. Fischer. (Die Form der skoliotischen Wirbelsäule. Vermessung und mathematische Analyse von Standard-Röntgenaufnahmen)*.

Drerup, B. (2014, December 12). Rasterstereographic measurement of scoliotic deformity [journal article]. *Scoliosis, 9*(1), 22. https://doi.org/10.1186/s13013-014-0022-7

Drerup, B., Ellger, B., Meyer Zu Bentrup, F. M., & Hierholzer, E. (2001, Apr). Functional rasterstereographic images. A new method for biomechanical analysis of skeletal geometry. *Orthopade, 30*(4), 242–250. https://doi.org/10.1007/s001320050603 (Rasterstereographische Funktionsaufnahmen. Eine neue Methode zur biomechanischen Analyse der Skelettgeometrie.).

Drerup, B., & Hierholzer, E. (1994, Jan). Back shape measurement using video rasterstereography and three-dimensional reconstruction of spinal shape. *Clinical Biomechanics (Bristol, Avon), 9*(1), 28–36. https://doi.org/10.1016/0268-0033(94)90055-8

Feipel, V., De Mesmaeker, T., Klein, P., & Rooze, M. (2001, Feb). Three-dimensional kinematics of the lumbar spine during treadmill walking at different speeds. *European Spine Journal, 10*(1), 16–22. https://doi.org/10.1007/s005860000199

Gipsman, A., Rauschert, L., Daneshvar, M., & Knott, P. (2014). Evaluating the reproducibility of motion analysis scanning of the spine during walking. *Advances in Medicine, 2014*, Article 721829. https://doi.org/10.1155/2014/721829

Gregersen, G. G., & Lucas, D. B. (1967, Mar). An in vivo study of the axial rotation of the human thoracolumbar spine. *The Journal of Bone and Joint Surgery. American Volume, 49*(2), 247–262. https://www.ncbi.nlm.nih.gov/pubmed/6018729.

Haimerl, M., Nebel, I., Linkerhägner, A., Konradi, J., Wolf, C., Drees, P., & Betz, U. (2022). Comprehensive visualization of spinal motion in gait sequences based on surface topography. *Human Movement Science, 81*. https://doi.org/10.1016/j.humov.2021.102919, 102919. 2022/02/01.

Hierholzer, E. (1993). *Objektive Analyse der Rückenform von Skoliosepatienten*. G. Fischer.

Horst, F., Kramer, F., Schafer, B., Eekhoff, A., Hegen, P., Nigg, B. M., & Schollhorn, W. I. (2016, Sep). Daily changes of individual gait patterns identified by means of support vector machines. *Gait & Posture, 49*, 309–314. https://doi.org/10.1016/j.gaitpost.2016.07.073

Horst, F., Lapuschkin, S., Samek, W., Muller, K. R., & Schollhorn, W. I. (2019, Feb 20). Explaining the unique nature of individual gait patterns with deep learning. *Scientific Reports, 9*(1), 2391. https://doi.org/10.1038/s41598-019-38748-8
Horst, F., Mildner, M., & Schollhorn, W. I. (2017, Oct). One-year persistence of individual gait patterns identified in a follow-up study - a call for individualised diagnose and therapy. *Gait & Posture, 58*, 476–480. https://doi.org/10.1016/j.gaitpost.2017.09.003
Huthwelker, J., Konradi, J., Wolf, C., Westphal, R., Schmidtmann, I., Drees, P., & Betz, U. (2022). Reference Values for 3D Spinal Posture Based on Videorasterstereographic Analyses of Healthy Adults. *Bioengineering, 9*(12), 809. https://doi.org/10.3390/bioengineering9120809
Kakushima, M., Miyamoto, K., & Shimizu, K. (2003, Nov 1). The effect of leg length discrepancy on spinal motion during gait: Three-dimensional analysis in healthy volunteers. *Spine (Phila Pa 1976), 28*(21), 2472–2476. https://doi.org/10.1097/01.Brs.0000090829.82231.4a
Kavanagh, J., Barrett, R., & Morrison, S. (2006, Jul). The role of the neck and trunk in facilitating head stability during walking. *Experimental Brain Research, 172*(4), 454–463. https://doi.org/10.1007/s00221-006-0353-6
Konradi, J. (2022a). *SPSS syntax script to create graphs of spinal motion for a Standardized Gait Cycle*. https://doi.org/10.17632/hbc5fz2xdw.1
Konradi, J. (2022b). *SPSS syntax script to create graphs of spinal motion relative to phases of gait*. https://doi.org/10.17632/5766pxrwh2.1
Konradi, J. (2022c). *Visualizations of rotational curves directly related to gait phases*. https://doi.org/10.17632/j4jwtt82zk.1
Konradi, J. (2022d). *Visualizations of rotational curves within a Standardized Gait Cycle*. https://doi.org/10.17632/m7tbn7vhpf.1
Konz, R. J., Fatone, S., Stine, R. L., Ganju, A., Gard, S. A., & Ondra, S. L. (2006, Nov 15). A kinematic model to assess spinal motion during walking. *Spine (Phila Pa 1976), 31*(24), E898–E906. https://doi.org/10.1097/01.brs.0000245939.97637.ae
Kouwenhoven, J. W., Bartels, L. W., Vincken, K. L., Viergever, M. A., Verbout, A. J., Delhaas, T., & Castelein, R. M. (2007, May 1). The relation between organ anatomy and pre-existent vertebral rotation in the normal spine: Magnetic resonance imaging study in humans with situs inversus totalis. *Spine (Phila Pa 1976), 32*(10), 1123–1128. https://doi.org/10.1097/01.brs.0000261563.75469.b0
Kouwenhoven, J. W., Vincken, K. L., Bartels, L. W., & Castelein, R. M. (2006, Jun 1). Analysis of preexistent vertebral rotation in the normal spine. *Spine (Phila Pa 1976), 31*(13), 1467–1472. https://doi.org/10.1097/01.brs.0000219938.14686.b3
Krott, N. L., Wild, M., & Betsch, M. (2020, Sep). Meta-analysis of the validity and reliability of rasterstereographic measurements of spinal posture. *European Spine Journal, 29*(9), 2392–2401. https://doi.org/10.1007/s00586-020-06402-x
Lamoth, C. J., Beek, P. J., & Meijer, O. G. (2002, Oct). Pelvis-thorax coordination in the transverse plane during gait. *Gait & Posture, 16*(2), 101–114. https://doi.org/10.1016/s0966-6362(01)00146-1
Lamoth, C. J., Meijer, O. G., Wuisman, P. I., van Dieen, J. H., Levin, M. F., & Beek, P. J. (2002, Feb 15). Pelvis-thorax coordination in the transverse plane during walking in persons with nonspecific low back pain. *Spine (Phila Pa 1976), 27*(4), E92–E99.
Leardini, A., Chiari, L., Della Croce, U., & Cappozzo, A. (2005, Feb). Human movement analysis using stereophotogrammetry. Part 3. Soft tissue artifact assessment and compensation. *Gait & Posture, 21*(2), 212–225. https://doi.org/10.1016/j.gaitpost.2004.05.002
Liljenqvist, U., Halm, H., Hierholzer, E., Drerup, B., & Weiland, M. (1998, Jan-Feb). Three-dimensional surface measurement of spinal deformities using video rasterstereography. *Zeitschrift für Orthopädie und Ihre Grenzgebiete, 136*(1), 57–64. https://doi.org/10.1055/s-2008-1044652
MacWilliams, B. A., Rozumalski, A., Swanson, A. N., Wervey, R. A., Dykes, D. C., Novacheck, T. F., & Schwartz, M. H. (2013, Dec 4). Assessment of three-dimensional lumbar spine vertebral motion during gait with use of indwelling bone pins. *The Journal of Bone and Joint Surgery. American Volume, 95*(23), e1841–e1848. https://doi.org/10.2106/JBJS.L.01469
McKay, M. J., Baldwin, J. N., Ferreira, P., Simic, M., Vanicek, N., Wojciechowski, E., … Burns, J. (2017, Oct). Spatiotemporal and plantar pressure patterns of 1000 healthy individuals aged 3-101 years. *Gait & Posture, 58*, 78–87. https://doi.org/10.1016/j.gaitpost.2017.07.004
Michalik, R., Hamm, J., Quack, V., Eschweiler, J., Gatz, M., & Betsch, M. (2020, Sep 8). Dynamic spinal posture and pelvic position analysis using a rasterstereographic device. *Journal of Orthopaedic Surgery and Research, 15*(1), 389. https://doi.org/10.1186/s13018-020-01825-0
Michalik, R., Siebers, H., Classen, T., Gatz, M., Rohof, B., Eschweiler, J., … Betsch, M. (2019, Mar). Comparison of two different designs of forefoot off-loader shoes and their influence on gait and spinal posture. *Gait & Posture, 69*, 202–208. https://doi.org/10.1016/j.gaitpost.2019.02.007
Mohokum, M., Mendoza, S., Udo, W., Sitter, H., Paletta, J. R., & Skwara, A. (2010, Jun 15). Reproducibility of rasterstereography for kyphotic and lordotic angles, trunk length, and trunk inclination: A reliability study. *Spine (Phila Pa 1976), 35*(14), 1353–1358. https://doi.org/10.1097/BRS.0b013e3181cbc157
Mohokum, M., Schülein, S., & Skwara, A. (2015). The validity of Rasterstereography: A systematic review. *Orthopedic Reviews, 7*(3). https://doi.org/10.4081/or.2015.5899, 5899–5899.
Myklebust, M., Magnussen, L., & Inger Strand, L. (2009). Back performance scale scores in people without back pain: Normative data. *Advances in Physiotherapy, 9*(1), 2–9. https://doi.org/10.1080/14038190601090794, 2007/01/01.
Needham, R., Naemi, R., Healy, A., & Chockalingam, N. (2016, Oct). Multi-segment kinematic model to assess three-dimensional movement of the spine and back during gait. *Prosthetics and Orthotics International, 40*(5), 624–635. https://doi.org/10.1177/0309364615579319
Needham, R., Stebbins, J., & Chockalingam, N. (2016). Three-dimensional kinematics of the lumbar spine during gait using marker-based systems: A systematic review. *Journal of Medical Engineering & Technology, 40*(4), 172–185. https://doi.org/10.3109/03091902.2016.1154616
Perry, J., & Burnfield, J. M. (2010). *Gait analysis - Normal and pathological function* (2nd. ed.). SLACK Incorporated.
Póvoa, L. C., Ferreira, A. P. A., Zanier, J. F. C., & Silva, J. G. (2018, Mar). Accuracy of motion palpation flexion-extension test in identifying the seventh cervical spinal process. *Journal of Chiropractic Medicine, 17*(1), 22–29. https://doi.org/10.1016/j.jcm.2017.11.005
Raspe, H. (2012). *Rückenschmerzen 53*. Gesundheitsberichterstattung des Bundes.
Schmidtmann, I., & Konradi, J. (2022). *SAS syntax script for merging export files*. https://doi.org/10.17632/mtd5x49mkc.1
Schöllhorn, W. I., Nigg, B. M., Stefanyshyn, D. J., & Liu, W. (2002, Apr). Identification of individual walking patterns using time discrete and time continuous data sets. *Gait & Posture, 15*(2), 180–186. https://doi.org/10.1016/s0966-6362(01)00193-x
Schubert, P., & Kirchner, M. (2014). Ellipse area calculations and their applicability in posturography. *Gait & Posture, 39*(1), 518–522. https://doi.org/10.1016/j.gaitpost.2013.09.001, 2014/01/01.
Schulte, T. L., Hierholzer, E., Boerke, A., Lerner, T., Liljenqvist, U., Bullmann, V., & Hackenberg, L. (2008, Feb). Raster stereography versus radiography in the long-term follow-up of idiopathic scoliosis. *Journal of Spinal Disorders & Techniques, 21*(1), 23–28. https://doi.org/10.1097/BSD.0b013e318057529b
Semaan, M. B., Wallard, L., Ruiz, V., Gillet, C., Leteneur, S., & Simoneau-Buessinger, E. (2022, Feb). Is treadmill walking biomechanically comparable to overground walking? A systematic review. *Gait & Posture, 92*, 249–257. https://doi.org/10.1016/j.gaitpost.2021.11.009
Suppé, B. (2014). In I. Spirgi-Gantert, & B. Suppé (Eds.), *FBL Klein-Vogelbach functional kinetics – Die Grundlagen* (7th ed.). Springer-Verlag.
Suppé, B., & Bongarz, M., & (Eds.).. (2013). *FBL Klein-Vogelbach Functional Kinetics praktisch angewandt. Gehen - Analyse und Intervention*. Springer. https://doi.org/10.1007/978-3-642-22076-0
Troendle, J. F., & Yu, K. F. (2003). Estimation of sample size for reference interval studies. *Biometrical Journal, 45*(5), 561–572.
Turner-Smith, A. R. (1988). A television/computer three-dimensional surface shape measurement system. *Journal of Biomechanics, 21*(6), 515–529. https://doi.org/10.1016/0021-9290(88)90244-8
Turner-Smith, A. R., Harris, J. D., Houghton, G. R., & Jefferson, R. J. (1988). A method for analysis of back shape in scoliosis. *Journal of Biomechanics, 21*(6), 497–509. https://doi.org/10.1016/0021-9290(88)90242-4
Vogt, L., Pfeifer, K., Portscher, & Banzer, W. (2001, Sep 1). Influences of nonspecific low back pain on three-dimensional lumbar spine kinematics in locomotion. *Spine (Phila Pa 1976), 26*(17), 1910–1919. https://doi.org/10.1097/00007632-200109010-00019
Westphal, R., & Konradi, J. (2022). *SAS syntax script for creation of a Standardized Gait Cycle*. https://doi.org/10.17632/k29mpr863y.1
Wolf, C., Betz, U., Huthwelker, J., Konradi, J., Westphal, R. S., Cerpa, M., … Drees, P. (2021, Dec 4). Evaluation of 3D vertebral and pelvic position by surface topography in asymptomatic females: Presentation of normative reference data. *Journal of Orthopaedic Surgery and Research, 16*(1), 703. https://doi.org/10.1186/s13018-021-02843-2

3 Diskussion

Das ursprüngliche Ziel dieses Dissertationsprojektes war die Erhebung von Referenzdaten für videorasterstereographische Wirbelsäulenparameter im Stand und im Gang bei verschiedenen Gehgeschwindigkeiten (2 km/h, 3 km/h, 4 km/h und 5 km/h). Diese sollten auf Messungen von 201 Gesunden im Alter von 18-70 Jahren basieren und bei der Auswertung das Geschlecht (weiblich; männlich), sowie das Alter („jung“: 18-30 Jahre; „mittel“: 31-50 Jahre; „alt“: 51-70 Jahre) der Probanden berücksichtigen. Dadurch sollte die Möglichkeit geschaffen werden, sowohl klinisch als auch wissenschaftlich erhobene VRS-Messergebnisse in Relation zu einer entsprechend gesunden Kontrollgruppe zu interpretieren und in einen funktionellen Kontext einordnen zu können. Diese Ziele konnten für den Stand (Huthwelker et al., 2022) und zum Teil auch für den Gang bei einer Gehgeschwindigkeit von 5 km/h in der Transversalebene (Huthwelker et al., 2023) erreicht werden.

Die vorliegende Arbeit unterscheidet sich dabei von früheren VRS-Referenzprojekten (Schröder et al., 2011, Schröder et al., 2014, Michalik et al., 2020, Degenhardt et al., 2020, Degenhardt et al., 2017), da die hier vorgestellten Ergebnisse auf einer vergleichsweise großen Anzahl inkludierter, gesunder Probanden, mit einer systematischen Zuordnung auf die drei beschriebenen Alterskohorten basieren. Dadurch konnte gewährleistet werden, dass jede Gruppe in sich über eine adäquate Anzahl an Teilnehmern verfügte (n=67) und die Gruppen durch ein konstantes Geschlechterverhältnis von 2:1 Probanden (44 weiblich; 23 männlich) untereinander vergleichbar waren.

Der vorangegangene gemeinsame Software-Entwicklungsprozess mit dem Hersteller ermöglichte zusätzlich die erstmalige dreidimensionale Darstellung der spezifischen videorasterstereographischen Wirbelsäulenparameter im Stand, sowie die Analyse dynamischer VRS-Daten (sowohl global als auch spezifisch) in zeitlicher Relation zum Gangzyklus. Daraus ließen sich, im Vergleich zu vorangegangenen Arbeiten (Michalik et al., 2020), neue Erkenntnisse gewinnen, welche bei reiner Betrachtung der globalen Wirbelsäulenparameter bzw. bei Auswertungen der dynamischen Parameter ohne zeitlichen Bezug zum Gangzyklus, nicht in dieser Form sichtbar geworden wären. So zeigten sich beispielsweise sowohl für den Stand, als auch für die Wirbelsäulenbewegung im Gang, gemittelt über aller Probanden, sehr systematische und harmonische Haltungs- und Bewegungsmuster der spezifischen Wirbelsäulenparameter. Entgegen der funktionellen Erwartung waren diese jedoch nicht symmetrisch. Stattdessen zeigte sich im aufrechten Stand, besonders in der Transversalebene, eine systematische, rechtsrotatorische Abweichung von der Nullstellung. Diese wurde bereits in der Literatur von anderen Arbeitsgruppen, basierend auf etablierten radiologischen Untersuchungen, beschrieben (Kouwenhoven et al., 2006) und konnten teilweise durch die Organanatomie begründet

werden (Kouwenhoven et al., 2007). Die dynamischen Bewegungsdaten der Wirbelsäule im Gang offenbarten eine vergleichbare rechtsrotatorische Asymmetrie. Diese Erkenntnis wirft zum einen die Frage auf, ob eine möglichst hohe Annährung an eine symmetrische Wirbelsäulenstatik (Wolf et al., 2021) bzw. Wirbelsäulendynamik unter funktionellen Gesichtspunkten überhaupt erstrebenswert ist. Zum anderen lässt sich daraus ein hoher funktioneller Zusammenhang zwischen der statischen Haltung und dem entsprechenden Bewegungsverhalten der Wirbelsäule im Gang ableiten, da die präsentierten dynamischen Wirbelsäulendaten vor der Auswertung nicht auf den Stand normiert wurden. Das bedeutet, dass die individuelle Wirbelsäulenform jedes Probanden seinen entsprechenden Bewegungsdaten zu Grunde liegt, wodurch das Referenzkoordinatensystem nicht auf „null“ steht, sondern jeweils die individuelle Haltung während des Gehens mitberücksichtigt. Die Vermutung liegt somit nah, dass jedes Individuum potentiell um seine persönliche Haltung „herum“ läuft. Dieser Frage sollte zukünftig unbedingt weiter nachgegangen werden. Eine möglicherweise geeignete Auswertemethodik hierfür könnte sich aus der Arbeit von Haimerl et al. (2023) ergeben. Ein Nachweis solch individueller, haltungsabhängiger Gangmuster hätte jedoch zur Folge, dass Messergebnisse verschiedener Personen zukünftig weitaus individueller auszuwerten und zu interpretieren wären, als dies bisher möglicherweise der Fall ist.

Hierfür wäre neben der vorhandenen hohen interindividuellen Varianz, welche sich in den beschriebenen Daten sowohl für den Stand, als auch für den Gang, deutlich durch die breite Streuung der individuellen Ergebnisse um ihre jeweiligen Mittelwerte zeigt, auch eine entsprechend hohe intraindividuelle Konstanz der spinalen Haltungs- und Bewegungsmuster erforderlich. Dadurch könnten, mit Hilfe personalisierter Bewertungskriterien, zielgerichtete Therapieempfehlungen abgeleitet und deren Erfolge durch intraindividuelle prä-post Messungen im Anschluss auch zuverlässig beurteilt werden. Erste Hinweise hierauf finden sich bereits in der Literatur, wo ähnlich den Bewegungsmustern der Becken-Bein-Region (Horst et al., 2016, Horst et al., 2017), auch für spinale Haltungs- und Bewegungsdaten bereits eine hohe intraindividuelle Konstanz beschrieben wurde (Dindorf et al., 2021b, Haimerl et al., 2023).

Der dringende Bedarf zur Entwicklung stärker individualisierter Bewertungskriterien für die Beurteilung spinaler Haltungs- und Bewegungsanalysen wird auf Basis dieser Erkenntnisse deutlich und wurde bereits in anderen Anwendungsbereichen der biomechanischen Ganganalyse gefordert (Horst et al., 2017). Nichtsdestotrotz sind klassische Referenzdaten aus Sicht der Autorin deshalb nicht komplett zu vernachlässigen und haben ihre Berechtigung und Aussagekraft. Sofern sich Anwender stets bewusst sind, dass in Referenzstudien allein aufgrund mathematischer Herangehensweisen bereits ein gewisser Prozentsatz der inkludierten gesunden Teilnehmer Messergebnisse aufweist, die außerhalb der Norm liegen

(Oppelt et al., 2020, Jöllenbeck, 2015) und somit nicht jeder Patient, der von einer Referenznorm abweicht, eine therapeutische Behandlung benötigt (Jöllenbeck, 2015), können sie durchaus einer ersten Orientierung und Einordnung von individuellen Messergebnissen in Relation zu einer entsprechend gesunden Vergleichsgruppe dienen und somit im konkreten Fall, einen wichtigen Beitrag zur klinischen und wissenschaftlichen Interpretierbarkeit VRS-basierter Messdaten leisten.

Neben den direkten Ergebnissen, welche überwiegend für klinische und wissenschaftliche Anwender vergleichbarer Messsysteme von Bedeutung sein dürften, konnten die funktionellen Erkenntnisse des vorliegenden Projektes auch für das allgemeine biomechanische Verständnis der Wirbelsäulenbewegung im Gang neue interessante Impulse liefern. Durch die alternative Messmethodik war es möglich, gleichzeitig Daten für das Bewegungsverhalten jedes einzelnen Wirbelkörpers (von C7-L4) und des Beckens in der Transversalebene zu erheben und diese im Vergleich zum bisherigen Verständnis der Wirbelsäulendynamik im Gang zu diskutieren. Die Erhebung solcher Daten gestaltete sich bisher schwierig, da es spezieller Markereigenschaften bedarf, um Bewegungen in der Transversalebene mit den gängigen markerbasierten Messsystemen zu erfassen (Konz et al., 2006, Needham et al., 2016). Zukünftige Untersuchungen werden zeigen müssen, ob die hier vorgestellten und vom bisherigen funktionellen Verständnis abweichenden Ergebnisse mit anderen Messverfahren reproduzierbar sind und welche Konsequenzen sich daraus potentiell für unser zukünftiges Verständnis der Wirbelsäulenbewegung im Gang ergeben. Aufgrund der hochstandardisierten Datenerhebung unter kontrollierten Laborbedingungen und der damit einhergehenden hohen internen Validität der Messergebnisse, sollte eine entsprechende Wiederholung des Studiendesigns durch andere Arbeitsgruppen und potentiell auch mit anderen Messsystemen jedoch möglich sein.

3.1 Schlussfolgerung

Die publizierten Arbeiten deuten darauf hin, dass es sich bei der VRS um ein geeignetes Messverfahren für die spinale Haltungsanalyse handelt, dessen Ergebnisse insbesondere von einer funktionellen Perspektive mit denen etablierter Untersuchungsverfahren vergleichbar sind. Dies unterstützt die klinische Einsetzbarkeit der VRS als nicht-invasives, schnelles und einfach durchzuführendes Untersuchungsverfahren im klinischen Alltag insbesondere dann, wenn funktionelle Fragestellungen beantwortet werden sollen. Durch den Weiterentwicklungsprozess der Software konnte außerdem der wissenschaftliche Anwendungsbereich der VRS vergrößert werden, da jetzt auch spezifische Wirbelsäulenparameter und alle Rohdaten in zeitlicher Relation zum Gangzyklus exportiert und dadurch vielfältige neue Forschungsfelder mit dieser strahlenfreien und wenig zeitaufwendigen Messmethodik erschlossen werden können.

Darüber hinaus hat die vorliegende Arbeit aber auch gezeigt, dass aufgrund der hohen interindividuellen Varianz der spinalen Haltungs- und Bewegungsdaten, eindeutige Schlussfolgerungen aus VRS-Messungen noch immer herausfordernd sind. Es wurde deutlich, dass systematische Referenzdaten, wie jene aus dem vorliegenden Projekt, zwar durchaus einer ersten Orientierung und funktionellen Einordnung von Messergebnissen in Relation zu einer entsprechend gesunden Vergleichsgruppe dienen können, dieser Vergleich aufgrund der hohen Komplexität der zu Grunde liegenden Daten jedoch allein nicht ausreicht, um zuverlässig zwischen physiologischen und pathologischen Messergebnissen zu differenzieren. Hier zeigte sich, ähnlich wie in anderen Anwendungsbereichen der biomechanischen Ganganalyse bereits gefordert, ein dringender Bedarf zur zusätzlichen Entwicklung stärker individualisierter Bewertungskriterien. Diese können dann, in Kombination mit Referenzdaten und adäquaten intraindividuellen prä-post Messungen, zukünftig noch gezielter zu Entscheidungsprozessen beitragen und individuelle Therapieeffekte potentiell noch zuverlässiger evaluieren.

3.2 Ausblick

Die bereits publizierten Referenzdaten werden sukzessiv durch die noch nicht ausgewerteten Datensätze dieses Forschungsprojektes erweitert. Dabei sollen Messergebnisse für alle erhobenen Gehgeschwindigkeiten, sowohl für die globalen als auch für die spezifischen Wirbelsäulenparameter, in allen drei Bewegungsebenen und in Abhängigkeit des Alters und des Geschlechts der Probanden zur Verfügung gestellt werden.

Basierend auf den Erkenntnissen der vorliegenden Arbeit wird parallel dazu ein zusätzlicher Schwerpunkt auf der Entwicklung stärker individualisierter Bewertungskriterien liegen. Hierbei bietet es sich auf Grund der hohen Komplexität der erhobenen Daten an, auf die Unterstützung künstlicher Intelligenz zurückzugreifen. Solche Programme wurden bereits im Bereich der Ganganalyse verwendet (Horst et al., 2019) und konnten in jüngster Vergangenheit außerdem erfolgreich für die Analyse von VRS-Daten sowohl für den Stand, als auch für den Gang herangezogen werden (Dindorf et al., 2021a, Dindorf et al., 2021b, Dindorf et al., 2020).

Die Beschreibung der noch verbliebenen Wirbelsäulendaten innerhalb des SGZ wird neben der reinen Präsentation von Referenzwerten und individualisierten Bewertungskriterien, außerdem einen wertvollen Beitrag zum allgemeinen Grundverständnis des funktionellen Bewegungsverhaltens der Wirbelsäule im Gang leisten können. Besonders vor dem Hintergrund der technischen Weiterentwicklung, die es mittlerweile ermöglicht VRS-Messungen im Bereich von Laufanalysen bei Geschwindigkeiten von bis zu 30 km/h einzusetzen (DIERS International GmbH, 2022), ist dieses Grundverständnis aus Sicht der Autorin von großer Bedeutung.

4 Literaturverzeichnis

APPLEBAUM, A., FERENCE, R. & CHO, W. 2020. Evaluating the role of surface topography in the surveillance of scoliosis. *Spine Deform*.

ARSHAD, R., PAN, F., REITMAIER, S. & SCHMIDT, H. 2019. Effect of age and sex on lumbar lordosis and the range of motion. A systematic review and meta-analysis. *Journal of Biomechanics,* 82**,** 1-19.

BETSCH, M., WILD, M., JOHNSTONE, B., JUNGBLUTH, P., HAKIMI, M., KUHLMANN, B. & RAPP, W. 2013. Evaluation of a novel spine and surface topography system for dynamic spinal curvature analysis during gait. *PLoS One,* 8**,** e70581.

BETSCH, M., WILD, M., RATH, B., TINGART, M., SCHULZE, A. & QUACK, V. 2015. [Radiation-free diagnosis of scoliosis : An overview of the surface and spine topography]. *Orthopade*.

BISCHOFF, H. A., STAHELIN, H. B., MONSCH, A. U., IVERSEN, M. D., WEYH, A., VON DECHEND, M., AKOS, R., CONZELMANN, M., DICK, W. & THEILER, R. 2003. Identifying a cut-off point for normal mobility: a comparison of the timed 'up and go' test in community-dwelling and institutionalised elderly women. *Age Ageing,* 32**,** 315-20.

BOHANNON, R. W., WANG, Y. C. & GERSHON, R. C. 2015. Two-minute walk test performance by adults 18 to 85 years: normative values, reliability, and responsiveness. *Arch Phys Med Rehabil,* 96**,** 472-7.

DEGENHARDT, B. F., STARKS, Z. & BHATIA, S. 2020. Reliability of the DIERS Formetric 4D Spine Shape Parameters in Adults without Postural Deformities. *BioMed research international,* 2020**,** 10.

DEGENHARDT, B. F., STARKS, Z., BHATIA, S. & FRANKLIN, G.-A. 2017. Appraisal of the DIERS method for calculating postural measurements: an observational study. *Scoliosis Spinal Disord,* 12**,** 28.

DIERS INTERNATIONAL GMBH. 2022. *DIERS 4D high performance Lab* [Online]. Available: https://diers.eu/de/produkte/komplett-systeme/diers-4dmotionlab-high-performance/ [Accessed 28.11.2023].

DINDORF, C., KONRADI, J., WOLF, C., TAETZ, B., BLESER, G., HUTHWELKER, J., DREES, P., FRÖHLICH, M. & BETZ, U. 2020. General method for automated feature extraction and selection and its application for gender classification and biomechanical knowledge discovery of sex differences in spinal posture during stance and gait. *Computer Methods in Biomechanics and Biomedical Engineering,* 24**,** 1-9.

DINDORF, C., KONRADI, J., WOLF, C., TAETZ, B., BLESER, G., HUTHWELKER, J., WERTHMANN, F., BARTAGUIZ, E., KNIEPERT, J., DREES, P., BETZ, U. & FRÖHLICH, M. 2021a. Classification and Automated Interpretation of Spinal Posture

Data Using a Pathology-Independent Classifier and Explainable Artificial Intelligence (XAI). *Sensors,* 21.

DINDORF, C., KONRADI, J., WOLF, C., TAETZ, B., BLESER, G., HUTHWELKER, J., WERTHMANN, F., DREES, P., FRÖHLICH, M. & BETZ, U. 2021b. Machine learning techniques demonstrating individual movement patterns of the vertebral column: the fingerprint of spinal motion. *Computer Methods in Biomechanics and Biomedical Engineering***,** 1-11.

DRERUP, B. 2014. Rasterstereographic measurement of scoliotic deformity. *Scoliosis,* 9**,** 22.

DRERUP, B., ELLGER, B., MEYER ZU BENTRUP, F. M. & HIERHOLZER, E. 2001. [Functional rasterstereographic images. A new method for biomechanical analysis of skeletal geometry]. *Orthopade,* 30**,** 242-50.

DRERUP, B. & HIERHOLZER, E. 1992a. Evaluation of frontal radiographs of scoliotic spines--Part I measurement of position and orientation of vertebrae and assessment of clinical shape parameters. *Journal of biomechanics,* 25**,** 1357-1362.

DRERUP, B. & HIERHOLZER, E. 1992b. Evaluation of frontal radiographs of scoliotic spines--Part II: Relations between lateral deviation, lateral tilt and axial rotation of vertebrae. *J Biomech,* 25.

FEDORAK, C., ASHWORTH, N., MARSHALL, J. & PAULL, H. 2003. Reliability of the visual assessment of cervical and lumbar lordosis: how good are we? *Spine (Phila Pa 1976),* 28**,** 1857-9.

FURIAN, T. C., RAPP, W., ECKERT, S., WILD, M. & BETSCH, M. 2013. Spinal posture and pelvic position in three hundred forty-five elementary school children: a rasterstereographic pilot study. *Orthop Rev (Pavia),* 5**,** e7.

GIPSMAN, A., RAUSCHERT, L., DANESHVAR, M. & KNOTT, P. 2014. Evaluating the Reproducibility of Motion Analysis Scanning of the Spine during Walking. *Adv Med,* 2014**,** 721829.

GREGERSEN, G. G. & LUCAS, D. B. 1967. An in vivo study of the axial rotation of the human thoracolumbar spine. *J Bone Joint Surg Am,* 49**,** 247-62.

HAIMERL, M., NEBEL, I., LINKERHÄGNER, A., KONRADI, J., WOLF, C., DREES, P. & BETZ, U. 2023. Consistency of vertebral motion and individual characteristics in gait sequences. *Human Movement Science,* 87**,** 103036.

HORST, F., KRAMER, F., SCHAFER, B., EEKHOFF, A., HEGEN, P., NIGG, B. M. & SCHOLLHORN, W. I. 2016. Daily changes of individual gait patterns identified by means of support vector machines. *Gait Posture,* 49**,** 309-314.

HORST, F., LAPUSCHKIN, S., SAMEK, W., MULLER, K. R. & SCHOLLHORN, W. I. 2019. Explaining the unique nature of individual gait patterns with deep learning. *Sci Rep,* 9**,** 2391.

HORST, F., MILDNER, M. & SCHOLLHORN, W. I. 2017. One-year persistence of individual gait patterns identified in a follow-up study - A call for individualised diagnose and therapy. *Gait Posture,* 58**,** 476-480.

HUTHWELKER, J., KONRADI, J., WOLF, C., WESTPHAL, R., SCHMIDTMANN, I., DREES, P. & BETZ, U. 2022. Reference Values for 3D Spinal Posture Based on Videorasterstereographic Analyses of Healthy Adults. *Bioengineering,* 9**,** 809.

HUTHWELKER, J., KONRADI, J., WOLF, C., WESTPHAL, R., SCHMIDTMANN, I., SCHUBERT, P., DREES, P. & BETZ, U. 2023. Reference values and functional descriptions of transverse plane spinal dynamics during gait based on surface topography. *Human Movement Science,* 88**,** 103054.

JANSSEN, M. M., DREVELLE, X., HUMBERT, L., SKALLI, W. & CASTELEIN, R. M. 2009. Differences in male and female spino-pelvic alignment in asymptomatic young adults: a three-dimensional analysis using upright low-dose digital biplanar X-rays. *Spine (Phila Pa 1976),* 34**,** E826-32.

JÖLLENBECK, T. Ganganalyse im Spannungsfeld zwischen Mensch und Technik. *In:* WITTE K., E.-N. J., ed. Sporttechnologie zwischen Theorie und Praxis IV, 2015. Aachen: Shaker-Verl., 67-75.

KONRADI, J. 2022a. SPSS syntax script to create graphs of spinal motion for a Standardized Gait Cycle. Mendeley Data.

KONRADI, J. 2022b. SPSS syntax script to create graphs of spinal motion relative to phases of gait. Mendeley Data.

KONRADI, J. 2022c. Visualizations of rotational curves directly related to gait phases. Mendeley Data.

KONRADI, J. 2022d. Visualizations of rotational curves within a Standardized Gait Cycle. Mendeley Data.

KONZ, R. J., FATONE, S., STINE, R. L., GANJU, A., GARD, S. A. & ONDRA, S. L. 2006. A kinematic model to assess spinal motion during walking. *Spine (Phila Pa 1976),* 31**,** E898-906.

KOUWENHOVEN, J. W., BARTELS, L. W., VINCKEN, K. L., VIERGEVER, M. A., VERBOUT, A. J., DELHAAS, T. & CASTELEIN, R. M. 2007. The relation between organ anatomy and pre-existent vertebral rotation in the normal spine: magnetic resonance imaging study in humans with situs inversus totalis. *Spine (Phila Pa 1976),* 32**,** 1123-8.

KOUWENHOVEN, J. W., VINCKEN, K. L., BARTELS, L. W. & CASTELEIN, R. M. 2006. Analysis of preexistent vertebral rotation in the normal spine. *Spine (Phila Pa 1976),* 31**,** 1467-72.

KROTT, N. L., WILD, M. & BETSCH, M. 2020. Meta-analysis of the validity and reliability of rasterstereographic measurements of spinal posture. *Eur Spine J,* 29**,** 2392-2401.

MICHALIK, R., HAMM, J., QUACK, V., ESCHWEILER, J., GATZ, M. & BETSCH, M. 2020. Dynamic spinal posture and pelvic position analysis using a rasterstereographic device. *J Orthop Surg Res,* 15**,** 389.

MYKLEBUST, M., MAGNUSSEN, L. & INGER STRAND, L. 2007. Back Performance Scale scores in people without back pain: Normative data. *Advances in Physiotherapy,* 9**,** 2-9.

NEEDHAM, R., STEBBINS, J. & CHOCKALINGAM, N. 2016. Three-dimensional kinematics of the lumbar spine during gait using marker-based systems: a systematic review. *J Med Eng Technol,* 40**,** 172-85.

OPPELT, K., HOGAN, A., STIEF, F., GRÜTZNER, P. A. & TRINLER, U. 2020. Movement Analysis in Orthopedics and Trauma Surgery - Measurement Systems and Clinical Applications. *Z Orthop Unfall,* 158**,** 304-317.

PERRY, J. & BURNFIELD, J. M. 2010. *Gait analysis - Normal and pathological function,* Thorofare, SLACK Incorporated.

SCHMIDTMANN, I. & KONRADI, J. 2022. SAS syntax script for merging export files. Mendeley Data.

SCHRÖDER, J., BRAUMANN, K. M. & REER, R. 2014. Wirbelsäulenform- und Funktionsprofile. *Der Orthopäde,* 43**,** 841-849.

SCHRÖDER, J., STILLER, T. & MATTES, K. 2011. [Reference data for spine shape analysis. Approaching a majority norm and deviations for unspecific low back pain]. *Manuelle Medizin,* 49**,** 161-166.

SUPPÉ, B. & BONGARZ, M. (eds.) 2013. *FBL Klein-Vogelbach Functional Kinetics praktisch angewandt. Gehen - Analyse und Intervention.,* Heidelberg: Springer.

WESTPHAL, R. & KONRADI, J. 2022. SAS syntax script for creation of a Standardized Gait Cycle. Mendeley Data.

WOLF, C., BETZ, U., HUTHWELKER, J., KONRADI, J., WESTPHAL, R. S., CERPA, M., LENKE, L. & DREES, P. 2021. Evaluation of 3D vertebral and pelvic position by surface topography in asymptomatic females: presentation of normative reference data. *J Orthop Surg Res,* 16**,** 703.

ZAPPALÁ, M., LIGHTBOURNE, S. & HENEGHAN, N. R. 2021. The relationship between thoracic kyphosis and age, and normative values across age groups: a systematic review of healthy adults. *J Orthop Surg Res,* 16**,** 447.

5 Danksagung

6 Tabellarischer Lebenslauf

Name:	Huthwelker, Janine
Geburtsort:	Kassel, Deutschland